DEGREE PROJECT

Progressive Landslides Analysis

Applications of a Finite Difference Method by Dr. Stig Bernander

Case Study of the North Spur at Muskrat Falls, Labrador, Canada

Robin DURY

Civil Engineering, master's level
2017

Luleå University of Technology
Department of Civil, Environmental and Natural Resources Engineering

LULEÅ UNIVERSITY OF TECHNOLOGY

The cover picture is a photography of Muskrat Falls hydro power plant construction site. It has been taken in August 2016 (Source: http://muskratfalls.nalcorenergy.com/).

Preface

The aim of this thesis is twofold: (1) To present an easy-to-use version of a finite difference method for progressive landslide analysis and (2) To apply the method to the study of a slope stability problem encountered on the construction site of a hydro power plant at Muskrat Falls in Churchill River, Labrador, Canada. The intension has been to carry out some analyses with an alternative approach to the traditional limit equilibrium method.

The progressive landslide analysis is based on a finite difference method developed by Dr. Stig Bernander.

The work with the thesis has been conducted under the guidance of Emeritus Professor Lennart Elfgren, Structural Engineering, and Professor Jan Laue, Soil Mechanics and Foundation Engineering, Luleå University of Technology, LTU. I am grateful to them for their help and commitment. I also wish to express my gratitude to Dr. Stig Bernander for the time and effort he took in sharing his knowledge on progressive landslides with me.

If you have any question about this report, please feel free to contact me by e-mail at the following address: robin.dury@hotmail.fr

Luleå in June 2017

Robin DURY

Abstract

An easy-to-use spreadsheet version of a finite difference method for progressive landslide analysis has been developed. The finite difference method was originally developed by Dr. Stig Bernander, earlier adjunct professor at Luleå University of Technology and head of the Design Department of Skanska AB in Gothenburg, Sweden..

The so called Muskrat Falls Project consists in the ongoing construction of a hydroelectric power plant in Churchill River Valley, Labrador, Canada. The site hosting the project includes a land ridge which is supposed to be used as a natural dam and thus be submitted to important water pressures. Yet, previous landslides in the area have shown that a stability analysis is worth to be carried out in order to ensure the safety of the facility.

Until now, investigations have only been carried out using the traditional limit equilibrium method and related elastic-plastic theory. For the sake of simplicity, this approach does not take into account deformations outside and inside the sliding body. However, because of the soil features in Churchill River Valley and particularly its 'deformation softening' behavior, there is increasing evidence that the conventional analysis is not relevant in this situation. Further, when analyzing the total stability of the ridge, only a horizontal failure surface has been used and not an inclined one, which is very optimistic and rather unrealistic..

In order to provide a more reliable study, a progressive failure analysis has been performed according to the finite difference method of Dr. Stig Bernander. The development of a spreadsheet adapted to this particular problem has allowed getting quickly and easily numerical results for several cases of study and assumptions. For assumed material properties and geometries of failure, the critical load-carrying capacity is below 1000 kN/m whereas a rise of the water level with 22 m will give an increased load of $N_q = 0{,}5\ \gamma_w H_d^2 = 0{,}5 \cdot 10 \cdot 22^2 =$ 2420 kN/m. This is more than twice of the what the ridge may stand with the assumed properties.

The investigation has led to the conclusion that the situation will be risky for many combinations of soil properties if the water level is raised as high as initially planned. The investigation also shows that more material tests are necessary and that stabilization work may be needed to eliminate the risk for a landslide.

Key words:
Downhill progressive landslides, Slope stability, Sensitive clay, Deformation softening, Finite difference method, Brittle failure in clay, Liquefaction, Muskrat Falls project

Sammanfattning på Svenska

Analys av jordskred på grund av progressiva brott

Tillämpning av en finit differensmetod utvecklad av Dr. Stig Bernander.
Fallstudie av North Spur i Muskrat Falls, Labrador, Kanada.

En lättanvändbar kalkylbladsversion har utvecklats för en finit differensmetod för analys av progressiva skred. Metoden utvecklades ursprungligen av Tekn. Dr. Stig Berander, tidigare adjungerad professor vid Luleå tekniska universitet och konstruktionschef på Skanska AB i Göteborg.

Projektet vid Muskrat Falls utgörs av ett kraftverksbygge i Churchillflodens dalgång i Labrador, Kanada. På projektplatsen finns en ås som man planerar att utnyttja som en naturlig damm och därmed utsätta den för betydande vattentryck. Tidigare skred i området gör det angeläget att studera den tilltänkta dammens stabilitet.
Hittills har beräkningar endast genomförts med traditionell jämviktsmetod baserad på elastiskt-plastiska förhållanden. För enkelhets skull tar denna metod inte hänsyn till några deformationer inne i skredmassorna eller utanför själva glidytan. På grund av de deformationsmjuknande egenskaperna hos jordmaterialet i Churchillflodens dalgång är det uppenbart att en traditionell analys inte ger relevanta resultat. Dessutom har man endast studerat horisontella glidytor och inga som lutar i släntens riktning. Detta är optimistiskt och orealistiskt.

En progressiv brottanalys har därför utförts med en finit differensmetod utvecklad av Stig Bernander. Ett kalkylblad har tagits fram som anpassats till det aktuella problemet och som möjliggör en snabb och enkel analys av olika antaganden om materialegenskaper och geometri. Med de antagna egenskaperna erhålls att den kritiska bärförmågan är mindre än 1000 kN/m. När vattennivån höjs med 22 m kommer horisontallaste att öka med N_q = 0,5 $\gamma_w H_d^2$ = 0,5·10·22^2 = 2420 kN/m. Detta är mer än dubbelt så mycket som åsen kan stå emot med de antagna förutsättningarna.

Undersökningen har lett till slutsatsen att situationen är mycket riskfylld för många kombinationer av materialegenskaper om vattennivån höjs så mycket som man planerar. Mer materialdata behövs och stabiliseringsarbeten kan också komma att visa sig nödvändiga för att undvika risken för att dammen skall raseras av ett skred.

Abstract en Français

Analyse des glissements de terrain progressifs

Application de la méthode des différences finies développée par Dr. Stig Bernander
Etude du cas de la digue Nord de Muskrat Falls, Labrador, Canada

Une feuille de calcul basée sur la méthode des différences finies appliquée à l'analyse des glissements de terrain progressifs a été développée. A l'origine, cette méthode a été développée par Dr. Stig Bernander, précédemment professeur adjoint à University of Technology of Luleå et chef du département conception de Skanska AB à Goteborg, Suède.

Muskrat Falls Project consiste en la construction d'une station hydro électrique dans la vallée de Churchill River, Labrador, Canada. Le site accueillant le projet contient une bande de terre qui est supposé être utilisée comme un barrage naturel et donc soumis à d'importantes pressions dues à l'eau. Cependant, les glissements de terrains ayant eu lieu précédemment dans cette zone ont montré qu'une analyse concernant la stabilité de la digue doit être menée pour assurer la pérennité de l'aménagement.

Jusqu'à présent, les études concernant l'installation ont seulement été menées en utilisant la méthode de l'équilibre limite, supposant un comportement élastico-plastique. Dans un souci de simplicité, cette approche ne tient pas compte des déformations environnant le corps glissant. Cependant, du fait des propriétés du sol dans la vallée de Churchill River, et particulièrement du comportement sensible de l'argile, il est évident que l'analyse conventionnelle n'est pas pertinente dans ce cas. De plus, les études menées précédemment se sont réduites à l'hypothèse d'une surface de glissement horizontale et non inclinée, ce qui est plutôt optimiste et éloigné de la réalité.

Afin d'apporter un point de vue plus sûr, une analyse a été menée en utilisant la méthode des différences finies de Dr. Stig Bernander. Le développement d'une feuille de calcul adaptée à ce problème particulier a permis d'obtenir rapidement de nombreux résultats pour des hypothèses et cas de figure différents. Pour des propriétés matériels et une géométrie hypothétiques, la charge critique supportable par la digue est inférieure à 1000 kN/m alors qu'une élévation du niveau d'eau de 22 m engendrerait une surcharge $N_q = 0{,}5\ \gamma_w\ H_d^2 = 0{,}5 \cdot 10 \cdot 22^2 = 2420$ kN/m. Cette valeur correspond à deux fois ce que la digue pourrait supporter.

L'analyse a conduit à tirer la conclusion suivante: la situation est risquée pour de nombreuses combinaisons de propriété de sol différentes si le niveau d'eau est élevé comme initialement prévu. L'étude montre aussi que d'autres tests des matériaux sont nécessaires et qu'un travail de stabilisation des pentes est requis pour éliminer le moindre risqué de glissement.

Contents

Notations

Upper case Roman letters (in alphabetical order)
E: Total earth pressure (kN/m)
E_0: In-situ earth pressure (kN/m)
E_{el}: Secant elastic modulus in down-slope compression (GPa)
E_p : Critical down-slope earth pressure resistance at passive Rankine failure (kN/m)
$F_s^{(I)}$: Safety factor for local failure (N_{cr} /N_q)
$F_s^{(II)}$: Safety factor for global failure (E_p /E)
G : Secant modulus in shear in the range $\tau\ (x,z) \rightarrow \tau\ (x,z) + \Delta\tau\ (x,z)$ (GPa)
$H_{x_i \rightarrow x_{i+1}}$: Height of element $i \rightarrow i+1$ (m)
K_0: Ratio between minor and major principal stresses
K_p: Rankine coefficient for lateral passive earth resistance
L_{cr} : Limit length of mobilization of shear stress at N_{cr} (m)
N_{cr} :Critical load effect initiating local slope failure (kN/m)
N_q : Additional load in the direction of the failure plane (kN/m)
N : Earth load increment due to additional load (kN/m)

Lower case Roman letters (in alphabetical order)
b: Width of the element considered (m)
c, c_u: Un-drained peak shear strength (kPa)
c_R: Residual shear strength (kPa)
c_s : Shear strength at layer interface (kPa)
g: Gravity (9,81 m/s^2)
q: Additional vertical load (kN/m^2)

Greek letters (in alphabetical order)
α: Coefficient defining the elevation of the earth pressure resultant
β : Slope gradient at coordinate x (°)
$\gamma(x,z)$: Deviator shear strain at point x,z
γ_{el}: Deviator strain at elastic limit
γ_f: Deviator strain for shear stress peak value
δ_{cr}: Critical displacement in terms of axial deformation (m)
δ_N: Down-slope displacement in terms of axial deformation generated by forces N (m)
δ_τ: Down-slope displacement in terms of deviator deformation (m)
δ_s: Slip in the failure surface during post peak deformation (m)
$\Delta\tau_{x_i \rightarrow x_{i+1}}$: Shear increment from step i to $i+1$ (kPa)
αH_x : Level at which the down-slope displacement is considered to be valid (m)
ρ: Soil density (kg/dm^3)
υ: Poisson coefficient
τ_{el} :Shear stress at elastic limit (kPa)
$\tau, \tau(x,z)$: Total shear stress in section x at elevation z (kPa)
$\tau_0(x,z)$: In situ shear stress in section x at elevation z (kPa)

1. Introduction

1.1. Background

A landslide is usually defined as a collapse of a mass of ground which is likely to transform an initially stable slope into a devastating earth flow. During the last century, a lot of such catastrophic phenomena have occurred, with consequences ranging from simple landscape modification to housing destructions and human deaths. With ongoing climate changes it is likely that the risks for landslides will increase.

The severity of the aftermaths of landslides demands us to develop reliable analysis methods allowing geo-technicians to predict landslides and set up sustainable actions to avoid them. The analysis of such complex phenomena requires models using many assumptions and simplifications. However, the problem must not be turned into something too far from reality. Thus, the difficulty of the task lies in finding a good balance between simplicity and accuracy. For this reason, different models and calculation methods have been developed over the years. Nowadays, the limit equilibrium method (LEM) is the most used and applied to perform landslides analysis, see e.g. Axelsson & Mattsson (2016). However, this method cannot properly explain numerous landslides in glacial deposits which have occurred in Sweden and other parts of the world during the last fifty years.

Dr. Stig Bernander has worked on this topic for many years; Bernander et al (1978, 1981, 2000, 2008, 2011, and 2016). He has developed an approach giving a satisfying analysis of landslides in Western Sweden such as Surte (1950), Tuve (1977) or more recently Småröd (2006).

This approach to solve stability problems in long natural slopes with soft Scandinavian or other glacial clays is based on a numerical finite difference model that, contrary to the traditional method, takes the deformation properties of the soil into consideration.

1.2. Aim and objectives

The aim of this work is to give a clear and simple explanation of the analysis method for downhill progressive failure in long natural slopes developed by Dr. Stig Bernander.

An objective is to set up software based on the method permitting to carry out rough landslide analyses. This tool is supposed to be user-friendly and accessible to any geotechnical engineer and consultant who want to assess the stability of a slope.

A final objective is to use the software to solve a problem encountered by Nalcor Company on the hydro power construction project of Muskrat Falls (Labrador, Canada), Leahy (2015). It concerns the study of the stability of a large natural dam caused by the building of the power plant at Muskrat Falls, which may have quite a high risk to cause a progressive landslide.

1.3. Method

A bibliographic study was performed to provide general knowledge on the subject of landslides, slope stability and progressive failure. A summary of this study is included in Chapter 2 to give the reader the necessary background to understand the rest of the report.

The theory underlying the method for downhill progressive failure is explained in the easiest way possible in Chapter 2. This part focuses on the scope of application, process and calculations with the method.

An overview of the stability problem encountered in the Muskrat Falls project is given in Chapter 3.

An explanation is then given of the architecture and the way of working of the spreadsheet developed in Chapter 4

Afterwards, the software is used to carry out a progressive failure analysis of the new dam close to the North Spur of Muskrat Falls. The input parameters and data chosen to perform the analysis are discussed and justified in Chapter 5.

The results of the analysis are then presented in chapter 5 and discussed in chapter 6.

1.4. Delimitation

This thesis has been written to develop a tool based on Stig Bernanders method to perform analysis for a very typical type of landslide. This tool is only made to study downhill progressive failure in long natural slopes. As it will be explained, it is not supposed to provide an analysis for other types of landslides.

This report does not provide a full account of Dr. Bernanders work and theory. For more details, the reader can study his doctoral thesis, Bernander (2011), with a summary in Bernander et al. (2016).

The study shows that a risk of downhill progressive failure may exist on the construction site at Muskrat Falls. This work is mainly based on rough assumptions as concerns the mechanics and geometric properties of the slope studied. Thus we cannot claim that the study gives an entirely accurate analysis. We simply bring to light the fact that there is a problem which should be studied in more a depth.

2. Theory

2.1. Progressive failure in long natural slopes

Stig Bernander developed his approach of progressive landslide failure to explain the many landslides which occurred in western Sweden. These landslides have until the last years mostly not been explained satisfactorily by post-slide investigations when applying the classic limit equilibrium method (LEM) using perfectly plastic soil properties.

The landslide of Tuve which occurred in 1977 is one of the catastrophic events that Bernander managed to explain with his method. This slide, which lasted not more than six minutes, destroyed 67 houses, killed 9, injured about 60 and made around 600 people homeless. It affected a huge area of 270 000 square meters, see Figure 2-1, Bernander (2000, 2011).

Figure 2-1. Aerial photograph of the Tuve slide in Gothenburg 1977 with East in the top. The slide started in the middle of the photo and moved beyond the Kville Creek (top). Copyright Gothenburg Museum of Natural History, Bernander et al (2016).

There exist three main categories of progressive landslides: downhill progressive slides, uphill progressive or retrogressive slides (often denoted 'spreads') and laterally progressive slides. In this paper, only the case of downhill progressive landslide will be investigated.

Downhill progressive failure starts in the upper part of the slope as a local instability that propagates downhill. It generally takes place in long gently sloping ground along a plane slip surface.

More information on theory of progressive landslides can be found in e.g. Bernander et al. (2011, 2016), Leroueil (2001), Thakur et al. (2006, 2007, 2017), Locat et al. (2011), Gylland (2012), and L.Heureux et al. (2013). Protection against mass movement hazards are discussed in e.g. FOEN (201&).

2.2. **Material Properties**

Progressive landslides occur in soils such as sensitive clays in which significant deformations are succeeded by an important reduction of shear resistance. (In contrast, elastic-plastic soils deform linearly with increasing shear stress). For this reason, the principle of plastic equilibrium cannot be applied to progressive failure analysis in long natural slopes made of soft sensitive clays.

A deformation softening behavior may be defined by a full nonlinear stress-strain relationship. see Figure 2-2. After an elastic phase with increasing shear resistance up to the linear limit, a non-linear phase begins and the peak value c is reached. At this point, the formation of a slip surface begins. Then a decline in shear strength follows until only the residual strength, c_r remains. The term 'deformation-softening' refers to the loss of shear resistance with increasing shear strains and displacements in the developing failure zone, the material is getting softer (less stiff) with increasing strains and deformations.

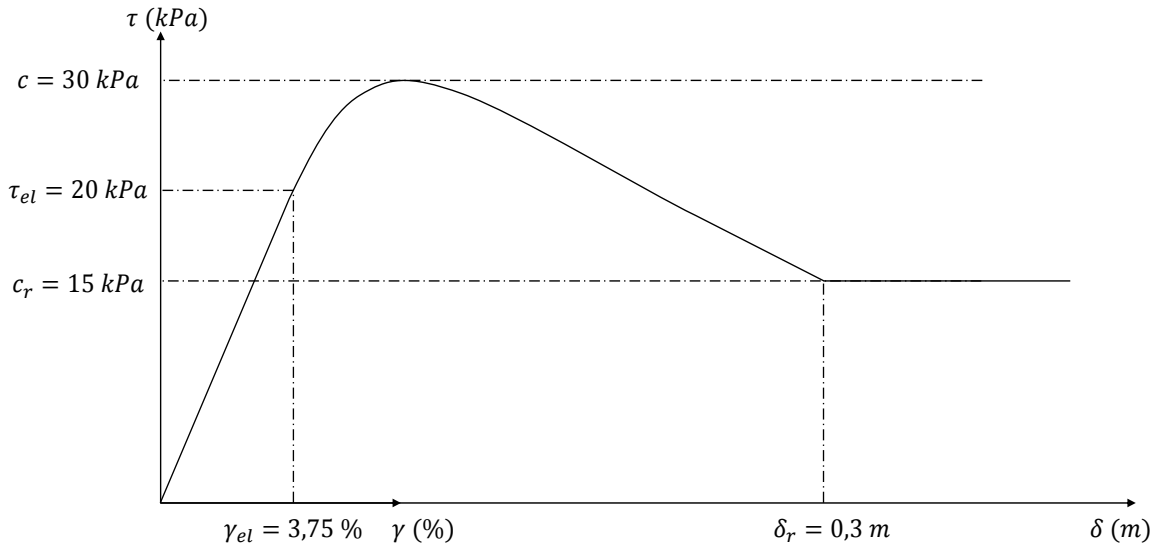

Figure 2-2. Stress-strain deformation relationship of a typical 'deformation softening' clay from southwestern Sweden

Shear resistance and shear stress-strain relations are not fixed or invariable properties. They remain dependent on various parameters.

For example, different time scales of load application give different stress-strain/deformation relationships. A fast loading gives a higher peak value and a lower residual value, which implies a quick, brittle failure. The ratio between the residual value, c_r and the peak value c, will in this case be low. As the difference between the peak strength and the residual strength lessen, the ratio tends to 1, and in that case the failure will be ductile. Figure 2-3 illustrates the relationship between these variables for three cases, with ratios ranging from of 0,3 to 1.

The creep of the soil is also of importance, see e.g. Grimstad et al. (2010) and Pusch et al (2016)

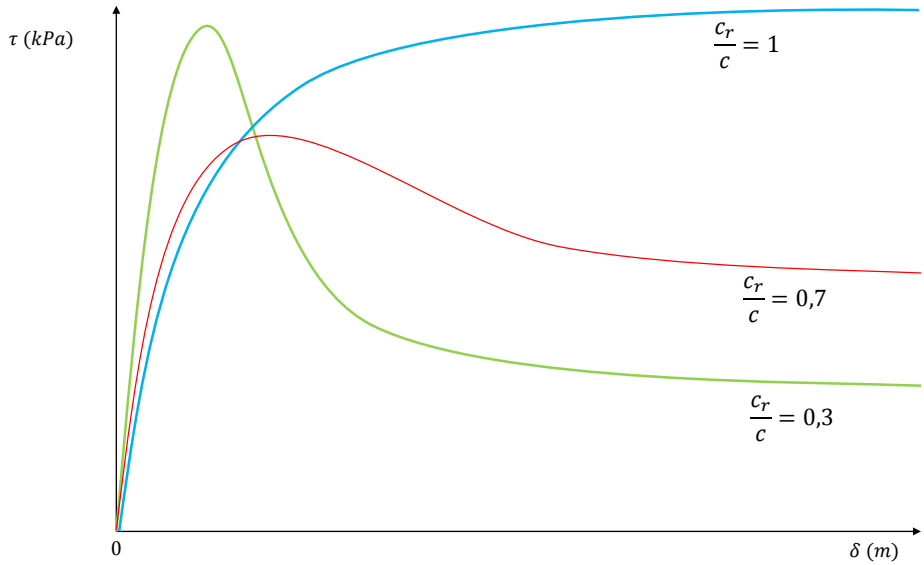

Figure 2-3. Stress-deformation relationships for different rates of loading. Initial condition c_r/c = 1, disturbance condition c_r/c = 0,7 and global failure conditions c_r/c = 0,3. Bernander et al. (2011, 2016).

This relationship is also depending on the following parameters:

- the rates of dissipation of excess pore pressure, e.g. the thickness and permeability of the soil layers neighboring the developing failure surface.
- the relationship between current porosity (n) and the value of critical porosity (n_{crit}); cf. Terzaghi, Peck & Mesri (1996).

The presence of sensitive clays in long natural slopes is the result of glacial and post-glacial deposits that emerged from the regressing sea after the last glacial period. The sediments deposited in seas at the end of this period, are now found on continental lands considerably above present sea level, forming deep layers of soft and silty clays. Over this metamorphosis, consolidation and creep movement have slowly affected the clay properties. Chemical reactions may have deteriorated the soil shear strength. Besides, the long-time upward ground water seepage has e.g. increased the sensitivity of the material. These two combined factors are enough to make an entire slope acutely vulnerable to progressive failure.

2.3. **Failure process**

A downhill progressive landslide is triggered by specific initiating agents acting along or on the top of the slope. They are local in time and space and they are often related to human construction activities. Here is a list of these agents which can seem insignificant at first glance.

- Stockpiling, earth fills, construction of supporting road embankments
- Excavation work
- Vibratory activity
- Rock blasting
- Man-made interference with hydrological conditions

One of these disturbing factors combined with a high shear stress level in the in situ condition of the slope can generate the phenomenon of brittle failure.

In many cases observed in Canada and Scandinavia, the slopes studied have remained stable for centuries or millennia, and yet, a seemingly insignificant local load has managed to trigger an extensive progressive landslide over wide area. (Bernander, 2015)

When the stress induced by the triggering agent reaches the peak shear strength of the material, a slip surface starts to develop in the slope. Then, when the deformations cause the residual shear resistance of the ground to decrease below the current in situ shear stress ($c_r \leq \tau_0$), a redistribution of earth pressures in the slope occurs in order to maintain overall equilibrium. Thus, a progressive downhill failure is triggered.

The final result of this phenomenon is a global ground displacement over more or less large areas.

In order to explain the progressive failure process, we use a simple example. The detailed calculations for the example are given in Appendix D. We consider a long natural slope made of soft sensitive clay. It has the mechanics properties of Figure 2-4. The ground portion considered has a constant inclination $\beta = 6{,}515\%$ ($3{,}728^{o}$) and an invariable depth $H = 20\,m$. The triggering agent likely to initiate the failure process is a load N_q caused by a vertical load q located at the top of the slope.

The ground below the presupposed failure plane consists of firmer soil and the ratio of horizontal to vertical stresses, K_0 is also presumed to be constant. Hence, the in situ stress conditions are readily defined.

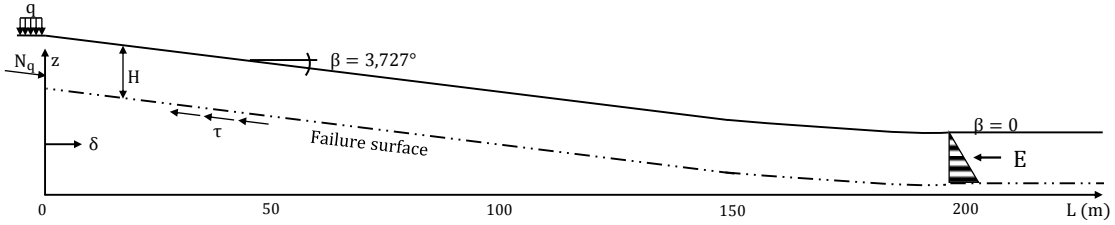

Figure 2-4. Slope submitted to the progressive failure process

The horizontal coordinate L has the value $L = 0$ where the additional load N_q is applied.
N is the earth load increment along the slope due to the additional load N_q.
The earth pressure is $E = E_0 + N$ with E_0 the in-situ earth pressure. The value of E_0 can approximately be taken as

$$E_0 = \frac{1}{2} K_0\, \rho g\, H^2 = 0{,}5 * 0{,}5 * 16 * 20^2 = 1600\ kN/m$$

Here $\rho g = 16\ kN/m^3$ is the weight of the soil.

τ_0 and τ are respectively the in-situ shear stress and the total shear stress in the failure surface along the slope.
The phenomenon of progressive failure is time-dependent. During the failure process, the parameters and conditions leading to the landslide may vary from one moment to another. The shear resistance may adopt very different values in the different phases of a slide. For this reason, progressive failure cannot be studied as a single and static event.

The process of progressive failure can be divided into five different phases illustrated by moments a-f below. .

Phase 1: The existing in situ stage; (moment a)

The additional load is $N_q = 0$. The initial in-situ shear stress along the potential failure surface is $\tau = \tau_0 = 20{,}8\ kPa$, see Figure 2-5.

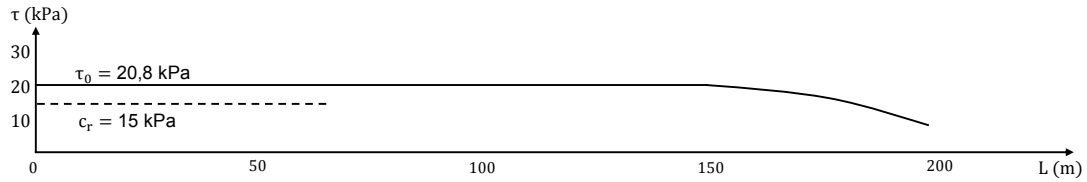

Figure 2-5. Global in situ shear stress τ_0 along the failure surface during phase 1

Phase 2: The disturbance phase, (moment b)

An additional load q generating the load N_q is placed at the top of the slope.
As a result, unbalanced upslope forces are transmitted further down-slope to more stable ground such that the resulting earth pressure distribution down the slope is $E = E_0 + N$.

After some load increment the applied load q gives τ = c = 30 kPa. The shear stresses can be integrated to the force N_q = 189 kN for an influence length L_b = 87,4 m, see Figure 2-6.

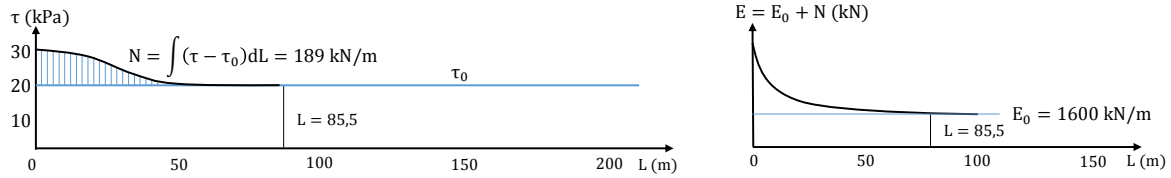

Figure 2-6. Global shear stress τ (left) and earth pressure (right) along the failure surface during moment b

End of Phase 2, start of Phase 3: The critical state, (moment c)

Further increase of the additional loading, makes the material strength decrease due to its strain-softening behavior. When the strength attains the original in situ value $\tau = \tau_0 = 20{,}8\ kPa$, all available shear resistance exceeding this value is used.
At this moment, N_q reaches its critical peak value $N_q = N_{crit} = 231\ kN/m$. (Moment c), see Figure 2-7. It corresponds to the step when the criterion for local failure and landslide initiation is fulfilled. The corresponding effective influential length is denoted $L = L_{crit} = 94{,}3\ m$ and the deformation at the point of load application is in this case $\delta_{crit} = 0{,}22\ m$.

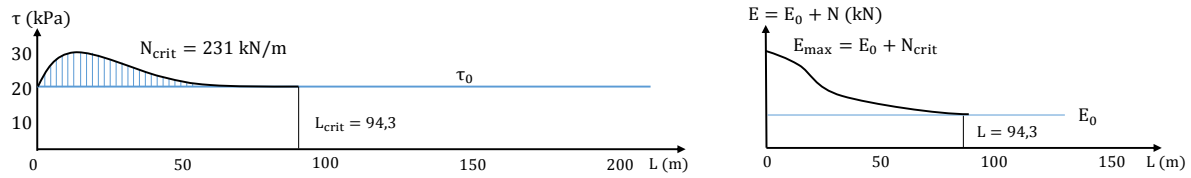

Figure 2-7. Global shear stress τ (left) and earth pressure (right) along the failure surface during moment c

Phase 3: An intermediate, virtually dynamic stage (moment d)

This is a new state of stress redistribution. Due to the failure initiation, unbalanced upslope forces are transmitted to more stable, less inclined ground further down the slope. The load that can be taken is reduced to N = 215 kN for an influence length of L_d = 99,7 m. The shear stress is reduced to its minimum value c_r= 15kPa, see Figure 2-8.

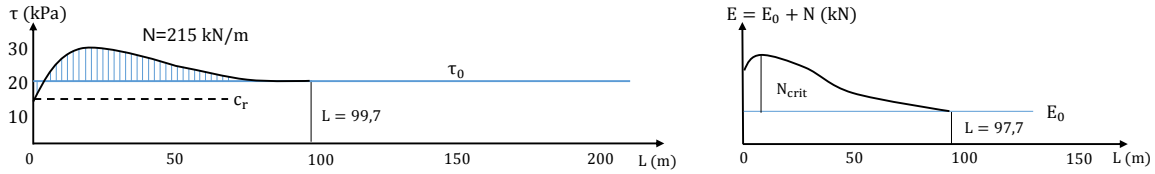

Figure 2-8. Global shear stress τ (left) and earth pressure (right) along the failure surface during moment d

End of Phase 3 (moment e):

At this state, the negative shear forces balance the positive forces so that N = 0 at the point of load application. The maximum shear force N_{instab}=231 kN has travelled downslope for a total influence length of L_{instab} = 139,6 m. The forced deformation corresponding δ_{instab} would trigger progressive failure even if N_{instab} would be removed instantly, see Figure 2-9.

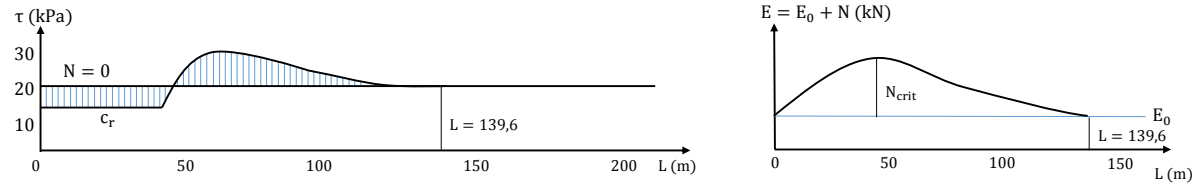

Figure 2-9. Global shear stress τ (left) and earth pressure (right) along the failure surface during moment e

Phase 4: A transitory state of equilibrium (moment f)

The shear resistance along the developing failure plane is effectively reduced. It leads to a massive earth pressure build-up further downslope in less sloping ground. This phase represents a condition, in which the earth pressure is permanently or temporarily balanced by passive resistance E_p., see Figure 2-10

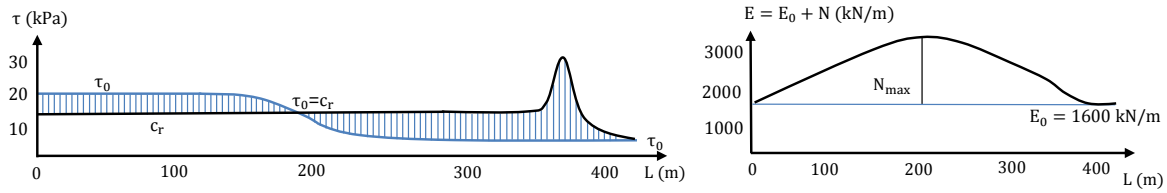

Figure 2-10. Global shear stress τ (left) and earth pressure (right) along the failure surface during moment f

The in situ shear stress τ_0 decreases from L = 150 m where the slope turns horizontal. The pressure N is caused by the weight of the sliding mass, $N = L * H * \rho * g * \sin(\beta)$. The residual shear stress c_r is reduced due to dynamic action. The pressure is "permanently" or "temporarily" balanced by passive resistance if $(E_0 + N)_{max} < E_{p,Rankine}$. The failure plane develops far into the unsloping ground before equilibrium is reached. If $(E_0 + N)_{max} > E_{p,Rankine}$ a final collapse will occur in Phase 5

Phase 5: Final collapse in passive failure

This phase is the actual slide movement

The deformation at the point of load application is illustrated by the following Figure 2-11

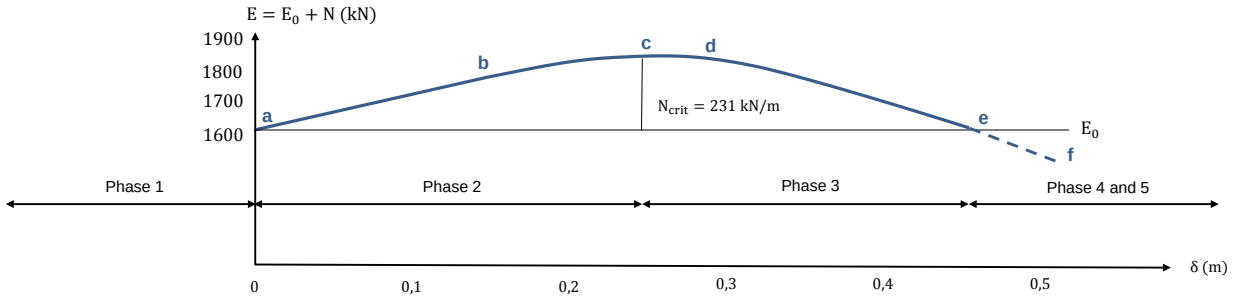

Figure 2-11. Deformation δ at L=0 during the different phases of the process

2.4. **Failure conditions**

For the process described above, Stig Bernander has defined two safety criteria:

1. The safety factor related to local failure at the end of Phase 2 is defined as:

$$F_s^{(I)} = \frac{N_{crit}}{N_q}$$

N_{crit} is the critical disturbing load and N_q is the applied local additional load.

If $F_s^{(I)} < 1$ the landslide is likely to be triggered.

In our example, $N_{crit} = 231\ kN/m$. This is then the maximum value N_q the slope may take to satisfy failure condition 1.

2. The safety factor related to global failure in Phase 4 is defined as:

$$F_s^{(II)} = \frac{E_p}{E_0 + N_{max}}$$

E_p is the passive earth resistance at failure (according to Rankine)

$E_0 + N_{max}$ is the earth pressure reached during the state of static equilibrium in phase 4 subsequent to the redistribution of earth pressures caused by the triggering load.

If $F_s^{(II)} < 1$ global failure occurs resulting in the real slide movement.

In the example above we may roughly assume that the passive earth resistance according to Rankine may be written.

$$E_p = K_0 \frac{\rho g H^2}{2} + 2cH \approx 0{,}5 * 16 * \frac{20^2}{2} + 2 * 30 * 20 = 2800\ kN/m$$

Here K_0 has been assumed to 0,5. If the slope gets flatter, e.g. at the bottom of a valley, a higher value may be used, see e.g. Bernander (2008), Appendix A, where K_0 = 1 is used.

In our example $E_0 + N_{max} = 1600 + 231 = 1731\ kN/m < E_p$ which indicates that

$F_s^{(II)} = \frac{2800}{1731} = 1{,}61 > 1$ and that no global failure will occur.

2.5. Calculation procedure

For many years (in most of the 20th century), progressive landslides investigations have been performed by using the elastic-plastic limit equilibrium method. Unfortunately, most of post slides analyses made have remained inconclusive.

The 'ideal plastic' failure analysis is based on a certain number of assumptions which are likely to question this method, especially when it comes to 'deformation softening' soils.
The basic assumptions of this method are that the soil mass is a rigid body and that the shear strength is mobilized simultaneously along the entire failure surface. This means that the conditions of deformations (within the sliding body and its surrounding environment) are neglected. This implies that the way in which the distribution of load, in situ stresses, stiffness properties and geometry affect the stress conditions in the slipping plane cannot be taken into account. Also, the 5 different phases of progressive failure can neither be identified nor accounted for.

For this reason, Stig Bernander developed an alternative method of analysis.
The aim in performing a downhill progressive landslide analysis is to learn if a slope is stable or not.
Hence, the calculation procedure has to provide us with the critical parameters N_{crit}, L_{crit} and δ_{crit} related to the triggering of progressive failure. These parameters are related to the critical

additional load the slope can support without failing. It actually corresponds to the end of phase 2 described in part 2.3.
The calculation can also provide L_{instab} and δ_{instab}, related to the situation, in which a forced deformation would trigger slope failure, even if the agent causing the deformation would be removed instantly.
The final goal of the calculation is to get the safety factors for local and global failure initiation.

Of course, the development of deformations due to additional stress depends on the stress-strain relationship of the soil studied. Clay tends to have a softening post-peak behavior. For this reason the calculation process is divided in two different stages:

Stage I: After an elastic phase with shear strength up to the linear limit, a plastic phase begins and the peak value *c* is reached. This last event corresponds to the beginning of the formation of the slip surface.

Stage II: A decline in strength occurs until only the residual strength remains and the slope finally collapses.

Calculations cannot be based on effective stress seepage analysis in the context of the fast development of progressive failure in deformation-softening soils, because in this case total stress conditions apply. During the rapid stress changes in the different phases of progressive failure, the water content of the soil is trapped in the pore system, and there is no time for water to seep away.

As concerns the stress-strain/deformation relationship, a linear dependence up to the elastic limit, τ_{el} is used. It is followed by a 2nd power parabolic law until the peak c is reached. In stage II, the strength is reduced according to a linear dependence set as a function of δ_s corresponding to the slip in the failure plane. After the point of residual strength, a slip deformation δ_{slip} is added, see Figure 2-12..

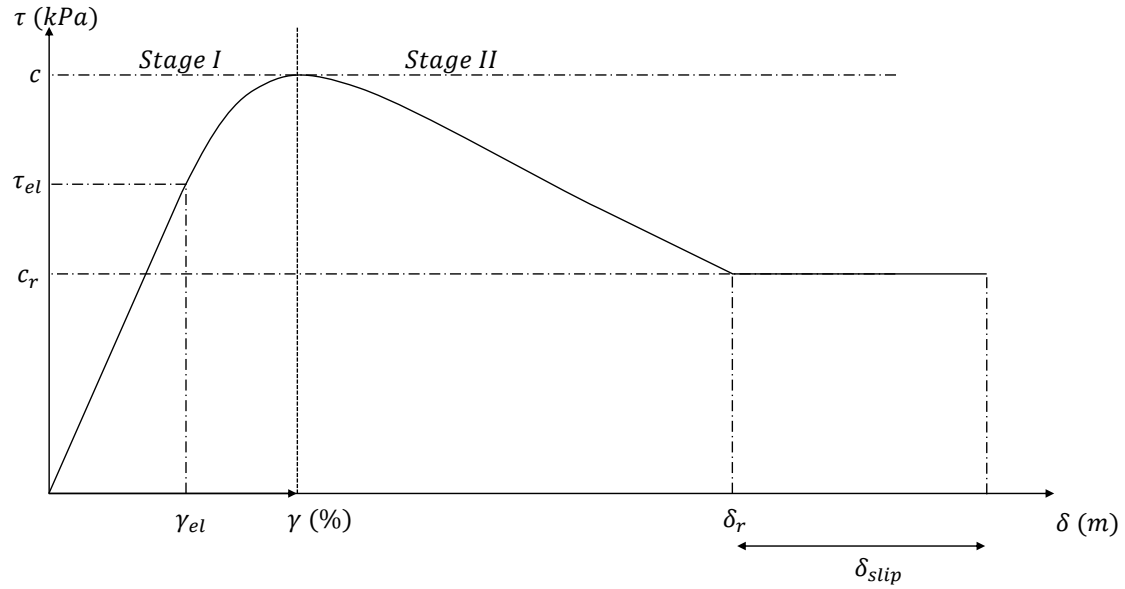

Figure 2-12. Stress-strain/deformation used by Bernander to carry out his downhill progressive failure analysis

To calculate the wanted parameters, a 2D finite difference method (FDM) is used. This is basically a stepwise process. The soil volume is divided into vertical elements of length Δx and each vertical slice is subdivided into rectangular elements of height Δz.

The location of the earth pressure resultant is set at the height of $z = \alpha H$.
α being equals to $\frac{1}{3}$ in this example.
The reason for doing so is that most of the shear deformations has taken place for z $\approx \frac{H}{3}$ in occurred slides, see Figure 2-15.

Stage I:

The calculation begins by determining the in-situ stress τ_0 at point $x = x_0 = 0$.

At this position, which corresponds to the lower boundary condition, the shear stress and the deformation due to the additional load N_q are respectively $N(x_0) = 0$ and $\delta_N(x_0) = 0$

As the additional load has no effect at this point, the total shear stress is equal to the in-situ shear stress $\tau(x_0) = \tau_0$

The formula for the in-situ shear stress is set as being:

$$\tau_0(x, 0) = \sum_0^{H(x)} \rho(x) * g * \Delta z * sin\beta(x)$$

Once the parameters at the lower boundary are calculated, we choose a first shear increment $\Delta\tau_{x_0 \to x_1}$ such that $\tau(x_1) = \tau(x_0) + \Delta\tau_{x_0 \to x_1}$

Thanks to the stress-strain relationship of the material considered, we determine $\gamma(x_1, z)$ the strain at position $x = x_1$ and vertical coordinate z. The shear deformation $\gamma(x, z)$ is defined with an equation in diagram in Figure 2-13 and given in full in Appendix A.

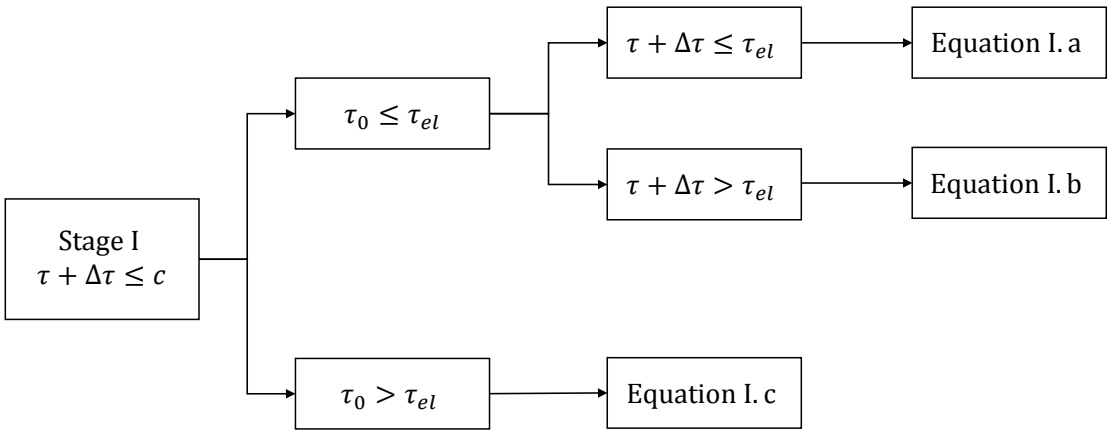

Figure 2-13. Diagram of conditions giving equations to determine $\gamma(x, z)$ during stage I. The different equations are given in Appendix A.

By integrating $\gamma(x_1, z)$ from $z = 0$ to $z = \alpha H_{x_0 \to x_1}$, we get $\delta_\tau(x_1)$, the deformation in section x_1 caused by the shear stress above the slip surface.

Then we calculate $\Delta N_{x_0 \to x_1}$ and $\delta_N(x_1)$ the deformation in section $x = x_1$ caused by the additional loading:

$$\Delta N_{x_0 \to x_1} = \left(\frac{\tau(x_0) + \tau(x_1)}{2} - \frac{\tau_0(x_0) + \tau_0(x_1)}{2} \right) * \Delta x_{0 \to 1}$$

$$\delta_N(x_1) = \frac{N(x_0) + N(x_1)}{2} * \frac{\Delta x_{0 \to 1}}{E_{el} * H_{x_0 \to x_1}}$$

Finally, we determine the unknown $\Delta x_{0 \to 1}$ corresponding to the $\Delta \tau_{x_0 \to x_1}$ stated by solving the following equation:

$$\sum_{x_0}^{x_1} \Delta \delta_N(x_i) = \delta_\tau(x_1)$$

This equation called 'compatibility criterion' means that the total mean down slope displacement δ_N to which a vertical element is subjected must be compatible with the shear deformation of the same elements relative to the ground below the slip surface, see Figure 2-15..

This process is repeated in every step $i \to i + 1$ until the shear stress reaches the maximal strength c and thus the slip surface forms.

The condition for completion of stage I is $\tau + \Delta\tau = c$

Stage II:

During the second part of the process, the slope is unloaded, i.e. the shear stress is decreased. For every step, a negative value for $\Delta \tau_{x_i \to x_{i+1}}$ is added.
To determine all the $\gamma(x_i, z)$ during this phase, the equations illustrated in Figure 2-14 are applied:

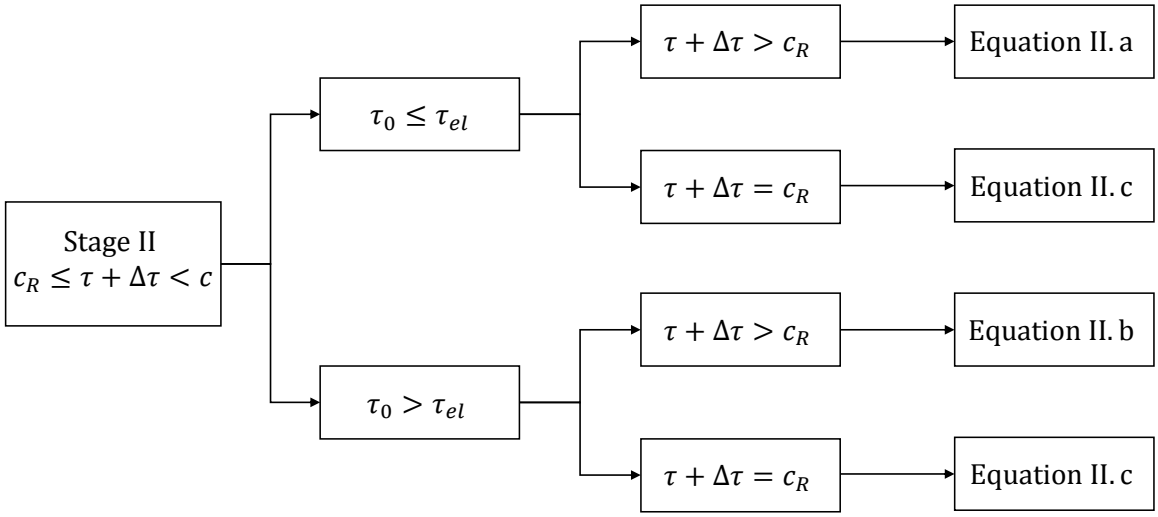

Figure 2-14. Diagram of conditions giving equations to determine $\gamma(x,z)$ during stage II. The different equations are given in Appendix A.

During stage II, the compatibility criterion is still applied. Nevertheless the equation differs a little because we now have a slip deformation in the failure plane.

$$\sum_{x_0}^{x_n} \Delta\delta_N(x_i) = \delta_\tau(x_n) + \delta_s(x_n)$$

δ_s is defined as the slip in the failure plane as being:

$$\delta_s(x) = \delta_{cr} \cdot \frac{c - \tau(x)}{c - c_r}$$

where δ_{cr} is the slip at which the residual strength c_r is reached.

For each calculation step upslope, the deformations are added and the procedure continues until the stress becomes equal to the in situ stress again $\tau + \Delta\tau = \tau_0$. At that point, all the additional bearing capacity is used and the maximum pressure value is reached. The critical load parameters N_{crit}, L_{crit} and δ_{crit} are then determined. The analysis of the progressive failure initiation is completed.

Then we keep on decreasing the global shear stress until we get $\tau + \Delta\tau = c_r$. Finally, we continue the iterative process until the value of N is equal to 0. This corresponds to the situation in which a forced deformation δ_{instab} would trigger slope failure, even if the agent causing the deformation would be removed instantly.

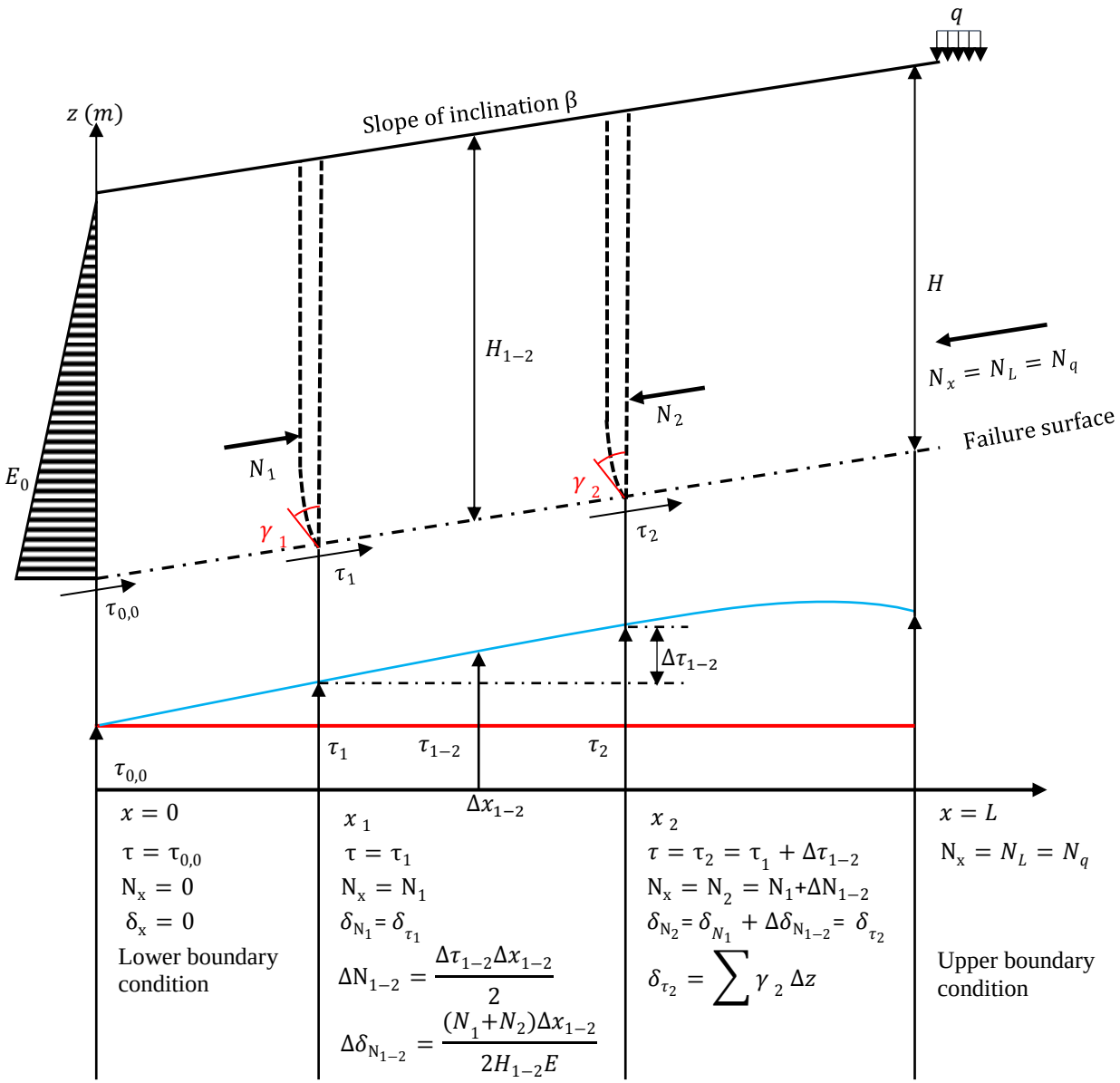

Figure 2-15. Illustration of the finite difference calculation.. Please observe that the load q' here is applied to the right and not to the left as in Figures 2-2 to 2-10.

3. Muskrat Falls Project

3.1. Background

Muskrat falls is a natural site composed of two waterfalls on the Lower Churchill River, in Labrador, Canada. This site, which represents a high hydro power potential, will host a dam, a spillway, and a powerhouse with four turbines and a total generating capacity of 824 MW. Nalcor Energy is the company responsible for the construction of the installation which began in 2013, see Figures 3-1 and 3-2.

Figure 3-1. Photo of Muskrat Falls by the contractor SNC-Lavalin (2017).

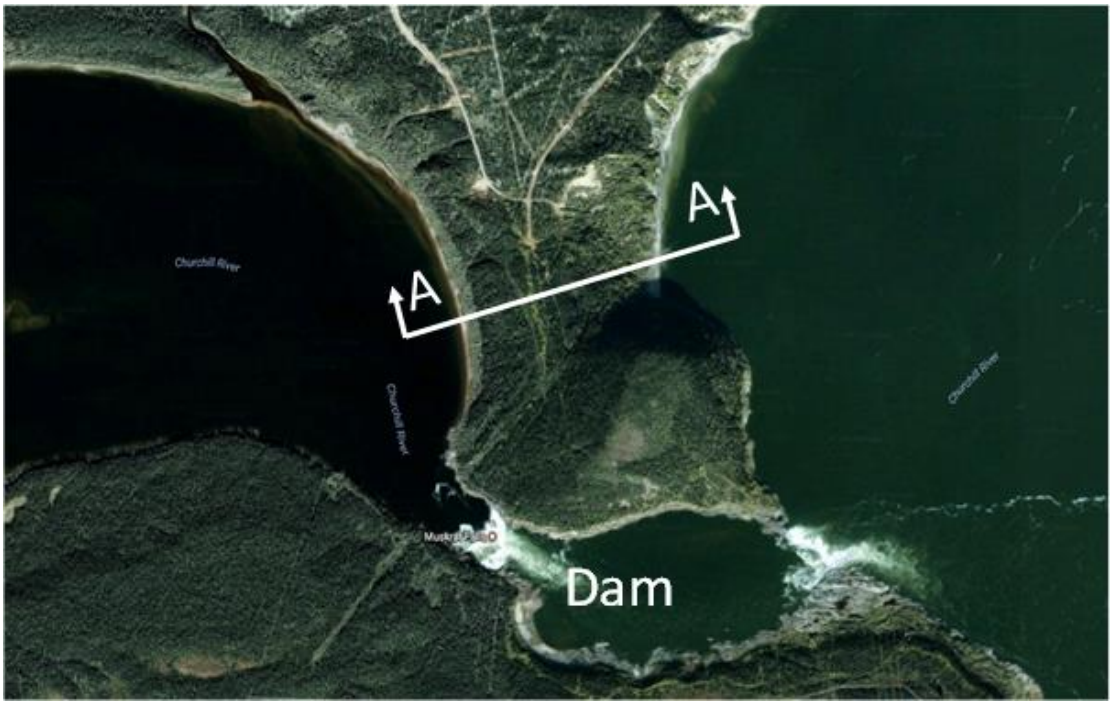

Figure 3-2. Satellite view of the North Spur including position of the future dam and section A-A

The North Spur on which the concrete dam is embanked is a post glacial deposit of marine and estuarine sediments which provide a partial closure of the Churchill River Valley at the Muskrat Falls site. It is about 1 km long between the Rock Knoll in the south and the Kettle Lakes in the north which represent natural boundaries. It has the following section, see Figure 3-3:

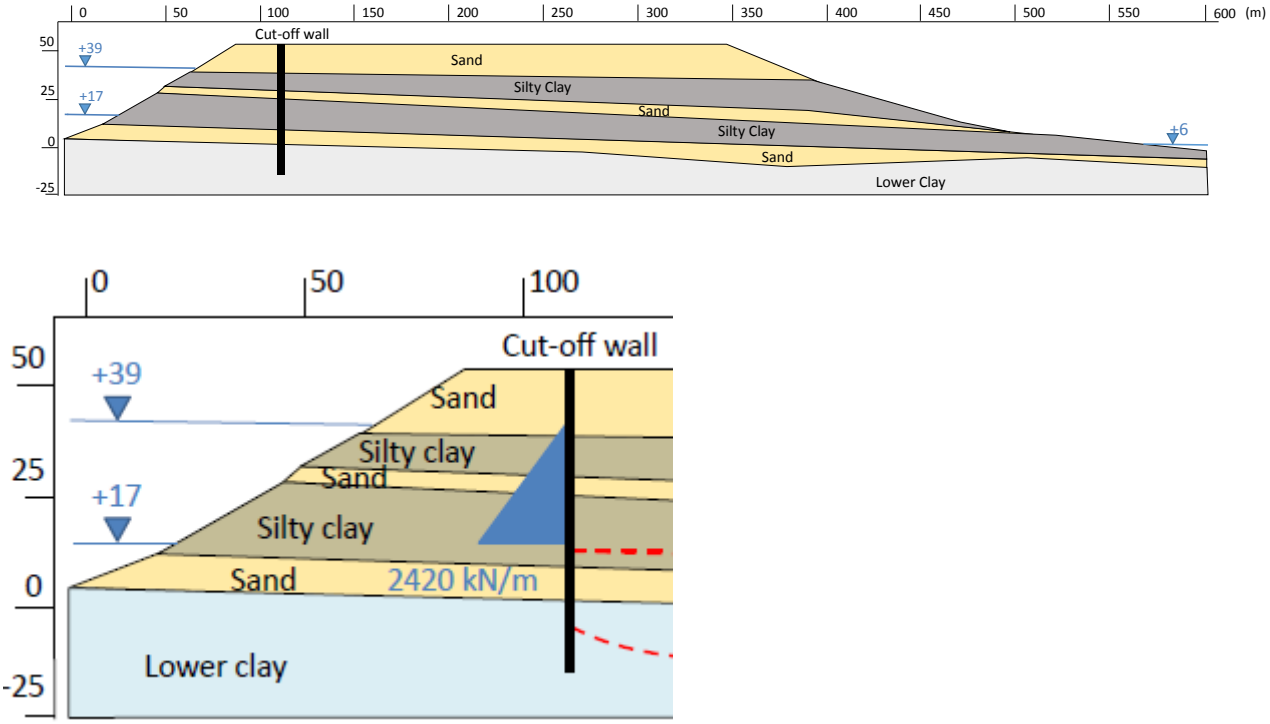

Figure 3-3. Section A-A of the North Spur above and detail below.

As one can see.in Figures 3.2 and 3-3, the North Spur is a natural dam consisting in a succession of soil layers. Among them, there are three different layers containing clay: Upper silty clay (1), Upper silty clay (2) and Lower clay (3).

The hydroelectric project could affect the integrity of the North Spur. The water level on the upstream shore will increase from 17 to 39 meters when the reservoir will be full. It will decrease on the downstream shore from 6,9 to 3 meters according to SNC-Lavallin Inc., Leahy (2015), Leahy et al.(2017)..

This huge amount of water contained in the reservoir will represents an important force applied on the spur which could trigger progressive failure.

A major slide on the downstream part of the Spur, in November 1978 (#2 on Figure 3.4) involved liquefaction of the stratified drift over a long lateral distance. This event has already revealed the fragility of this natural deposit. Some other minor slides which occurred upstream (#5, 6, 7, 8 on Figure 3.4) have confirmed this concern.

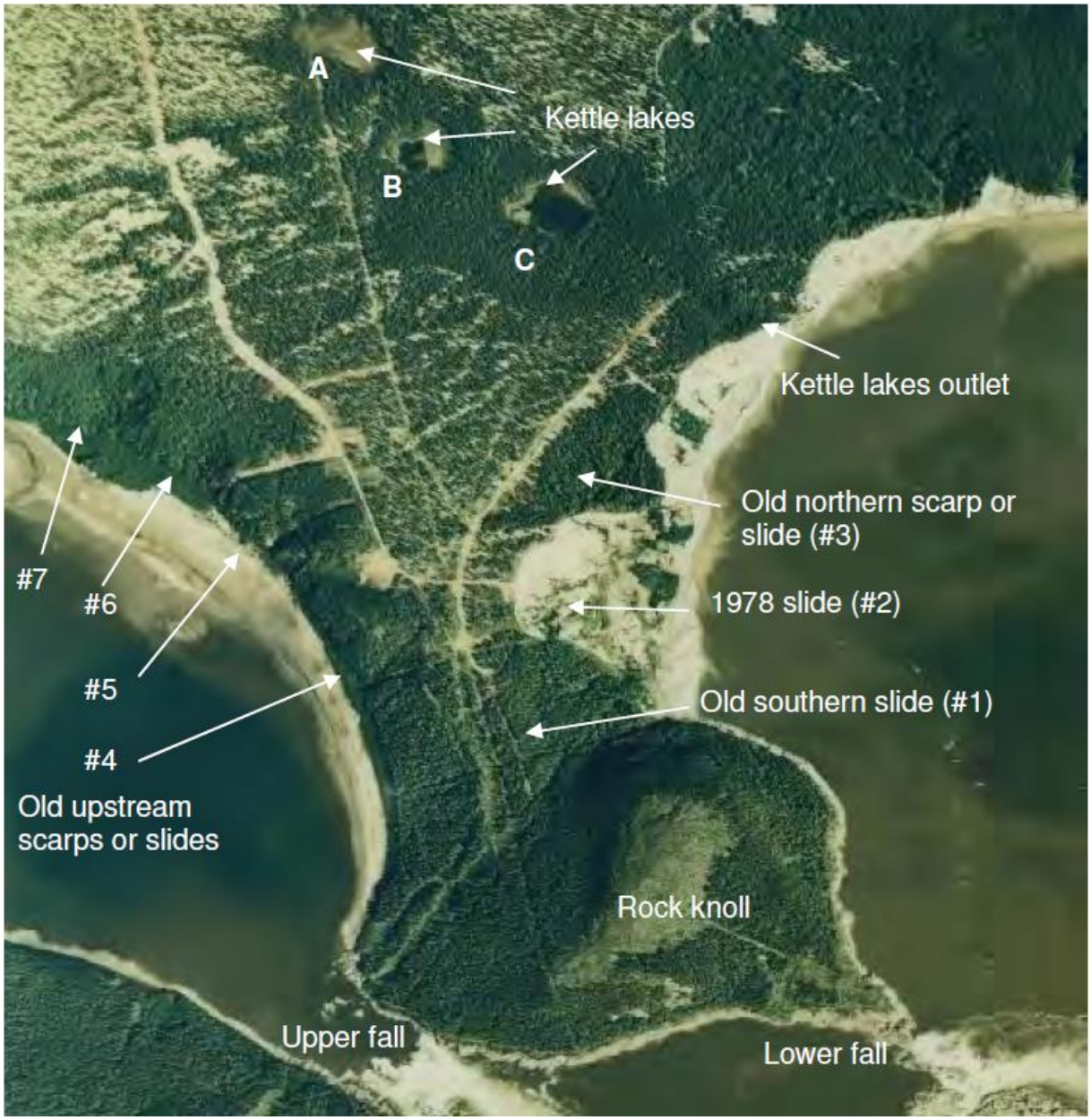

Figure 3-4. Aerial photo of the North Spur (1988). SNC-Lavalin Inc, Leahy.(2015)

3.2. **Material properties**

In the process of assessing the stability of the North Spur, the Muskrat Falls project team has provided some information about the material properties of the North Spur. The three different layers containing clay notified in Figure 3-3 are particularly interesting to study.

3.2.1. **Upper Clay Layers**

According to Nalcor, the upper silty clay layers (1) and (2) belong to the Stratified Drift, which is referred to as a 'heterogeneous mix of clays, silts and sands', Leahy (2015).Their properties are given in Table 3-1.

Table 3-1. Summary of the properties of the upper silty layers, Leahy (2015).

Property	General Range	Average	Number of tests
Percent finer than 2 microns	35 – 45	_	19
Water content, w %	17 – 43	31	199
Liquid limit, LL %	17 – 43	30	168
Plastic limit, PL %	13 – 32	19	168
Plasticity Index, PI %	2 – 22	11	168
Liquidity Index, LI	0.6 – 2.8	1.3	168
Intact Undrained shear strength, S_u kPa	35 – 135	_	_
Remoulded Undrained shear strength, S_u kPa	60 – 2	_	_
Sensitivity, in-situ, S_t	1 – 36	10	43
Large strain friction angle, ϕ'_{cv} º	30 – 32	_	_
Effective cohesion, c', kPa	0 – 10	_	_
Unit weight, γ kN/m^3	18.4 – 19.7	_	11
Initial void ratio, e_0	0.93 – 1.06	_	_
Compression index, c_c	0.32 – 0.5	_	_
Recompression index, c_r	0.03 – 0.06	_	_
Hydraulic Conductivity, k, m/s	10^{-7} – 10^{-9}	_	_
Salt content, g/l	0.8 – 1.5	_	_

On the basis of these data, Bernander (2015) noted concerning the upper silty clays : 'the water content for all of the soils type, including the average value, exceeds the Liquid Limit, a condition which in Soil Mechanics is indicative of high sensitivity.'

3.2.2. **Lower Clay Layer**

The Lower Clay Layer is located between the stratified drift and lower aquifer.
Table 3-2 is a summary of the properties of this layer:

Table 3-2. Summary of the properties of the Lower Clay Layer, Leahy (2015).

Property	General Range	Average	Number of tests
Percent finer than 2 microns	15 – 35		
Water content, w %	17 – 45	29	201
Liquid limit, LL %	22 – 48	37	123
Plastic limit, PL %	13 – 27	21	123
Plasticity Index, PI %	7 – 25	16	123
Liquidity Index, LI	0.1 – 2	0.6	123
Intact Undrained shear strength, S_u, kPa	53 – 200	_	_
Remoulded Undrained shear strength, S_u, kPa	8 – 96	_	_
Sensitivity in-situ, s_t	2 – 11	4	35
Large strain friction angle, ϕ'_{cv} º	33	_	_
Effective cohesion, c', kPa	6	_	_
Salt content, g/l	8 – 22	_	8
Unit weight, γ , kN/m^3	19.2 – 19.5	_	3
Hydraulic Conductivity, k, m/s	10^{-7} – 10^{-9}	_	_

Although a reassuring average value smaller than 1, the values of liquidity index vary widely between 0.1 and 2.0. It may indicate the presence of sensitive material and the possibility of developing a progressive failure. (i.e. those in excess 1,0)

3.3. **Prevention measures**

3.3.1. **Stability analysis**

Nalcor has performed its own stability analysis by using the traditional limit equilibrium method. The main issue is that this procedure is not justifiable for soils having such a high porosity. In fact, high porous materials have a 'deformation softening' behavior far from the perfect elastic plastic behavior assumed with the LEM. Thus, the analysis and safety factors calculated by Nalcor cannot be reliable.

Besides, the failure analysis shown in the Nalcor report by Leahy (2015) shows an analysis assuming a circular slip surface extending over 200 meters. The studies carried by Bernander during his post slides investigations in Scandinavia have clearly shown that as soon as the length of a potential landslide exceeds 50–80 meters, safety factors based on LEM tend to become seriously unreliable.

Finally, Leahy (2015) and Leahy et al.(2017) have only carried out an analysis considering a horizontal failure plane, exempting inclined surfaces. This is not sufficient due to the fact that

failure planes do not always propagate horizontally. In fact, progressive landslides initiation is typically triggered by locally steep failure surfaces in the initiation zone.

3.3.2. **Stabilization works**

Some stabilization works have been performed along the slopes of the spur to try to prevent any type of slope failure. According to SNC-Lavalin Inc, Leahy (2015) and Leahy et al. (2017), the objectives are numerous.

First, water drainage controls have to be set up by using cut-off walls, see Figure 3-7, to stop seepage and drainage systems to remove water from the dam area.

The stability has to be directly enhanced. The idea is to reduce slopes and to remove high sensitive clay on the upstream and downstream sides of the Spur.

Finally a preventive action has to be taken to avoid erosion at the upstream and downstream shorelines.

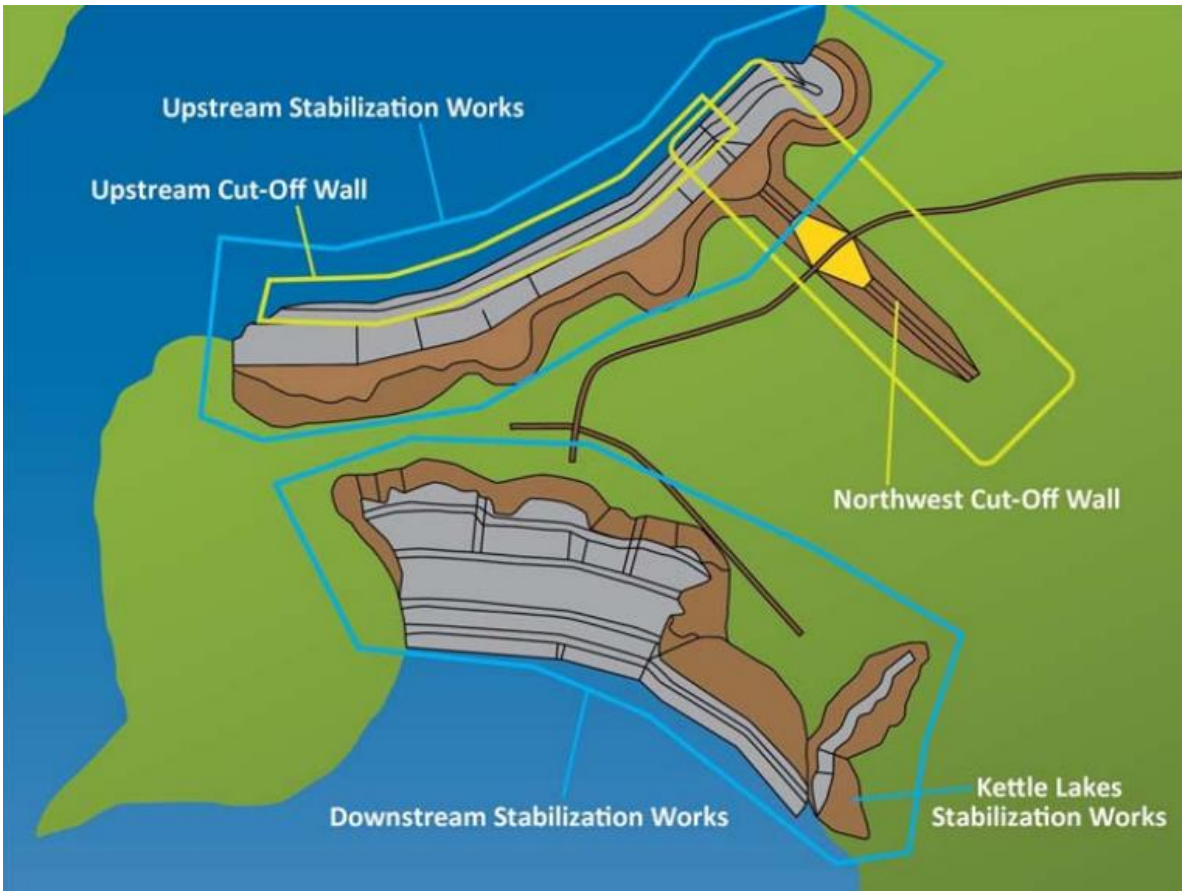

Figure 3-5. Sketch of the North Spur showing the different stabilization works driven by Nalcor to enhance the Spur stability. SNC-Lavalin Inc., Leahy.(2015).

4. Software development

In order to perform a progressive failure analysis and to assess the North Spur stability using the approach by Stig Bernander, a spreadsheet has been developed in the scope of this thesis.

4.1. Features

The software developed during this thesis work is an Excel spreadsheet allowing every geotechnical engineer or consultant to assess quickly downhill progressive failures
.
The user has simply to enter into the spreadsheet the geometric and mechanics parameters of the slope and the value of the triggering load. Then, the software calculates automatically $N_{crit}, \delta_{crit}, L_{crit}, \delta_{instab}, L_{instab}$ and the safety factor for local failure.

It also provides different charts, showing the shear stress along the slope for two different cases of loading:

- The moment c, when the slope is submitted to the critical load (cf .2.3).
- The moment e, when the slope is submitted to a forced deformation triggering landslide failure.

The spreadsheet allows you to deal with two different slope geometries.
First, it permits to model a really simple slope with constant depth and gradient, see Figure 4-1 below.

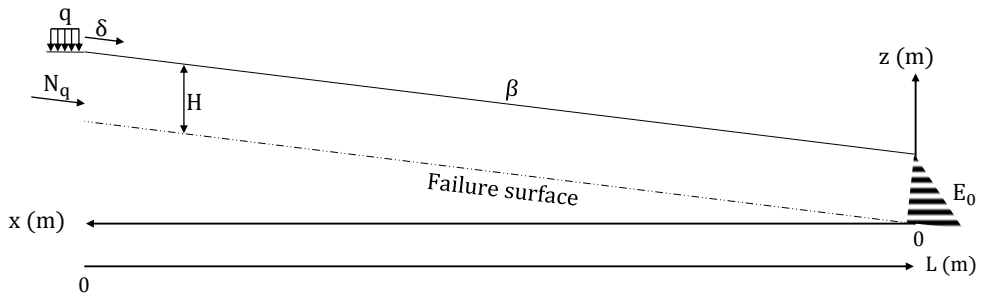

Figure 4-1. First slope configuration processed by the spreadsheet

Second, as this specific spreadsheet was firstly developed to investigate the problem encountered with the Muskrat Falls project, the spreadsheet allows to deal with the following conditions, see Figure 4-2.

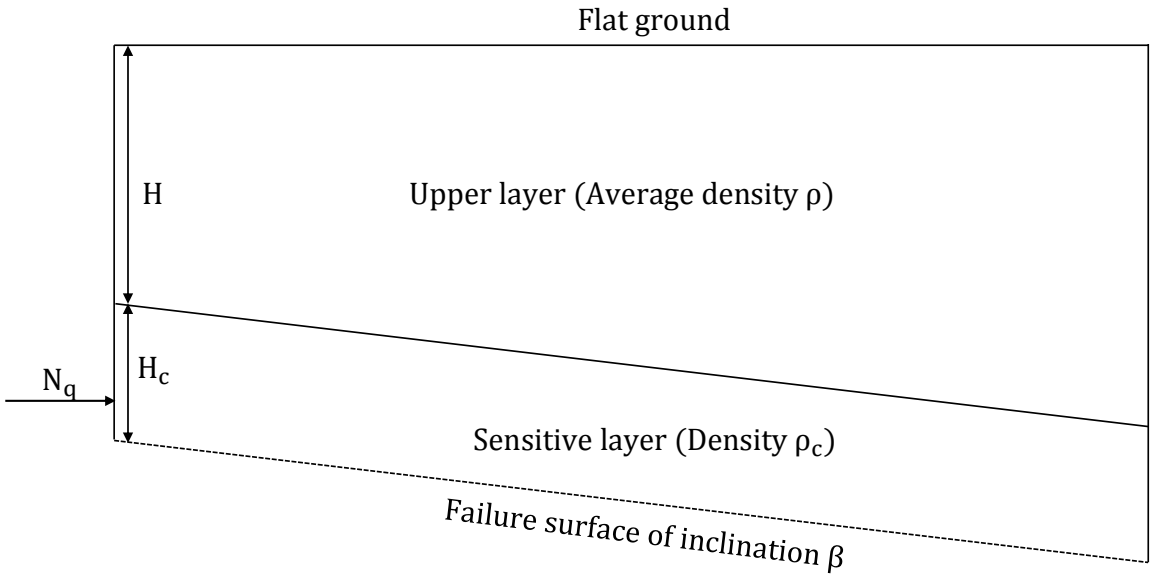

Figure 4-2. Second slope configuration processed by the spreadsheet

The layer above the 'sensitive layer' is considered as only one layer with an average density, even if it is in reality made of several layers.

The user can vary a separate parameter by giving it an increment. The software then calculates quickly and automatically all the safety factors corresponding to these parameters. For example, if one wants to study the impact of the inclination of the failure plane, one can vary β from 0 to 5° with an increment of 0,1°. Then one just needs to press 'run the calculation' and all the corresponding safety factors are displayed.

4.2. **How it works**

The calculation process is divided in two stages.

During the first stage, the shear stress τ is increased automatically ten times such that the value of the increment $\Delta\tau$ gets smaller and smaller until the peak shear strength is reached.

During the second stage, the shear stress is decreased linearly five times. It is decreased from the peak shear strength c to the in-situ shear stress τ_0. These steps permit getting the critical parameters.

Then, the shear stress is decreased till the residual strength of the clay c_R.

Finally, the instability parameters are directly calculated on the basis of the previous step by reducing the additional load effect to $N = 0$.

All along the process, the in-situ stress is calculated with the geometric and mechanics input entered by the user. The shear deformation corresponding on the stress level is automatically calculated on the basis of the mechanical in-put and equations given in Figures 2-13 and 2-13 and in Appendix A.

The ground surface is considered here to be flat. Nevertheless the user, can give the values he wants to the geometric parameters H_c defining the depth of the clay layer -H defining the depth of the upper layer and β defining the inclination of failure plane.

It is considered that the in situ shear stress is modeled by the equation (Bernander, 2017), compare with Fig. 5-1:

$$\tau_0 = H_c * \rho_c * \sin\beta \cos\beta + H * \rho * \sin\beta \cos\beta - \frac{\Delta E_0}{\Delta x}$$

Here, ΔE_0 denotes the passive earth pressure resistance caused by the depth difference between two consecutive slices of the upper layer defined such that:

$$\Delta E_0 = K_p * \rho * (\frac{H_{x_{i+1}}^2 - H_{x_i}^2}{2})$$

The depth partitioning of the slope from the slip surface ($z = 0$) to the level at which the down-slope displacement is considered to be valid ($z = \alpha H_x$) is arbitrary divided in 7 equal parts.

The analysis is automatically made thanks to a macro. For each step, the equation corresponding to the compatibility criterion is solved with the solver function of Excel.

4.3. **Accuracy**

The procedure used is slightly revised in comparison to the one used by Bernander (2000, 2008 and 2011) in accordance with a MSc thesis by Liw Rehnström (2013). The principal difference likely to affect the outcome is the partitioning of the slope. This is by Bernander done manually by regulation of the shear stress addition, Δτ. In the version used here, the number of calculation steps has been fixed and the intervals for the shear stress are regulated in order to divide the spacing so that the length distance decreases closer to the peak value. As it is a finite difference problem, the number of intervals and partitioning can have an impact on the results.

To approve the accuracy of this spreadsheet, some comparisons have been carried with the results got by Stig Bernander with his own manual spreadsheet.

Results for a slope with a constant gradient:

Table 4-1 Comparison between the results obtained with the manual sheet developed by Dr. Bernander and the new spreadsheet developed by Robin Dury in this project.

	Previous sheet by Dr. Bernander	New sheet by Robin Dury	Difference (%)
L_{crit}	92,08	92,59	0,55
δ_{crit}	0,21	0,22	5,24
N_{crit}	221,9	231,05	3,96

5. Slope analysis for North Spur Ridge

In this chapter, some slope analyses with two models based on the elastic plastic theory are first presented. We used both a basic simplified limit equilibrium method and a finite element model.

Second, several analyses with the finite difference method developed by Stig Bernander are presented.

5.1. Traditional calculation

5.1.1. LEM hand calculation

A basic hand calculation has first been carried to have a rough idea of the factor of safety obtained with a very basic LEM assuming a failure surface appearing in the upper clay layer (2).

The infinite slope analysis has been used.

The different assumptions allowing applying this method are the following (Axelsson & Mattsson, 2016):

- Translational failure along a single failure plane with failure surface parallel to slope surface.
- Ground water table parallel to slope surface
- Ratio of depth to failure surface to length of failure zone is small (<10%)
- Applies to surface raveling in granular materials or slab slides in cohesive materials

The geometry assumed is the following, see Figure 5-1.:

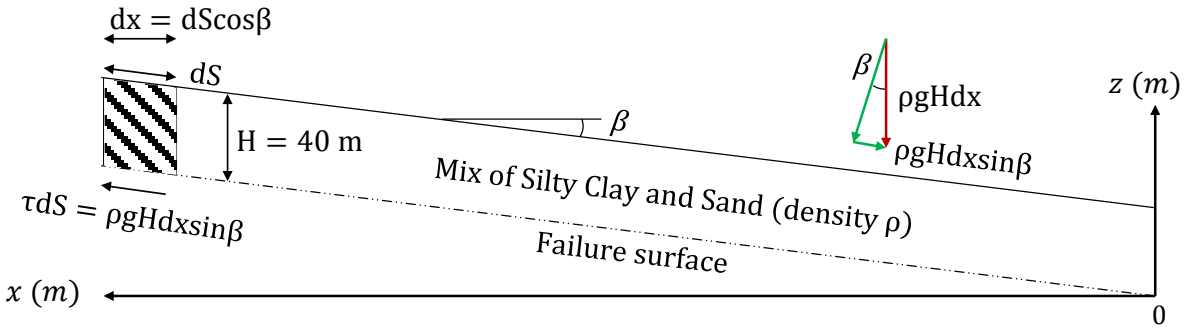

Figure 5-1. Geometric simplification of the slope

The calculation of the safety factor relies on the following principle:

$$F_s = \frac{available\ shear\ strength\ of\ the\ soil\ (c_u)}{equilibrium\ shear\ stress\ (\tau_0)}$$

with: $\tau_0 = \rho g H sin\beta cos\beta$

If we deal with total shear stresses, the safety factor is given by the following formula:

$$F_s = \frac{c_u}{\tau_0}$$

Assuming an undrained shear strength $c_u = 60\ kPa$, a volume weight $\rho g = 18\ kN/m^3$ and a depth $H = 40\ m$, one have the following results:

Table 5-1. Factors of safety obtained for different slope and failure plane inclination β

$\beta(\%)$	1	2	3	4	5	6	7	8	9	10
$\beta(degrees)$	0,573	1,146	1,718	2,291	2,862	3,434	4,004	4,574	5,142	5,711
$\tau_0\ (kPa)$	7,20	14,39	21,58	28,75	35,91	43,05	50,15	57,23	64,28	71,29
F_s	8,33	4,2	2,8	2,1	1,7	1,4	1,2	1	0,9	0,8

According to this basic calculation, no slide should occur in the upper clay layer (2) assuming a slope with a failure plane having an inclination less than 7%.

Nonetheless, the geometry of the spur is according to this model extremely simplified and inaccurate.

5.1.2. **Plaxis 2D calculation**

To get more reliable results, we used Plaxis 2D 2017 which is a finite element software for soil and rock analysis.
This computer program is applicable to many geotechnical problems, including stability analyses and steady-state groundwater flow calculations.

Material properties including shear strength parameters were defined for each soil layer according to the Nalcor report, Leahy (2015):

Table 5-2. Mechanical parameters used to model the North Spur (table 6-1 and 7-2 of the report SNC-Lavallin Inc., Leahy (2015))

Material	**Total unit weight**	**Porosity**	**Cohesion**	**Internal friction angle**	**Poisson's Ratio**	**Young Modulus**
	$\gamma(\frac{kN}{m^3})$	n	$c'(kPa)$	$\varphi'(\circ)$	υ	$E\ (kPa)$
Upper Sand	19	0,36	0	35	0,334	400
Intermediate Sand	19,5	0,41	0	35	0,334	600
Upper Clay	18,5	0,48	6	31	0,334	300
Lower Clay	18,5	0,48	6	31	0,334	500

An accurate geometry of the North Spur with the cut-off wall has been defined as on the following Figure 5-2:

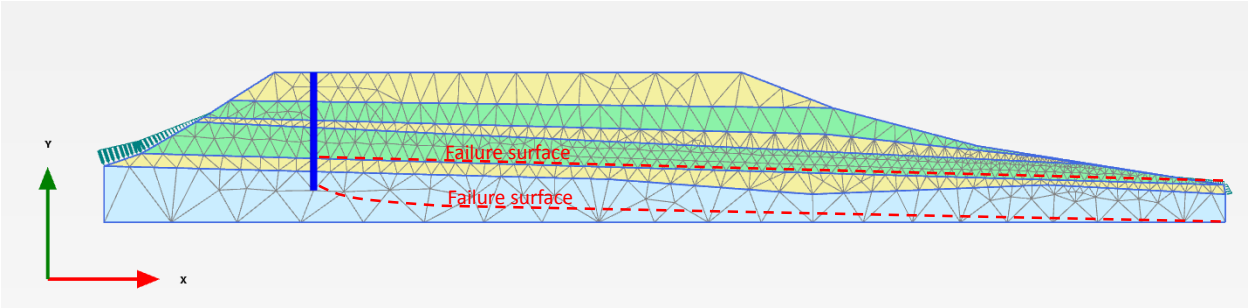

Figure 5-2. Geometry of the slope modeled in PLAXIS 2D

We investigated both failure surfaces represented on Figure 5.2. The first one, located in the second silty clay layer has a constant inclination of 4%. The second one, located in the lower clay layer has a curvy shape close to the cut-off wall and then a constant inclination of 4%

A plain strain model of 15 noded triangular elements was used to generate the finite element mesh. Pore pressure distributions were generated based on the steady-state groundwater calculation. Moreover, a Mohr-Coulomb material model based on the elastic-perfectly plastic theory of soil mechanics is selected for the stability analysis. Accordingly, both elastic parameters (E, ν) and plastic parameters (c', φ') are used in the model.

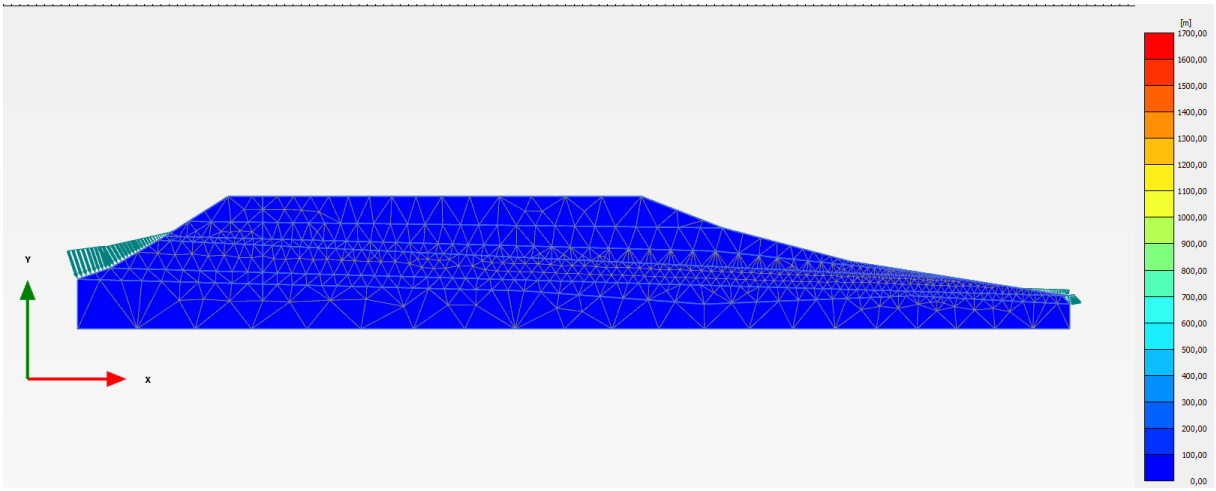

Figure 5-3. Incremental deformation within the North Spur

The safety factor is computed by using the 'c-φ reduction' procedure. (Aryal, 2006) The strength parameters are automatically reduced until the final calculation step results in a fully developed failure mechanism. In this way, PLAXIS computes the FOS as the ratio of the available shear strength to the strength at failure by summing up the incremental multiplier (M_{sf}) as defined by:

$$F_s = \frac{available\ shear\ strength}{shear\ stress\ at\ failure} = value \sum M_{sf}\ at\ failure$$

For both of the failure surfaces studied, the safety factors obtained are respectively equals to 1,45 for the silty clay layer and 1,35 for the lower clay layer.

As expected, and as Nalcor has already shown, the LEM do not show any risk of failure whatever the accuracy of the model used.
However, the method used does not take into account the fact that clay has a strain softening behavior. Besides, the deformations within and outside the sliding body are neglected.

5.2. **Bernander's method for investigation in upper clay**

A first analysis is carried with fixed parameters. The calculation is explained step by step from the choice of the parameters till the result in order to illustrate the theory previously explained and to make it easy to understand..

Then, some results are presented for a number of different parameters.

5.2.1. **Geometry**

The failure plane assumed for this calculation is located at an altitude $z = 17\ m$. It corresponds to the initial level of water in the reservoir (Figure 5-4).

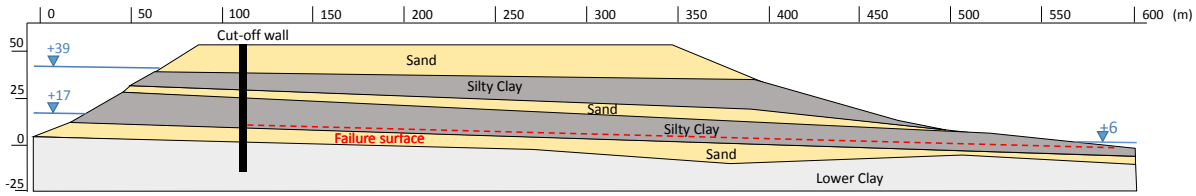

Figure 5-4. Section of the North Spur and location of the assumed failure plane

Regarding the section of the North Spur, one can observe that the upper contour of the layer considered drops about 16 meters along the length coordinate x ≈ 100 m to x ≈ 500 m. This is an inclination of about 4%.
We assume that if a failure surface appears in this layer, it is likely to be parallel to this plane. So, for this first calculation, we will take an inclination of 4% for the failure plane.

At the upstream edge of the spur (directly after the cut off wall), the thickness of ground above the clay layer studied is 28 meters. The thickness of the clay layer above the failure plane is 15 meters. The water level is considered as maximal in front of the cut-off wall (39 meters when the reservoir is full). The cut-off wall makes it drop. To simplify the calculation it is considered as being under the failure surface.

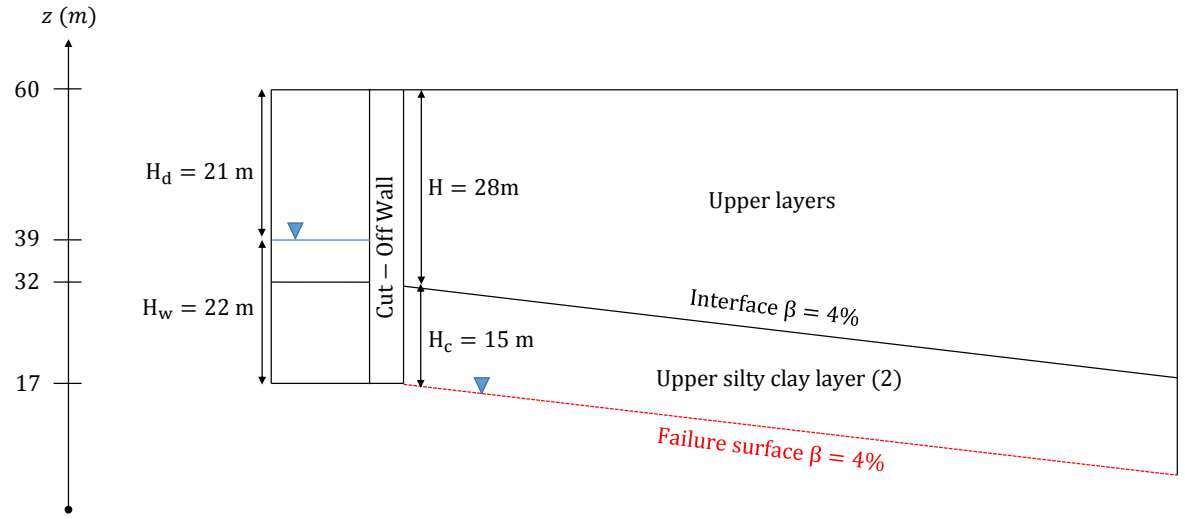

Figure 5-5. Geometric simplification of the problem studied

5.2.1. **Triggering agent**

In Muskrat Falls Project, the triggering agent might be the water pressure which will increase because of the water level being raised from $z = 17\ m$ to $z = 39\ m$.

We will first only consider the influence of the increased water level giving:

$$N_q = 0.5 * \gamma_w H_d^2 = 2420\ kN/m$$

5.2.2. **Mechanical properties**

The mechanical properties chosen for the analysis are summarized in the Table 5-3. For all the following calculations, the strength parameters used are chosen considering that the slope is un-drained. The value of Poisson ratio and of the volume masses are based on Nalcor report, Leahy (2015).

Table 5-3. Mechanical parameters of the slope studied

Poisson ratio	**Peak shear strength**	**Deviator strain at failure limit**	**Residual shear strength**	**Shear strength at interface**	**Sensitivity ratio**	
ν	$c_u\ (kN/m^2)$	$\gamma_f\ (\%)$	$c_R\ (kN/m^2)$	$c_s\ (kN/m^2)$	c_R/c	
0,334	*60*	*0,07*	*12*	*45*	*0,2*	
Shear stress at elastic limit	**Deviator strain at elastic limit**	**Secant modulus in shear**	**Elastic modulus**	**Slip for residual shear strength**	**Volume weight upper layer**	**Volume weight clay layer**
$\tau_{el}\ (kN/m^2)$	$\gamma_{el}\ (\%)$	$G\ (kN/m^2)$	$E_{mean}\ (kN/m^2)$	$\delta_{cr}\ (m)$	$\rho\ (kN/m^2)$	$\rho_c\ (kN/m^2)$
40	*0,035*	*1143*	*3000*	*0,3*	*18,8*	*18*

The peak shear strength has been chosen on the basis of the average value found in Nalcor document, Leahy (2015) p.49 for the upper clay layer.
We first carried out the calculation with a low sensitivity ratio in order to model a sensitive clay.

The other parameters (shear and strain at elastic limit) have been chosen so that they correspond to what can be expected for the layers in the North Spur. The calculations are given in detail in Appendix D.

5.2.3. **Calculation**

Stage I:

Step 0 → 1:
The calculation begins by determining the in-situ stress τ_0 at point $x = x_0 = 0$.

At this position, which corresponds to the lower boundary condition, the shear stress and the deformation due to the additional load N_q are respectively $N(x_0) = 0$ and $\delta_N(x_0) = 0$

As the additional load has no effect at this point, the total shear stress is equal to the in-situ shear stress $\tau(x_0) = \tau_0$

$$\tau_0(x_{0\to1}, 0) = [\sum_0^H \rho * g * \Delta z * sin\beta + \sum_0^{H_c} \rho_c * g * \Delta z * sin\beta - K_p \rho g \left(\frac{H_{x_1}^2 - H_{x_0}^2}{2}\right)]/\Delta x_{0\to1}$$

Once the parameters at the lower boundary are established, we chose a first shear increment corresponding to the difference between the in situ shear stress and the shear stress at the elastic point.

$$\Delta\tau_{x_0\to x_1} = \tau_{el} - \tau_0$$

Then we get $\tau(x_1) = \tau(x_0) + \Delta\tau_{x_0\to x_1}$

Thanks to Figure 5-6, $\gamma(x_1, z)$, the strain at position $x = x_1$ is determined for each Δz all along the section.

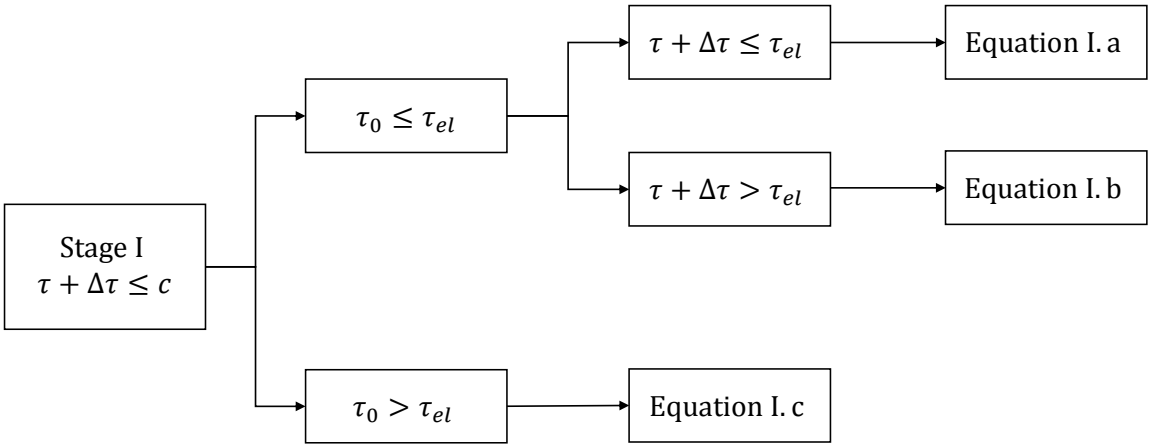

Figure 5-6. Diagram of conditions leading to the equations adapted to determine $\gamma(x,z)$ during analysis stage I. The different equations are included in appendix A.

By integrating $\gamma(x_1)$ from $z = 0$ to $z = 0{,}33 * H_{x_0 \to x_1}$, we get $\delta_\tau(x_1)$, the deformation in section x_1 caused by the shear stress.

Then we calculate $\Delta N_{x_0 \to x_1}$ and $\delta_N(x_1)$ the deformation in section $x = x_1$ caused by the additional loading:

$$\Delta N_{x_0 \to x_1} = \left(\frac{\tau(x_0) + \tau(x_1)}{2} - \frac{\tau_0(x_0) + \tau_0(x_1)}{2} \right) * \Delta x_{0 \to 1}$$

$$\delta_N(x_1) = \frac{N(x_0) + N(x_1)}{2} * \frac{\Delta x_{0 \to 1}}{E_{el} * H_{x_0 \to x_1}}$$

Finally, the unknown $\Delta x_{0 \to 1}$ corresponding to the $\Delta\tau_{x_0 \to x_1}$ stated is determined by solving the following equation thanks to solver function of excel:

$$\sum_{x_0}^{x_1} \Delta\delta_N(x_i) = \delta_\tau(x_1)$$

Then, we get $\Delta x_{0 \to 1} = 38{,}5\ m$

This value allows us to get:

$\tau_0(x_{0 \to 1}, 0) = 22{,}470\ kPa$

$\tau(x_1) = 40\ kPa$

$\Delta N_{x_0 \to x_1} = 335\ kN/m$

$\delta_N(x_1) = \delta_\tau(x_1) = 0{,}07\ mm$

Step 1 → 2:

We choose a second shear increment $\Delta\tau_{x_1 \to x_2} = 2{,}222\ kPa$.

Then we get $\tau(x_2) = \tau(x_1) + \Delta\tau_{x_1 \to x_2} = 40 + 2{,}222 = 42{,}222$

Thanks to figure 5-6, the values of $\gamma(x_2, z)$, are determined.

$\tau(x_2) < c$, $\tau_0 < \tau_{el}$ and $\tau(x_2) > \tau_{el}$ so we apply equation I.b.

Then we calculate $\Delta N_{x_1 \to x_2}$ and $\delta_N(x_2)$ and determine the unknown $\Delta x_{1 \to 2}$ corresponding to the $\Delta\tau_{x_1 \to x_2}$ stated by solving the following equation thanks to the solver function of excel:

$$\sum_{x_0}^{x_2} \Delta\delta_N(x_i) = \delta_\tau(x_2)$$

Then, we get $\Delta x_{1 \to 2} = 2{,}45\ m$

And $\delta_N(x_2) = \delta_\tau(x_2) = 0{,}08\ mm$

Step $i \to i + 1$:

This process is repeated in every step $i \to i + 1$ until the shear stress reaches the peak shear strength c and thus the slip surface forms.

At the end of stage I, we get:

$x_{10} = 56{,}35\ m$ and $\delta_N(x_{10}) = \delta_\tau(x_{10}) = 0{,}18\ mm$

Stage II:

During the second part of the process, the slope is unloaded, i.e. the shear stress is decreased.

Step 10 → 11:

We chose a shear increment $\Delta\tau_{x_{10} \to x_{11}} = (c - \tau_0)/5 = -7{,}57\ kPa$.

Then we get $\tau(x_{11}) = \tau(x_{10}) + \Delta\tau_{x_{10} \to x_{11}}$

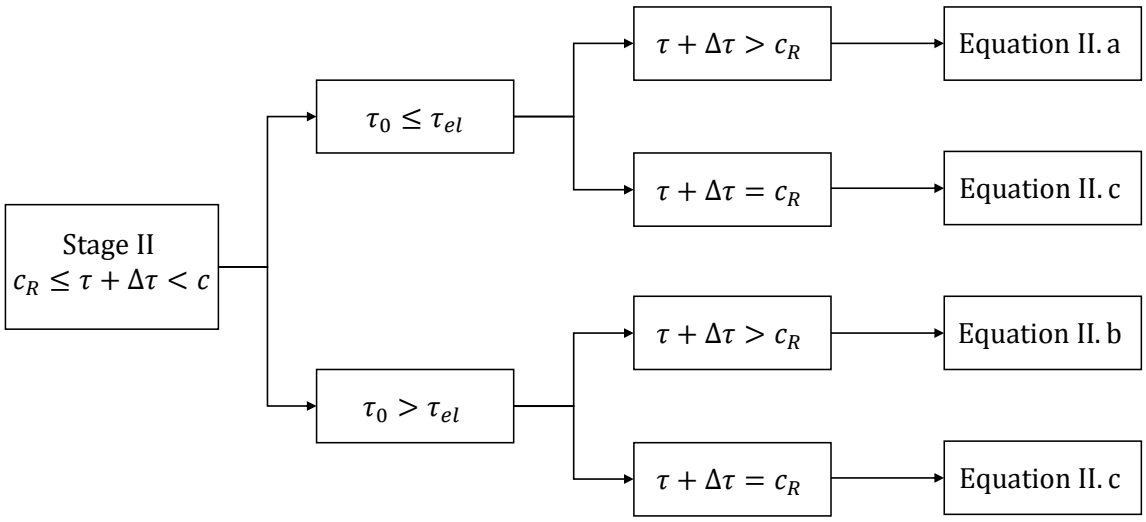

Figure 5-7 Diagram of conditions leading to the equations adapted to determine $\gamma(x,z)$ during analysis stage II. The different equations are included in appendix A.

Thanks to figure 5-7, we get $\gamma(x_{11}, z)$, the strain at position $x = x_{11}$

$c_R < \tau(x_{12}) < c$ and $\tau_0 < \tau_{el}$ so we apply equation II.b.

Then we calculate $\Delta N_{x_{10}\to x_{11}}$ and $\delta_N(x_{11})$ and determine the unknown $\Delta x_{10\to 11}$ corresponding to the $\Delta\tau_{x_{10}\to x_{11}}$ stated by solving the following equation thanks to solver function of excel:

$$\sum_{x_0}^{x_{11}} \Delta\delta_N(x_i) = \delta_\tau(x_{11}) + \delta_s(x_{11})$$

δ_s is defined as the slip in the failure plane as being:

$$\delta_s(x_{11}) = \delta_{cr}\left(\frac{c - \tau(x_{11})}{c - c_r}\right)$$

Where δ_{cr} is the slip at which the residual strength c_r is reached

Then, we get $\Delta x_{10\to 11} = 1{,}80\ m$

Step 11 → 15:

We repeat the process until we get $\tau(x_{15}) = \tau(x_{14}) + \Delta\tau_{x_{14}\to x_{14}} = \tau_0$

It implies $x_{15} = L_{crit} = 63{,}7\ m$

And $\delta_N(x_{15}) = \delta_\tau(x_{15}) = \delta_{crit} = 0{,}29\ m$

Also $N_{15} = N_{crit} = 981{,}7\ kN/m$

These are the critical parameters. They correspond to the additional load which would trigger progressive failure, see Figure 5-8.

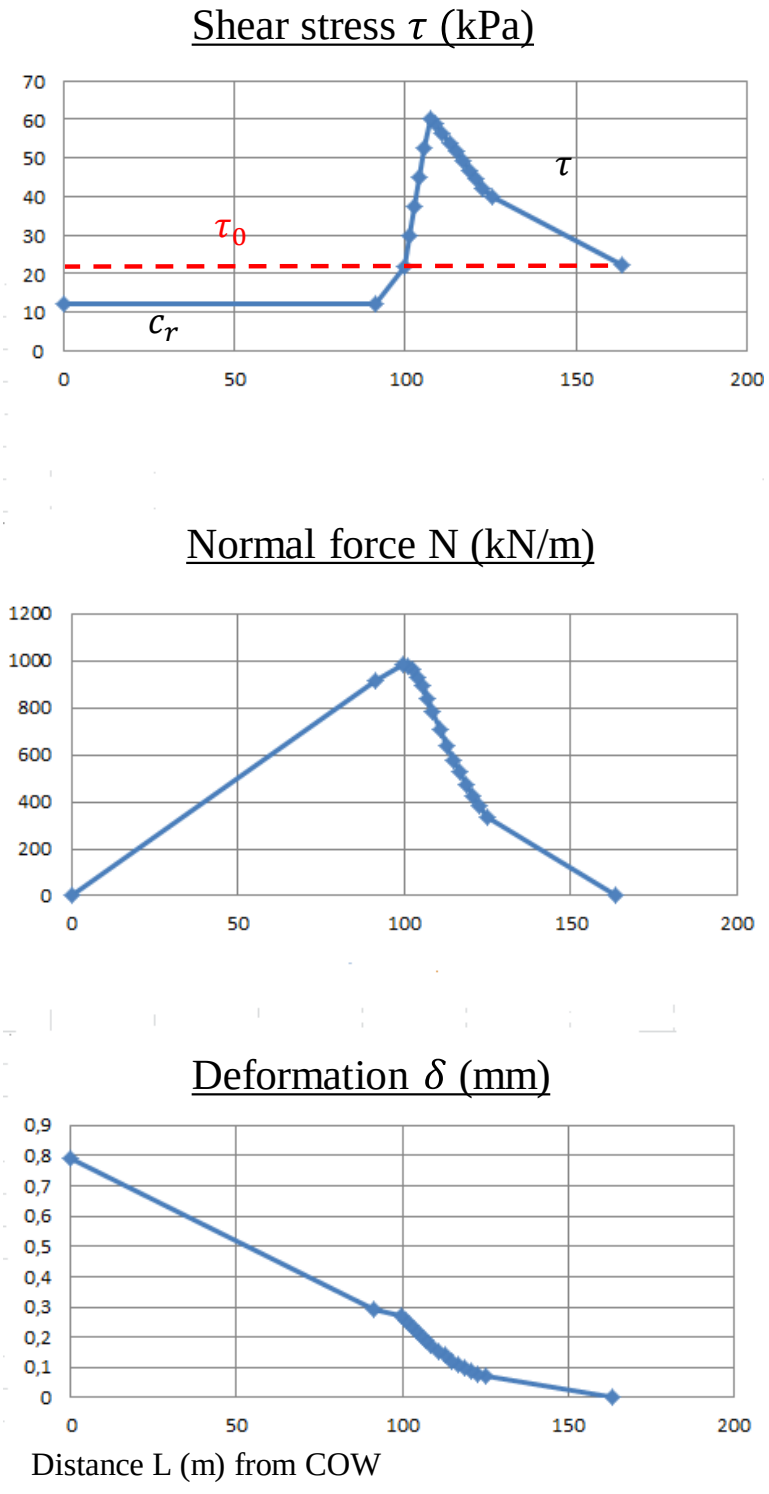

Figure 5-8. Shear stresses τ, normal force N and deformation δ as function of the distance L from the Cut-Off Wall (COW).

Step 15 → 16:

We now chose a shear increment $\Delta\tau_{x_{15}\to x_{16}} = \tau_0 - c_R = -22{,}27\ kPa.$

Then we get $\tau(x_{16}) = \tau(x_{15}) + \Delta\tau_{x_{15}\to x_{16}} = c_R$

Then we calculate $\Delta N_{x_{15}\to x_{16}}$ and $\delta_N(x_{16})$ and determine the unknown $\Delta x_{15\to 16}$ corresponding to the $\Delta\tau_{x_{15}\to x_{16}}$ stated by solving the following equation thanks to solver function of excel:

$$\sum_{x_0}^{x_{16}} \Delta\delta_N(x_i) = \delta_\tau(x_{16}) + \delta_s(x_{16})$$

Then, we get $\Delta x_{15\to 16} = 9{,}00\ m$
And $\delta_N(x_{16}) = \delta_\tau(x_{16}) = 0{,}304\ m$
Also $N_{16} = 938 kN/m$

Step 16 → 17:

The instability parameters are calculated directly on the basis of the previous step:

$$\Delta x_{16\to 17} = \frac{N_{crit}}{\tau_0(x_{16}) - c_R} = 134\ m$$

$$L_{instab} = x_{16} + \Delta x_{16\to 17} = 208\ m$$

$$\delta_\tau(x_{17}) = \delta_{instab} = \delta_\tau(x_{16}) + \frac{N_{16} * \Delta x_{16\to 17}}{2 * E_{el} * H} = 1{,}04\ m$$

The charts below show the stress and the incremental earth pressure repartition along the slope caused by a forced deformation δ_{instab} likely to trigger failure:

The whole calculation with intermediate results is enclosed in appendix D.

Safety Factor

The safety factor related to local failure in this case is defined as:

$$F_s^{(I)} = \frac{N_{crit}}{N_q} = \frac{981{,}7}{2420} = 0{,}38$$

$F_s^{(I)} < 1$, it means progressive failure is likely to be triggered considering this combination of properties.

5.2.4. **Results**

This part of the study focuses on the results that we obtained for several different assumptions as concerns the mechanics and geometric parameters of the slope. It will mainly be focused on the safety factor for local failure as it is a good indicator to say if the situation is risky.

First, the impact of the sensitivity ratio is studied for different peak shear strengths of the clay. The constant parameters studied are repeated in the following table:

Poisson ratio	**Thickness of the failure layer**	**Thickness of ground of the upper layer**	**Inclination of failure plane**	**Slip for residual shear strength**	**Deviator strain at failure limit**
ν	H_c (m)	H (m)	β	δ_{cr} (m)	γ_f (%)
0,334	15	28	0,04	0,3	0,07
Shear stress at elastic limit	**Deviator strain at elastic limit**	**Secant modulus in shear**	**Elastic modulus**	**Volumic weight upper layer**	**Volumic weight clay layer**
τ_{el} (kN/m²)	γ_{el} (%)	G (kN/m²)	E_{mean} (kN/m²)	ρ (kN/m²)	ρ_c (kN/m²)
40	0,035	1143	3000	18,8	18

Table 5-4 Constant parameters of the case studied

The different safety factors for a full reservoir (water level of 39 meters) are displayed on the chart below:

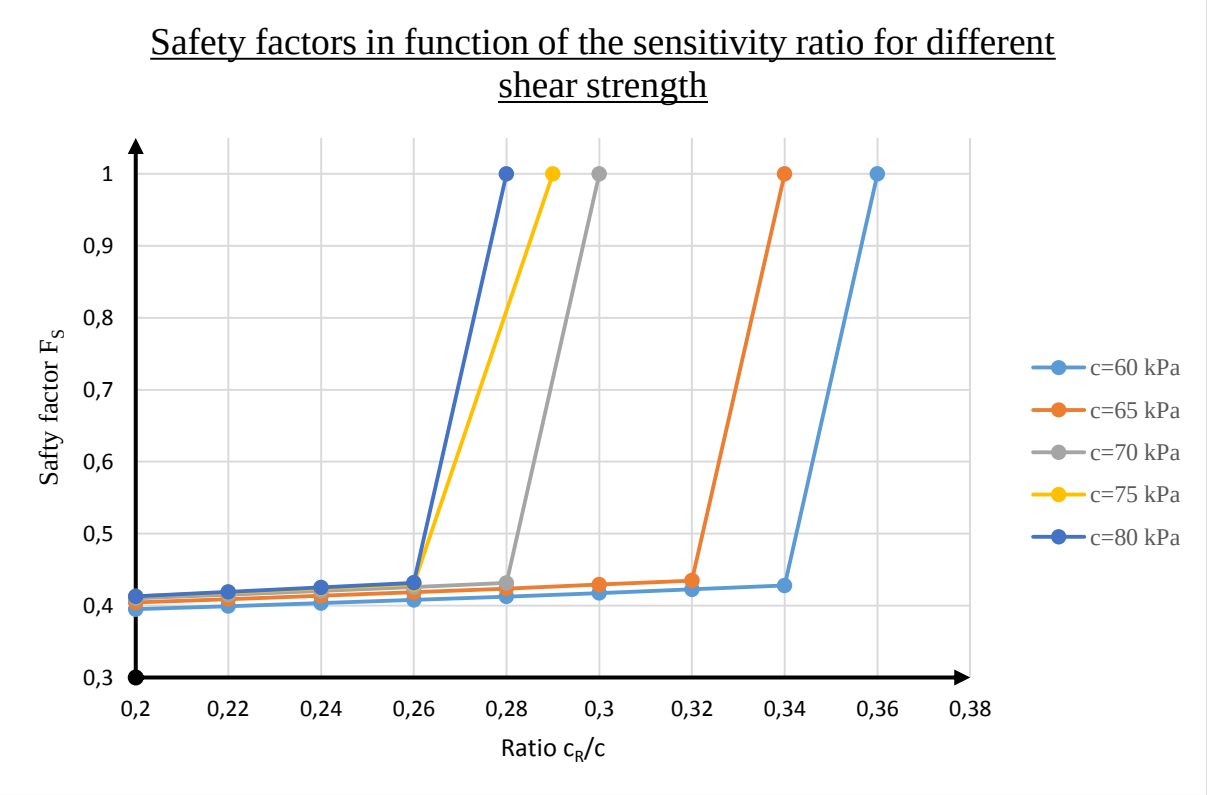

Figure 5-8 Safety factors obtained for different sensitivity ratios and different peak shear strengths of clay studied

The chart shows that there is an important risk of brittle failure whatever the peak shear strength of the clay if its sensitivity ratio is around 0,4.

For example, considering a material with a shear strength of 60 kPa, with a sensitivity ratio below 0,36 the safety factor resulting is equal to 0,42, meaning that brittle failure can be triggered.
However, when $\frac{c_r}{c} > 0{,}36$, the safety factor is bigger than 1 because brittle failure cannot occur. In fact, in those cases the residual strength of the material is bigger than the in-situ shear stress of the clay. This case is illustrated by the figure below:

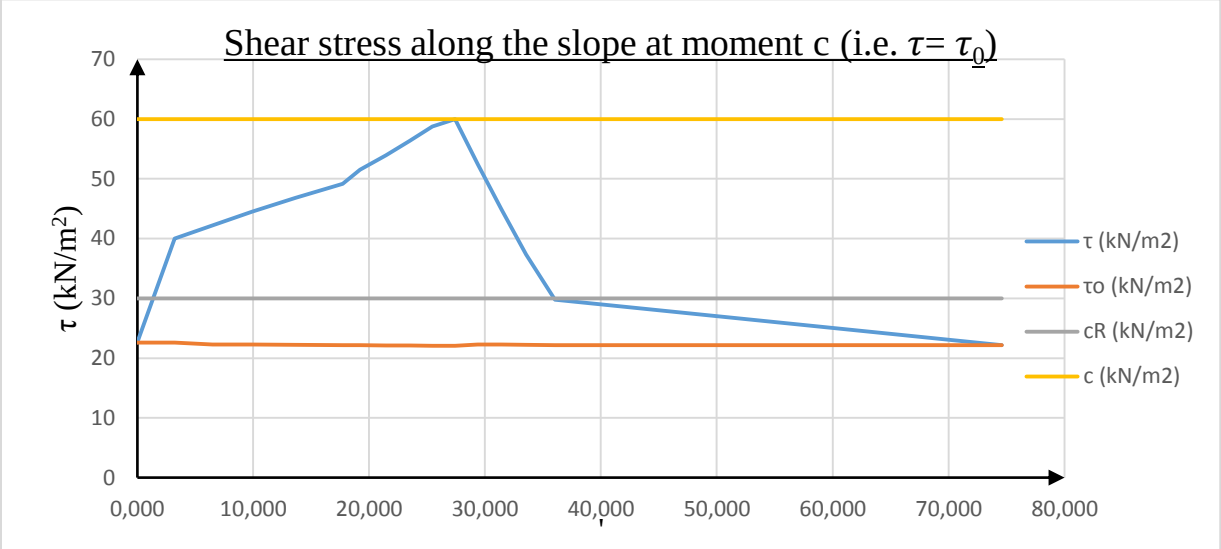

Figure 5-9 Shear stress along the slope for c=60 kPa and c_r/c=0,5; in-situ shear stress is below the residual strength: brittle failure cannot occur

As expected, the safety is increased when the peak shear strength increases. When the sensitivity ratio increases for a constant peak shear strength, the safety increases too.

Variation of the failure plane gradient β

The impact of the failure plane gradient is studied for a slope having the following constant parameters:

Poisson ratio	Thickness of the failure layer	Thickness of ground of the upper layer	Shear strength at interface	Deviator strain at failure limit	Peak shear strength	Residual shear strength
ν	H_c (m)	H (m)	c_s (kN/m²)	γ_f (%)	c (kN/m²)	c_R (kN/m²)
0,334	15	28	45	0,07	60	12
Shear stress at elastic limit	**Deviator strain at elastic limit**	**Secant modulus in shear**	**Elastic modulus**	**Slip for residual shear strength**	**Volumic weight upper layer**	**Volumic weight clay layer**
τ_{el} (kN/m²)	γ_{el} (%)	G (kN/m²)	E_{mean} (kN/m²)	δ_{cr} (m)	ρ (kN/m²)	ρ (kN/m²)
40	0,035	1143	3000	0,3	18,8	18,8

Table 5-5 Constant parameters of the case studied

With an inclination bigger than $\beta = 0{,}022$, the safety factors obtained are far below 1, meaning that the situation is risky.

With an inclination of $\beta = 0{,}022$, the in situ shear stress is below the residual strength, and so brittle failure can't occur. It means that below a 2% gradient, the safety factor is above 1 and the situation is not risky anymore.

5.3. Bernander's method for investigation in lower clay

5.3.1. Geometry

The failure surface most likely to appear and propagate in the lower clay is circular at the top of the slope and then linear. This shape is assumed because we suppose that the layers having a high porosity within the lower clay can have this kind of shape.

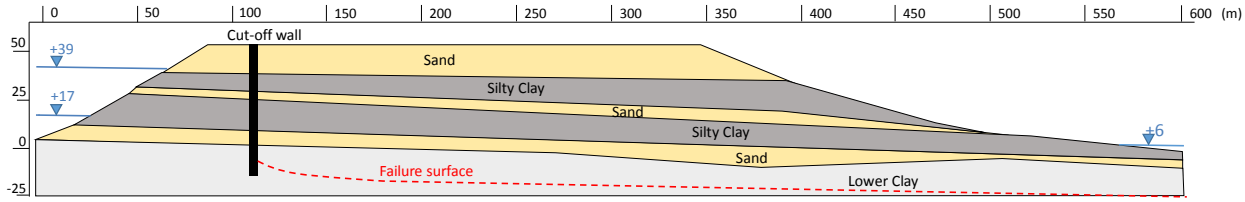

Figure 5-10 Section of the north spur and location of the assumed failure plane

At the upstream edge of the spur (directly after the cut off wall), the thickness of ground above the lower clay layer studied is 50 meters. The thickness of the clay layer above the failure plane is 10 meters. The water level is considered as maximal before the cut-off wall (39 meters when the reservoir is full). The cut-off wall makes it drop a bit. To simplify the calculation the water level after the cut-off wall is considered as being at the same level as the failure surface.

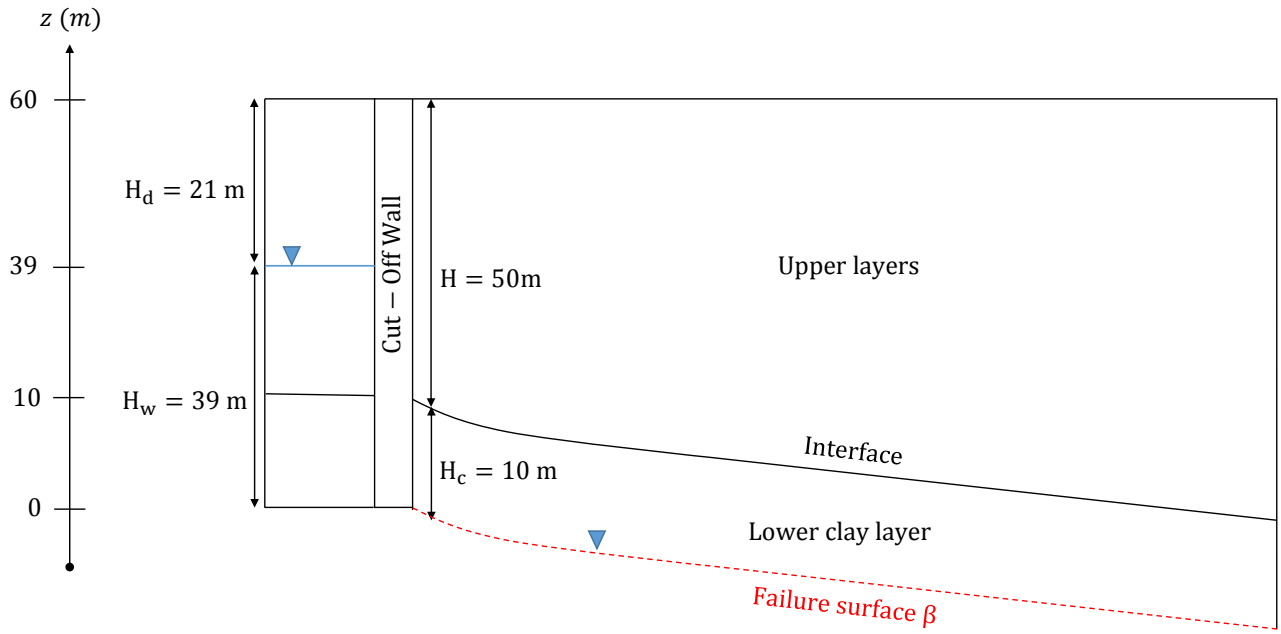

Figure 5-11 Geometric simplification of the problem studied

5.3.2. **Triggering agent**

In Muskrat Falls Project, the triggering agent would essentially be the water pressure which will increase because of the raising level from $z = 17\ m$ to $z = 39\ m$. As a result the total additional load N_q likely to trigger progressive failure is the earth pressure acting on the cut-off wall.

It may be considered that the upper layers have an average humid mass density $\rho = 18{,}8\ kg/m^3$

As concern the clay layer studied, it has a water saturated mass $\rho_c = 18\ kg/m^3$
It has a cohesion $c' = 6\ kPa$.

The triggering load is defined as:

$$N_q = 0.5 * \gamma_w H_d^2 = 2420\ kN/m$$

5.3.3. **Results**

To get the results necessary for the analysis, we carry the same calculation as in chapter 5.2.3. A detailed calculation can be found in Appendix E.
We just chose different gradient values for each slice of the slope. Hence the slices located at the upstream edge of the spur have a steeper failure inclination than the one located downstream.

The chart below represents the shape of the failure surface for an analysis carried with $c = 60\ kPa$ and $c_r = 12\ kPa$.

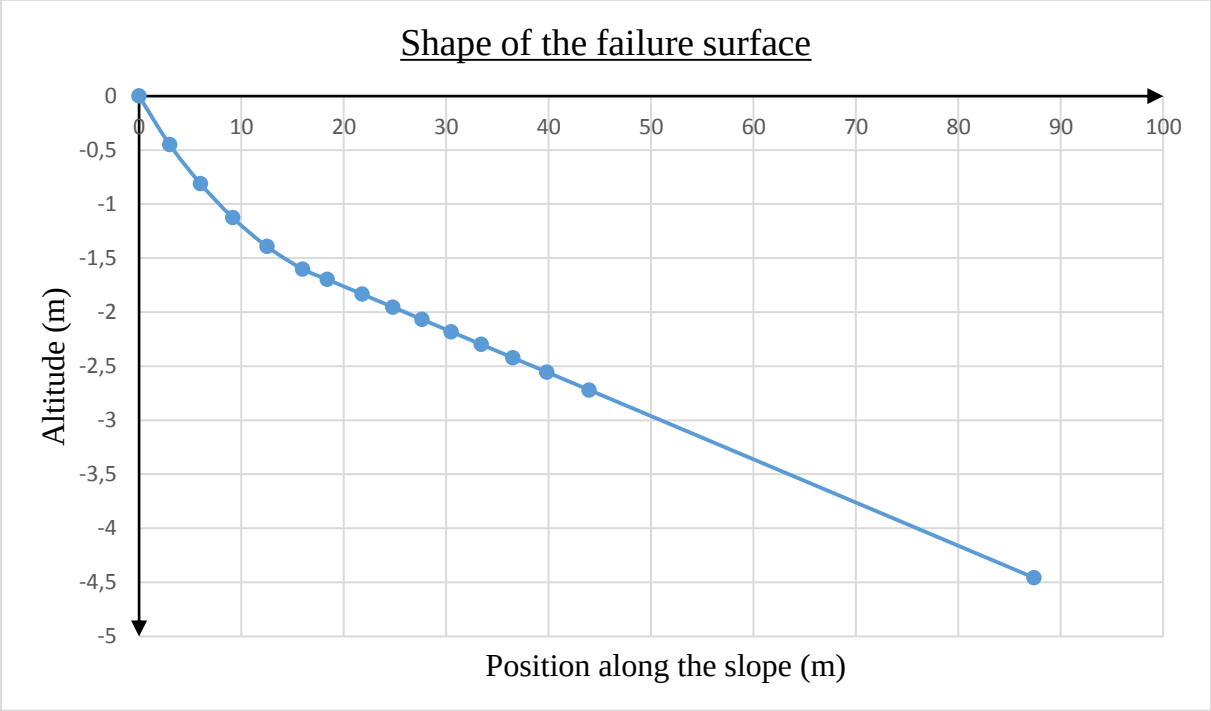

Figure 5-12 Shape and location of the failure surface along the lower clay layer

Variation of the sensitivity ratio and the peak shear strength:

The impact of the sensitivity ratio is studied for different peak shear strengths of the clay. The constant parameters are repeated in the following table.

Poisson ratio	Thickness of the failure layer	Thickness of ground of the upper layer	Slip for residual shear strength	Deviator strain at failure limit	
ν	H_c (m)	H (m)	δ_{cr} (m)	γ_f (%)	
0,334	10	50	0,3	0,07	
Shear stress at elastic limit	**Deviator strain at elastic limit**	**Secant modulus in shear**	**Elastic modulus**	**Volumic weight clay layer**	**Volumic weight upper layer**
τ_{el} (kN/m²)	γ_{el} (%)	G (kN/m²)	E_{mean} (kN/m²)	ρ_c (kN/m²)	ρ (kN/m²)
40	0,035	1143	3000	18	18,8

Table 5-6 Constant parameters of the case studied

The different safety factors for a full reservoir (water level of 39 meters) are displayed on the following chart:

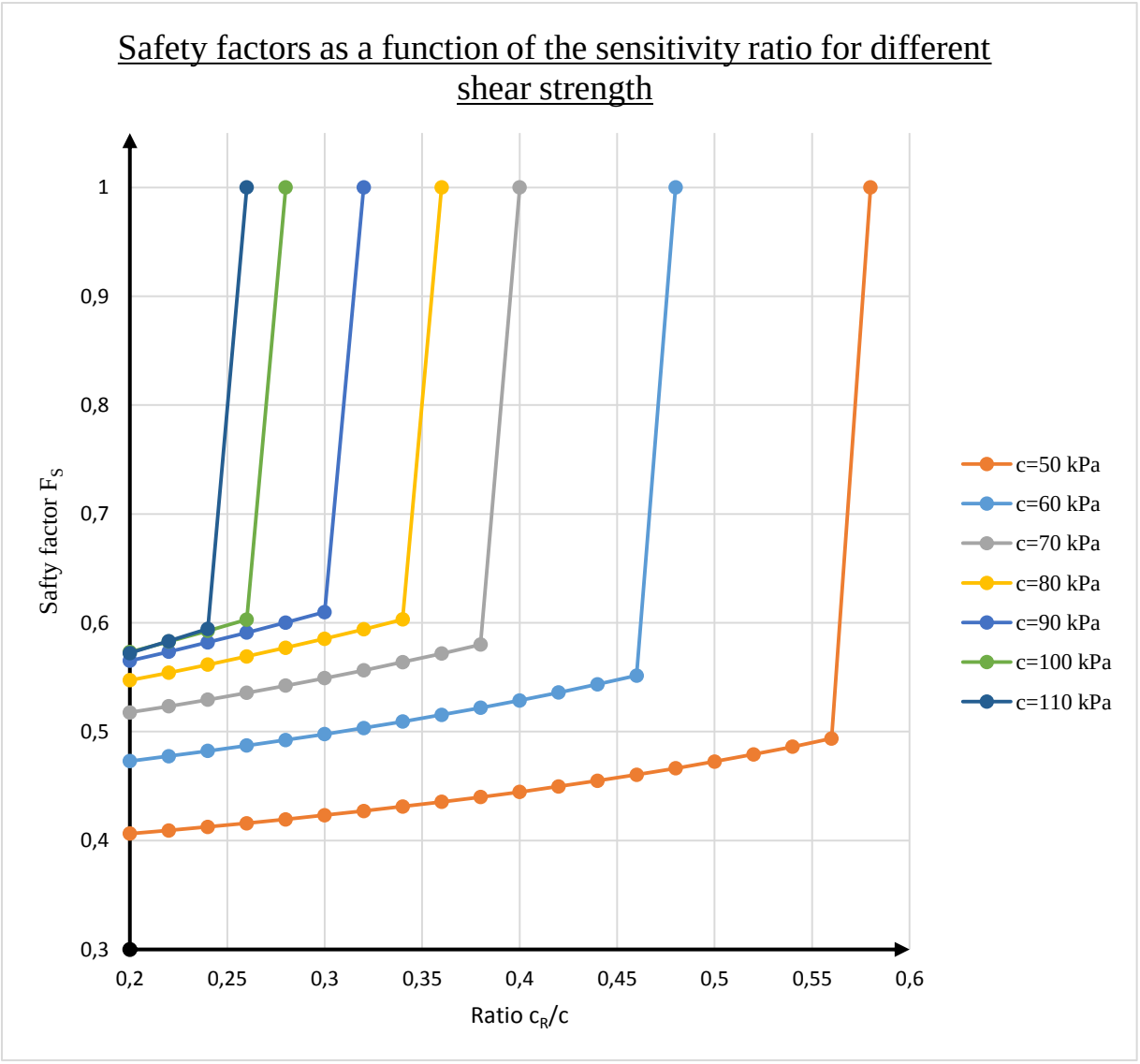

Figure 5-13 Safety factors obtained for different sensitivity ratios and different peak shear strengths of clay studied

This chart shows that for a certain range of sensitivity, progressive failure is likely to be triggered with a safety factor far below 1.

We notice that as the peak shear strength is decreased, the range of sensitivity corresponding to a risky situation increases. For example $c = 50\ kPa$, the slope is likely to slide for ${}^{c_r}/_{c} \in [0{,}2; 0{,}56]$. On the contrary, for $c = 110\ kPa$ progressive failure can occur for ${}^{c_r}/_{c} \in [0{,}2; 0{,}24]$.

The detail of the calculation carried for $c = 60\ kPa$ and for ${}^{c_r}/_{c} = 0{,}2$ can be found in appendix E.

6. Discussion

6.1. Interpretation of results

As expected and as Nalcor already showed, Leahy (2015), the limit equilibrium method does not indicate any significant risk of failure (cf. chapter 5.1). In fact, none of the two traditional limit equilibrium method we used (FEM or infinite slope) show a significant failure risk in the clay layers investigated. This means that if the clay layers investigated would have an elastic plastic behavior, the stability of the spur would be safe.

Nonetheless, if the ground studied would have a high in-situ porosity, which is very likely, the plastic limit equilibrium method would not be relevant at all. And if this assumption is verified, the clay layers must be analyzed as a 'deformation-softening' ground.

On the basis of this assumption it is shown using Bernander's progressive failure method that there exists a certain risk of landslides triggering in both the upper and lower clay layers.
Those risks relate to a range of soil properties (peak shear strength and residual shear strength) and certain failure plane locations and inclinations.
Besides, in the North Spur configuration, there is no phase 4, during which the earth pressure is permanently or temporarily balanced by passive resistance E_p. In fact there is nothing after the ridge that may stop the slide once it has started.

6.2. Criticism of the method

Making a stability problem manageable require both simplifications and assumptions. Building a model without compromising the accuracy of the results is a difficult task and whatever the method used, there will always be discrepancies between models and actual conditions.

First, the study has been performed with an assumed stress-deformation relationship.
To prevent the worst possible case and because no dynamic shear tests have been carried out on the soils studied, it has been chosen to model a wide range of sensitive materials.

Second the analysis has been performed assuming that the mechanical properties of the clay are constant all along the section of the North Spur.
Obviously this is not the case and it would be interesting to perform an analysis with the results of dynamic shear strength tests carried at different locations along the North Spur.

This investigation has been performed for a optimistic case with N_q only being caused by the rising water, More conservative assumptions wher the triggering load has been considered as being the whole earth pressure on the cut-off wall for a full reservoir are tried in Appendices E and F.

Moreover, the geometry of the North Spur is simplified. This aspect should be developed in further versions of the spreadsheet by allowing the user to deal with more complex geometries. All the stabilization constructions built since the beginning of the project are not taken into account in the calculations. We only included the effect of the cut-off wall. Furthermore we considered only one homogeneous layer above the layer likely to contain the

failure plane. Besides, the soil layers have been assumed to be fully saturated. Yet, this aspect may have a negligible impact on the in-situ stress calculated.

For those reasons, the landslides analysis performed on the North Spur with Stig Bernander's method are not supposed to give exacts odds for progressive failure. Yet, as the values are really low, we can say that it still represents a warning of an existing risk of landslide.

6.3. **Preventive actions**

Since the beginning of the project (1979), only a few dynamic tests have been performed in situ by the company responsible for the construction. In fact, dynamic stress conditions are extrapolated from static data with help of software models. Yet, these computer models are based on elastic-plastic conditions and the limit equilibrium method which do not fit to the North Spur configuration. For this reason, dynamic hydro-geological testing that would better quantify the risk of a progressive failure has to be carried out (Bernander, 2015).

Besides, the general character and development of the Churchill River Valley indicate that the in-situ porosities of some soil layers of the North Spur are probably critically high.
Thus, in-situ porosity tests should be carried to assess if the safety factors already calculated by Nalcor with the LEM are reliable.

Bernander has proposed, in his report (2015), a practical method for making a simple, effective in-situ assessment of the stability of the North Spur even while construction proceeds. The idea of Bernander is to submit violent vibratory treatment to the soil and measure the subsequent changes. This can be done by gradually step-wise driving down a group of piles into the soil while measuring the deformations for each step the piles are driven further down. If the settlements generated in the tested soil are moderate, then the reliability of the results of the analyses made by Nalcor will be confirmed.

If, on the other hand, the settlements indicate a high degree of compaction— i.e. the mean in-situ porosity (n) is clearly in excess of the critical porosity, then it will be necessary to strengthen the affected soil structures.

Stig Bernander (2015) suggests that the best way to stabilize the North Spur would be to compact the upper soils over a wide area with driving piles down below the level of the cot-off wall. The time required for such compaction, and its interaction with the construction program, is a further compelling reason for carrying out the required vibrational testing immediately.

7. Conclusion

The spreadsheet developed in this thesis allows its users to perform easy and quick analyses regarding downhill progressive failure problems in long slopes made of sensitive materials.

This tool is based on a finite difference method and can be adapted to a variety of geometries material properties.

The software has been used to assess the risk of a progressive landslide encountered on the Muskrat Falls construction project. On the basis of the outcome of this study, we can affirm that the North Spur does not form a safe and reliable part of the impoundment wall. For assumed material properties and geometries of failure, the critical load are below 1000 kN/m whereas a rise of the water level with 21 m will give an increased load of $N_q = 0{,}5\ \gamma_w H_d^2 = 0{,}5 \cdot 10 \cdot 21^2 = 2420$ kN/m which is more than twice what the ridge can stand with the assumed properties.

For this reason, it is recommended to test the in-situ porosity of the slope soil in order to assess its sensitivity to liquefy. Depending on the results, some stabilization work has to be performed to ensure the safety and the sustainability of the slope.

8. References

Andresen, L & Jostad H. P. (2004). Analyses of progressive failure in long naturals slopes. Proc. Num. Mod. Geomech. – NUMOG IX, Ottawa, Canada, pp 603-608.

Aryal, Krishna P. (2006). Slope Stability Evaluations by Limit Equilibrium and Finite Element Methods.Trondheim: Norwegian University of Science and Technology, Department of Civil and Transport Engineering, Doctoral Thesis 2006:66, 124 pp, ISBN 82-471-7881-8

Axelsson, Kennet & Matsson, Hans (2016). Geoteknik (Soil Mechanicsd and Foundation Engineering. In Swedish). Lund: Studentlitteratur, 464 pp, ISB 978-91-33-08072-7.

Bernander, Stig (1978). Brittle Failures in Normally Consolidated Soils. Väg- & Vattenbyggaren (Stockholm), No 8- 9, pp 49-52. Available at http://ltu.diva-portal.org/

Bernander, Stig & Olofsson, Ingvar (1981). On formation of progressive failure in slopes. In Proceedings of the 10th International Conference on Soil Mechanics and Foundation Engineering,(ICSMFE), Stockholm 1981. Vol 3, 11/6, pp 357-362. Available at http://ltu.diva-portal.org/

Bernander, Stig (2000). Progressive Landslides in Long Natural Slopes. Formation, potential extension and configuration of finished slides in strain-softening soils. Licentiate Thesis 2000:16, Luleå University of Technology, Available at http://ltu.diva-portal.org/

Bernander, Stig (2008). Down-hill Progressive Landslides in Soft Clays. Triggering Disturbance Agents. Slide Prevention over Horizontal or Gently Sloping Ground. Sensitivity related to Geometry. Research Report 2008:11, Luleå University of Technology, ISSN: 1402-1528, 16+101 pp. Available at http://ltu.diva-portal.org/

Bernander, Stig (2011). Progressive landslides in long natural slopes. Formation, potential extension and configuration of finished slides in strain-softening soils. Doctoral thesis, Lulea University of Technology, ISBN 978-91-7439-283-8. Available at http://ltu.diva-portal.org/

Bernander, Stig (2015). Comments on the Engineering Report by Nalcor/SNC-Lavalin of December 2015 prepared for Grand Riverkeeper, Labrador, Inc. Churchill, 31 pp.

Bernander, Stig, Kullingsjö, A., Gylland, A. S., Bengtsson, P. E., Knutsson, S., Pusch, R., Olofsson, J., & Elfgren, L. (2016). Downhill progressive landslides in long natural slopes: triggering agents and landslide phases modelled with a finite difference method. Canadian Geotechnical Journal, Vol. 53, No. 10, pp. 1565-1582, dx.doi.org/10.1139/cgj-2015-0651

Bernander, Stig (2017): Personal communication. Prof. Stig Bernnader, Tegelformsgatan 10, SE-43136 MÖLNDAL, Sweden, stig,bernander@telia.com.

FOEN (2016). Protection against Mass Movement Hazards. Guideline for the integrated hazard management of landslides, rockfall and hillslope debris flows. Federal Office for

the Environment FOEN, Swiss confederation, Report UV-1608-E, Bern 2016, 97 pp. Available at www.bafu.admin.ch/uv-1608-e

Grimstad, G. Degago, S. A., Nordal, S. & Karstunen, M. (2010). Modelling of creep and rate effects in structured anisotropic soft clays. Acta Geotechnica Journal, Vol.5, No 1, pp 69-81. Available at: http//www.springerlink.com/content/0415473702752105/ (21 April 2011)

Gylland, Anders S. (2012). Material and slope failure in sensitive clays. Trondheim: Norwegian University of Science and Technology, Department of Civil and Transport Engineering, Doctoral Thesis 2012:352, 238 pp.

L´Heureux, Jean-Sébastien, Locat, A., Leroueil, S., Demers, D. and Locat, J., Editors (2013). Landslides in Sensitive Clays. From Geoscience to Risk Management. Springer, 418 pp, ISBN 978-94-007-7078-2.

Leahy, Denise (2015). North Spur Stabilization Works. Progressive Failure Study. Lower Churchill Project, Engineering Report, SNC-Lavalin, Nalcor, SLI Document No. 505573-3281-4GER-0001-01, Nalcor Reference No. MFA-SN-CD-2800-GT-RP-0001 Rev B2, 21 Dec 2015, 128 pp. Available at https://muskratfalls.nalcorenergy.com/wp-content/uploads/2016/01/North-Spur-Stabilization-Works-Progressive-Failure-Study.pdf

Leahy, Denise; Bouchard, R. and Leroueil, S. (2017). Potential Landslide at the North Spur, Churchill River Valley. In "Landslides in Sensitive Clays. From Research to Implementation" Ed. by Tharkur, V., L'Heureux, J.-S. & Locat, A., Springer Cham, pp 213-223. ISBN 978-3-319-56486-9.

Leroueil, Serge (2001). Natural slopes and cuts - Movement and failure mechanisms. 39th Rankine Lecture. Géotechnique, Vol 51, No 3, pp 197-243.

Locat, Ariane, Leroueil, S., Bernander, S., Demers, D., Jostad, H.P., and Ouehb, L. (2011). Progressive failures in eastern Canadian and Scandinavian sensitive clays. Canadian Geotechnical Journal, 48(11): 1696-1712, doi:10.1139/t11-059.

Pusch, Roland, Knutsson, S., Liu, X. and Yang, T. (2016). Creep can strengthen clay: A matter of long-term slope stability. Journal of Earth Sciences and Geotechnical Engineering, vol. 6, no.1, 2016, 1-18 ISSN: 1792-9040 (print), 1792-9660 (online) Scienpress Ltd, 2016.

Rehnström, Liw (2013). Analysis of Progressive Landslides. A review of the simplified calculation model. M Sc Thesis 2013:5, Div. of Geo Engineering, Chalmers University of Technology, Göteborg, 55 pp. Available at http://publications.lib.chalmers.se/records/fulltext/185611/185611.pdf

SNC-Lavalin (2017), Lower Churchill Project. North Spur Information Session, January 2017, Slide Presentation available at http://muskratfalls.nalcorenergy.com/wp-content/uploads/2017/01/North-Spur-Information-Session-Presentation__Jan-2017_Website-posting.pdf

Terzaghi, Karl; Peck, Ralph B. & Mesri, Gholamreza (1996). *Soil Mechanics in Engineering Practice*, 3rd Edition. New York, Wiley, 592 pages, ISBN: 978-0-471-08658-1.

Thakur, V., Nordal, S. & Grimstad, G. (2006). Phenomenological issues related to strain softening in sensitive clays. Geotechnical and Geological Engineering, Vol. 24, No 6, pp. 1729-1747.

Thakur, V. (2007). Strain Localization in Sensitive Soft Clays. Ph D Thesis, Geotechnical Division, Department of Civil and Transport Engineering, Norwegian Institute of Science and Technology, NTNU. Trondheim and Norwegian Centre of Excellence: International Centre for Geohazards, ISBN 9788247139097, 188 pp.

Tharkur, V., L'Heureux, J.-S. & Locat, A., Editors (2017). Landslides in Sensitive Clays. From Research to Implementation. Cham: Springer, 604 pp, ISBN 978-3-319-56486-9.

Appendices

A. Equations related to the calculation process

The following figures remind the stress-strain/deformation relationship of clay with the equations used during the calculation procedure to model each part of the curve.

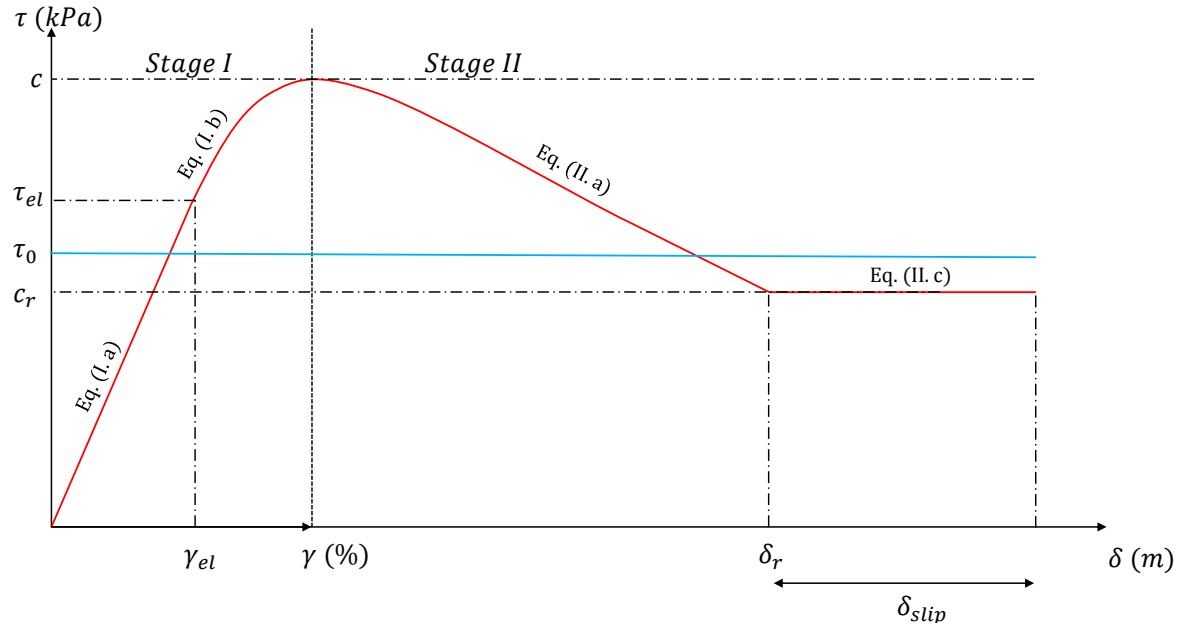

Figure 0-1 Stress-strain/deformation relationship of clay with the equations corresponding to the different part of the curve when $\tau_0 < \tau_{el}$

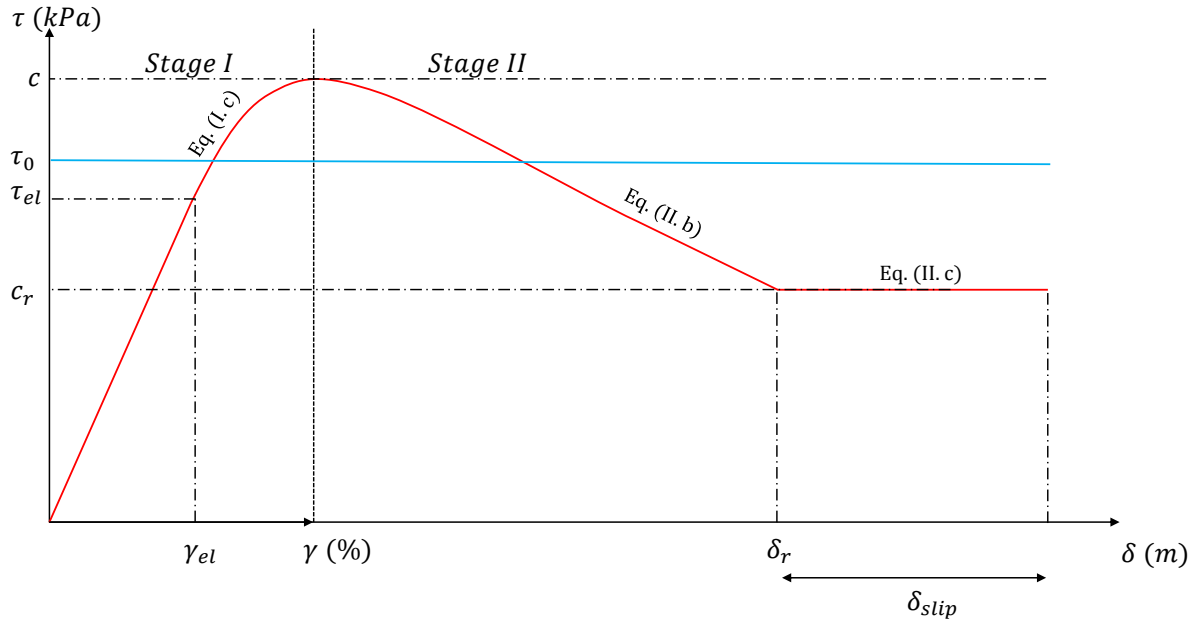

Figure 0-2 Stress-strain/deformation relationship of clay with the equations corresponding to the different part of the curve when $\tau_0 > \tau_{el}$

Note: To alleviate the equations, we don't write $\tau\,(x,z)$ but $\tau\,(z)$. Yet, the different terms are obviously functions of x.

Equation (I. a) Applied during stage I for: $\tau+\Delta\tau\le c,\ \tau_0\le\tau_{el},\ \tau+\Delta\tau\le\tau_{el}$

$$\gamma(z)=\left(\tau\,(z)+\Delta\tau(z)-\tau_0(z)\right)*\frac{\gamma_{el}}{\tau_{el}(z)}$$

Equation (I. b) Applied during stage I for: $\tau+\Delta\tau\le c,\ \tau_0\le\tau_{el},\ \tau+\Delta\tau>\tau_{el}$

$$\gamma(z)=\frac{\tau_{el}(z)-\tau_0(z)}{\tau_{el}(z)}*\gamma_{el}+\left(\gamma_f-\gamma_{el}\right)*\left(1-\sqrt{1-\frac{\tau\,(z)+\Delta\tau\,(z)-\tau_{el}(z)}{c(z)-\tau_{el}(z)}}\right)$$

Equation (I. c) Applied during stage I for: $\tau+\Delta\tau\le c,\ \tau_0>\tau_{el},\ \tau+\Delta\tau>\tau_{el}$

$$\gamma(z)=\left(\gamma_f-\gamma_{el}\right)*\left(1-\sqrt{1-\frac{\tau_0(z)-\tau_{el}(z)}{c(z)-\tau_{el}(z)}}-\sqrt{1-\frac{\tau\,(z)+\Delta\tau\,(z)-\tau_{el}(z)}{c(z)-\tau_{el}(z)}}\right)$$

Equation (II. a) Applied during stage II for: $c_R\le\tau+\Delta\tau\le c,\ \tau_0\le\tau_{el},\ \tau+\Delta\tau>c_R$

$$\gamma(z)=\left(\tau_{max}(z)-\tau_0(z)\right)*\frac{\gamma_{el}}{\tau_{el}(z)}+\left(\gamma_f-\gamma_{el}\right)*\left(1-\sqrt{1-\frac{\tau_{max}(z)-\tau_{el}(z)}{c(z)-\tau_{el}(z)}}\right)+\left(\tau\,(z)+\Delta\tau\,(z)-\tau_{max}(z)\right)*\frac{\gamma_{el}}{\tau_{el}(z)}$$

Equation (II. b) Applied during stage II for: $c_R\le\tau+\Delta\tau\le c,\ \tau_0>\tau_{el},\ \tau+\Delta\tau>c_R$

$$\gamma(z)=\left(\gamma_f-\gamma_{el}\right)*\left(\sqrt{1-\frac{\tau_0(z)-\tau_{el}(z)}{c(z)-\tau_{el}(z)}}-\sqrt{1-\frac{\tau_{max}(z)-\tau_{el}(z)}{c(z)-\tau_{el}(z)}}\right)-)+\left(\tau_{max}(z)-\tau\,(z)-\Delta\tau\,(z)\right)*\frac{\gamma_{el}}{\tau_{el}(z)}$$

Equation (II. c) $c_R\le\tau+\Delta\tau\le c,\ \tau+\Delta\tau=c_R$

$$\gamma(z)=\left(\gamma_f-\gamma_{el}\right)*\left(\sqrt{1-\frac{\tau_0(z)-\tau_{el}(z)}{c(z)-\tau_{el}(z)}}-\sqrt{1-\frac{\tau_{max}(z)-\tau_{el}(z)}{c(z)-\tau_{el}(z)}}\right)-)+\left(\tau_{max}(z)-\tau\,(z)-\Delta\tau\,(z)\right)*\frac{\gamma_{el}}{\tau_{el}(z)}-\left(\tau_{max}(z)-c_R\right)*\frac{\gamma_{el}}{\tau_{el}(z)}$$

B. Spreadsheet notice

This appendix is a notice to use the spreadsheet developed during this thesis work.

In the sheet called ‘Calculation’

1) Verify that the solver is well installed

From the main window:
FILE → Options → Add-Ins → Go… → Check Problemlosaren or Solver

Back to the main window
VIEW → Macros → Edit → Tools → References → Check Solver

2) Fill the input parameters of your slope (orange cells)

3) Click on the button “Run the calculation”

4) You can read N_{crit}, L_{crit}, δ_{crit}, L_{instab} and δ_{inst}ab and observe all the charts related to the calculation.

C. Introductory Example in Chapter 2

This is the detailed calculation for the example of landslide investigation carried in chapter 2.3 with the excel spreadsheet developed during this work.

PARAMETERS												
Poisson ratio	Peak shear strength	Residual shear strength	Shear strength at surface	Sensitivity ratio	Shear stress at elastic limit	Deviator strain at elastic limit	Deviator strain at failure limit	Secant modulus in shear	Elastic modulus	Slip for residual shear stregth	Depth	Gradient
v	c (kN/m^2)	c_R (kN/m^2)	c_S (kN/m^2)	c_R/c	τ_{el}	γ_{el}	γ_f	G	E_{mean}	δ_{cr}	H (m)	dx/dy
0,5	30	15	15	0,5	20	3,75E-02	7,50E-02	533,33333	1200	0,3	20	6,52E-02

Stage I:

Step n° 1									
Position from slip surface (z)	Volumic weight (kN/m2)	τ_o (kN/m^2)	τ_{el} (kN/m^2)	c(kN/m^2)	τ	$\Delta\tau$	$\tau+\Delta\tau$	γ_τ	$\delta(\tau)$ (m)
0,00	16,00	20,80	20,00	30,00	20,80	0,50	21,30	9,91E-04	
									9,20E-04
0,95	16,00	19,81	19,52	29,29	19,81	0,48	20,29	9,40E-04	
									8,73E-04
1,90	16,00	18,82	19,05	28,57	18,82	0,45	19,27	8,93E-04	
									8,37E-04
2,86	16,00	17,83	18,57	27,86	17,83	0,43	18,26	8,65E-04	
									8,12E-04
3,81	16,00	16,84	18,10	27,14	16,84	0,40	17,25	8,39E-04	
									7,86E-04
4,76	16,00	15,85	17,62	26,43	15,85	0,38	16,23	8,11E-04	
									7,58E-04
5,71	16,00	14,86	17,14	25,71	14,86	0,36	15,22	7,81E-04	
									7,29E-04
6,67	16,00	13,87	16,67	25,00	13,87	0,33	14,20	7,50E-04	

H (m)	20,00
Gradient	6,52E-02
ΔN (kN/m^2)	8,28
N (kN/m^2)	8,28
$\delta_{\Delta N}$ (m)	5,71E-03
$\Sigma\delta_N$ (m)	5,71E-03
δ_τ (m)	5,71E-03
Δx (m)	33,13
Compatibility criterion	0,00
x (m)	33,13

Step n° 2									
Position from slip surface (z)	Volumic weight (kN/m2)	τ_o (kN/m^2)	τ_{el} (kN/m^2)	c(kN/m^2)	τ	$\Delta\tau$	$\tau+\Delta\tau$	γ_τ	$\delta(\tau)$ (m)
0,00	16,00	20,80	20,00	30,00	21,30	0,92	22,22	2,89E-03	
									2,68E-03
0,95	16,00	19,81	19,52	29,29	20,29	0,88	21,17	2,74E-03	
									2,54E-03
1,90	16,00	18,82	19,05	28,57	19,27	0,83	20,11	2,59E-03	
									2,41E-03
2,86	16,00	17,83	18,57	27,86	18,26	0,79	19,05	2,47E-03	
									2,31E-03
3,81	16,00	16,84	18,10	27,14	17,25	0,74	17,99	2,38E-03	
									2,23E-03
4,76	16,00	15,85	17,62	26,43	16,23	0,70	16,93	2,30E-03	
									2,15E-03
5,71	16,00	14,86	17,14	25,71	15,22	0,66	15,87	2,22E-03	
									2,07E-03
6,67	16,00	13,87	16,67	25,00	14,20	0,61	14,82	2,13E-03	

H (m)	20,00
Gradient	6,52E-02
ΔN (kN/m^2)	15,39
N (kN/m^2)	23,67
$\delta_{\Delta N}$ (m)	1,07E-02
$\Sigma\delta_N$ (m)	1,64E-02
δ_τ (m)	1,64E-02
Δx (m)	16,04
Compatibility criterion	0,00
x (m)	49,16

Step n°	3								
Position from slip surface (z)	Volumic weight (kN/m2)	τ_o (kN/m^2)	τ_{el} (kN/m^2)	c(kN/m^2)	τ	$\Delta\tau$	$\tau+\Delta\tau$	γ_τ	$\delta(\tau)$ (m)
0,00	16,00	20,80	20,00	30,00	22,22	0,96	23,19	5,01E-03	
									4,63E-03
0,95	16,00	19,81	19,52	29,29	21,17	0,92	22,08	4,73E-03	
									4,37E-03
1,90	16,00	18,82	19,05	28,57	20,11	0,87	20,98	4,46E-03	
									4,13E-03
2,86	16,00	17,83	18,57	27,86	19,05	0,82	19,87	4,22E-03	
									3,93E-03
3,81	16,00	16,84	18,10	27,14	17,99	0,78	18,77	4,02E-03	
									3,75E-03
4,76	16,00	15,85	17,62	26,43	16,93	0,73	17,67	3,86E-03	
									3,61E-03
5,71	16,00	14,86	17,14	25,71	15,87	0,69	16,56	3,72E-03	
									3,47E-03
6,67	16,00	13,87	16,67	25,00	14,82	0,64	15,46	3,57E-03	

H (m)	20,00
Gradient	6,52E-02
ΔN (kN/m^2)	16,46
N (kN/m^2)	40,13
$\delta_{\Delta N}$ (m)	1,15E-02
$\Sigma\delta_N$ (m)	2,79E-02
δ_τ (m)	2,79E-02
Δx (m)	8,66
Compatibility criterion	0,00
x (m)	57,82

Step n°	4								
Position from slip surface (z)	Volumic weight (kN/m2)	τ_o (kN/m^2)	τ_{el} (kN/m^2)	c(kN/m^2)	τ	$\Delta\tau$	$\tau+\Delta\tau$	γ_τ	$\delta(\tau)$ (m)
0,00	16,00	20,80	20,00	30,00	23,19	0,99	24,17	7,34E-03	
									6,78E-03
0,95	16,00	19,81	19,52	29,29	22,08	0,94	23,02	6,90E-03	
									6,38E-03
1,90	16,00	18,82	19,05	28,57	20,98	0,89	21,87	6,49E-03	
									6,00E-03
2,86	16,00	17,83	18,57	27,86	19,87	0,85	20,72	6,12E-03	
									5,67E-03
3,81	16,00	16,84	18,10	27,14	18,77	0,80	19,57	5,79E-03	
									5,38E-03
4,76	16,00	15,85	17,62	26,43	17,67	0,75	18,42	5,50E-03	
									5,13E-03
5,71	16,00	14,86	17,14	25,71	16,56	0,71	17,27	5,27E-03	
									4,91E-03
6,67	16,00	13,87	16,67	25,00	15,46	0,66	16,12	5,05E-03	

H (m)	20,00
Gradient	6,52E-02
ΔN (kN/m^2)	17,44
N (kN/m^2)	57,58
$\delta_{\Delta N}$ (m)	1,23E-02
$\Sigma\delta_N$ (m)	4,03E-02
δ_τ (m)	4,03E-02
Δx (m)	6,07
Compatibility criterion	0,00
x (m)	63,89

Step n°	5								
Position from slip surface (z)	Volumic weight (kN/m2)	τ_o (kN/m^2)	τ_{el} (kN/m^2)	c(kN/m^2)	τ	$\Delta\tau$	$\tau+\Delta\tau$	γ_τ	$\delta(\tau)$ (m)
0,00	16,00	20,80	20,00	30,00	24,17	1,01	25,18	9,93E-03	
									9,15E-03
0,95	16,00	19,81	19,52	29,29	23,02	0,96	23,98	9,30E-03	
									8,57E-03
1,90	16,00	18,82	19,05	28,57	21,87	0,91	22,78	8,71E-03	
									8,03E-03
2,86	16,00	17,83	18,57	27,86	20,72	0,86	21,58	8,17E-03	
									7,55E-03
3,81	16,00	16,84	18,10	27,14	19,57	0,81	20,38	7,69E-03	
									7,12E-03
4,76	16,00	15,85	17,62	26,43	18,42	0,77	19,18	7,26E-03	
									6,74E-03
5,71	16,00	14,86	17,14	25,71	17,27	0,72	17,99	6,89E-03	
									6,40E-03
6,67	16,00	13,87	16,67	25,00	16,12	0,67	16,79	6,57E-03	

H (m)	20,00
Gradient	6,52E-02
ΔN (kN/m^2)	18,52
N (kN/m^2)	76,10
$\delta_{\Delta N}$ (m)	1,33E-02
$\Sigma\delta_N$ (m)	5,36E-02
δ_τ (m)	5,36E-02
Δx (m)	4,78
Compatibility criterion	0,00
x (m)	68,67

Step n°	6								
Position from slip surface (z)	Volumic weight (kN/m2)	τ_o (kN/m^2)	τ_{el} (kN/m^2)	c(kN/m^2)	τ	Δτ	τ+Δτ	γ_τ	δ(τ) (m)
0,00	16,00	20,80	20,00	30,00	25,18	1,02	26,20	1,28E-02	
									1,18E-02
0,95	16,00	19,81	19,52	29,29	23,98	0,97	24,95	1,20E-02	
									1,10E-02
1,90	16,00	18,82	19,05	28,57	22,78	0,92	23,71	1,11E-02	
									1,03E-02
2,86	16,00	17,83	18,57	27,86	21,58	0,88	22,46	1,04E-02	
									9,59E-03
3,81	16,00	16,84	18,10	27,14	20,38	0,83	21,21	9,73E-03	
									8,99E-03
4,76	16,00	15,85	17,62	26,43	19,18	0,78	19,96	9,14E-03	
									8,45E-03
5,71	16,00	14,86	17,14	25,71	17,99	0,73	18,72	8,61E-03	
									7,98E-03
6,67	16,00	13,87	16,67	25,00	16,79	0,68	17,47	8,14E-03	

H (m)	20,00
Gradient	6,52E-02
ΔN (kN/m^2)	19,78
N (kN/m^2)	95,87
$\delta_{\Delta N}$ (m)	1,45E-02
$\Sigma\delta_N$ (m)	6,81E-02
δ_τ (m)	6,81E-02
Δx (m)	4,05
Compatibility criterion	0,00
x (m)	72,72

Step n°	7								
Position from slip surface (z)	Volumic weight (kN/m2)	τ_o (kN/m^2)	τ_{el} (kN/m^2)	c(kN/m^2)	τ	Δτ	τ+Δτ	γ_τ	δ(τ) (m)
0,00	16,00	20,80	20,00	30,00	26,20	1,03	27,23	1,62E-02	
									1,49E-02
0,95	16,00	19,81	19,52	29,29	24,95	0,98	25,94	1,50E-02	
									1,37E-02
1,90	16,00	18,82	19,05	28,57	23,71	0,94	24,64	1,39E-02	
									1,27E-02
2,86	16,00	17,83	18,57	27,86	22,46	0,89	23,34	1,28E-02	
									1,18E-02
3,81	16,00	16,84	18,10	27,14	21,21	0,84	22,05	1,20E-02	
									1,10E-02
4,76	16,00	15,85	17,62	26,43	19,96	0,79	20,75	1,12E-02	
									1,03E-02
5,71	16,00	14,86	17,14	25,71	18,72	0,74	19,45	1,04E-02	
									9,65E-03
6,67	16,00	13,87	16,67	25,00	17,47	0,69	18,16	9,81E-03	

H (m)	20,00
Gradient	6,52E-02
ΔN (kN/m^2)	21,31
N (kN/m^2)	117,18
$\delta_{\Delta N}$ (m)	1,60E-02
$\Sigma\delta_N$ (m)	8,41E-02
δ_τ (m)	8,41E-02
Δx (m)	3,60
Compatibility criterion	0,00
x (m)	76,32

Step n°	8								
Position from slip surface (z)	Volumic weight (kN/m2)	τ_o (kN/m^2)	τ_{el} (kN/m^2)	c(kN/m^2)	τ	Δτ	τ+Δτ	γ_τ	δ(τ) (m)
0,00	16,00	20,80	20,00	30,00	27,23	1,04	28,28	2,04E-02	
									1,85E-02
0,95	16,00	19,81	19,52	29,29	25,94	0,99	26,93	1,85E-02	
									1,69E-02
1,90	16,00	18,82	19,05	28,57	24,64	0,94	25,59	1,69E-02	
									1,55E-02
2,86	16,00	17,83	18,57	27,86	23,34	0,89	24,24	1,56E-02	
									1,43E-02
3,81	16,00	16,84	18,10	27,14	22,05	0,85	22,89	1,44E-02	
									1,32E-02
4,76	16,00	15,85	17,62	26,43	20,75	0,80	21,55	1,33E-02	
									1,23E-02
5,71	16,00	14,86	17,14	25,71	19,45	0,75	20,20	1,24E-02	
									1,14E-02
6,67	16,00	13,87	16,67	25,00	18,16	0,70	18,85	1,16E-02	

H (m)	20,00
Gradient	6,52E-02
ΔN (kN/m^2)	23,36
N (kN/m^2)	140,54
$\delta_{\Delta N}$ (m)	1,80E-02
$\Sigma\delta_N$ (m)	1,02E-01
δ_τ (m)	1,02E-01
Δx (m)	3,36
Compatibility criterion	0,00
x (m)	79,68

Step n°	9								
Position from slip surface (z)	Volumic weight (kN/m2)	τ_o (kN/m^2)	τ_{el} (kN/m^2)	c(kN/m^2)	τ	Δτ	τ+Δτ	γ_τ	δ(τ) (m)
0,00	16,00	20,80	20,00	30,00	28,28	1,05	29,33	2,63E-02	
									2,35E-02
0,95	16,00	19,81	19,52	29,29	26,93	1,00	27,93	2,30E-02	
									2,08E-02
1,90	16,00	18,82	19,05	28,57	25,59	0,95	26,54	2,06E-02	
									1,87E-02
2,86	16,00	17,83	18,57	27,86	24,24	0,90	25,14	1,87E-02	
									1,71E-02
3,81	16,00	16,84	18,10	27,14	22,89	0,85	23,74	1,71E-02	
									1,56E-02
4,76	16,00	15,85	17,62	26,43	21,55	0,80	22,35	1,57E-02	
									1,44E-02
5,71	16,00	14,86	17,14	25,71	20,20	0,75	20,95	1,45E-02	
									1,33E-02
6,67	16,00	13,87	16,67	25,00	18,85	0,70	19,55	1,35E-02	

H (m)	20,00
Gradient	6,52E-02
ΔN (kN/m^2)	26,61
N (kN/m^2)	167,15
$\delta_{\Delta N}$ (m)	2,13E-02
$\Sigma\delta_N$ (m)	1,23E-01
δ_τ (m)	1,23E-01
Δx (m)	3,33
Compatibility criterion	0,00
x (m)	83,01

Step n°	10								
Position from slip surface (z)	Volumic weight (kN/m2)	τ_o (kN/m^2)	τ_{el} (kN/m^2)	c(kN/m^2)	τ	Δτ	τ+Δτ	γ_τ	δ(τ) (m)
0,00	16,00	20,80	20,00	30,00	29,33	0,67	30,00	3,60E-02	
									2,99E-02
0,95	16,00	19,81	19,52	29,29	27,93	0,64	28,57	2,68E-02	
									2,39E-02
1,90	16,00	18,82	19,05	28,57	26,54	0,60	27,14	2,34E-02	
									2,11E-02
2,86	16,00	17,83	18,57	27,86	25,14	0,57	25,71	2,10E-02	
									1,90E-02
3,81	16,00	16,84	18,10	27,14	23,74	0,54	24,29	1,90E-02	
									1,73E-02
4,76	16,00	15,85	17,62	26,43	22,35	0,51	22,86	1,74E-02	
									1,59E-02
5,71	16,00	14,86	17,14	25,71	20,95	0,48	21,43	1,60E-02	
									1,46E-02
6,67	16,00	13,87	16,67	25,00	19,55	0,45	20,00	1,47E-02	

H (m)	20,00
Gradient	6,52E-02
ΔN (kN/m^2)	22,00
N (kN/m^2)	189,15
$\delta_{\Delta N}$ (m)	1,84E-02
$\Sigma\delta_N$ (m)	1,42E-01
δ_τ (m)	1,42E-01
Δx (m)	2,48
Compatibility criterion	0,00
x (m)	85,49

Stage II:

Step n°	1								
Position from slip surface (z)	Volumic weight (kN/m2)	τ_o (kN/m^2)	τ_{el} (kN/m^2)	c (kN/m^2)	τ	Δτ	τ+Δτ	γ_τ	δ(τ) (m)
0,00	16,00	20,80	20,00	30,00	30,00	-1,84	28,16	3,25E-02	
									2,66E-02
0,95	16,00	19,81	19,52	29,29	28,57	-1,75	26,82	2,34E-02	
									2,07E-02
1,90	16,00	18,82	19,05	28,57	27,14	-1,66	25,48	2,01E-02	
									1,81E-02
2,86	16,00	17,83	18,57	27,86	25,71	-1,58	24,14	1,78E-02	
									1,61E-02
3,81	16,00	16,84	18,10	27,14	24,29	-1,49	22,80	1,59E-02	
									1,44E-02
4,76	16,00	15,85	17,62	26,43	22,86	-1,40	21,46	1,44E-02	
									1,31E-02
5,71	16,00	14,86	17,14	25,71	21,43	-1,31	20,11	1,31E-02	
									1,19E-02
6,67	16,00	13,87	16,67	25,00	20,00	-1,23	18,77	1,20E-02	

H	20,00
Gradient	6,52E-02
ΔN	16,07
N	205,23
$\delta_{\Delta N}$ (m)	1,60E-02
$\Sigma\delta_N$ (m)	1,58E-01
δ_τ (m)	1,58E-01
Δx	1,94
Compatibility criterion	0,00
Slip in the failure plane	0,04
x (m)	87,43

Step n°	2								
Position from slip surface (z)	Volumic weight (kN/m2)	τ_o (kN/m^2)	τ_{el} (kN/m^2)	c (kN/m^2)	τ	$\Delta\tau$	$\tau+\Delta\tau$	γ_τ	$\delta(\tau)$ (m)
0,00	18,50	20,80	20,00	30,00	28,16	-1,84	26,32	2,91E-02	
									2,34E-02
0,95	18,50	19,81	19,52	29,29	26,82	-1,75	25,07	2,01E-02	
									1,76E-02
1,90	18,50	18,82	19,05	28,57	25,48	-1,66	23,81	1,69E-02	
									1,50E-02
2,86	18,50	17,83	18,57	27,86	24,14	-1,58	22,56	1,46E-02	
									1,31E-02
3,81	18,50	16,84	18,10	27,14	22,80	-1,49	21,31	1,29E-02	
									1,16E-02
4,76	18,50	15,85	17,62	26,43	21,46	-1,40	20,05	1,14E-02	
									1,03E-02
5,71	18,50	14,86	17,14	25,71	20,11	-1,31	18,80	1,02E-02	
									9,27E-03
6,67	18,50	13,87	16,67	25,00	18,77	-1,23	17,55	9,23E-03	

H	20,00
Gradient	6,52E-02
ΔN	11,68
N	216,90
$\delta_{\Delta N}$ (m)	1,60E-02
$\Sigma\delta_N$ (m)	1,74E-01
δ_τ (m)	1,74E-01
Δx	1,81
Compatibility criterion	0,00
Slip in the failure plane	0,07
x (m)	89,24

Step n°	3								
Position from slip surface (z)	Volumic weight (kN/m2)	τ_o (kN/m^2)	τ_{el} (kN/m^2)	c (kN/m^2)	τ	$\Delta\tau$	$\tau+\Delta\tau$	γ_τ	$\delta(\tau)$ (m)
0,00	18,50	20,80	20,00	30,00	26,32	-1,84	24,48	2,56E-02	
									2,02E-02
0,95	18,50	19,81	19,52	29,29	25,07	-1,75	23,32	1,67E-02	
									1,44E-02
1,90	18,50	18,82	19,05	28,57	23,81	-1,66	22,15	1,36E-02	
									1,19E-02
2,86	18,50	17,83	18,57	27,86	22,56	-1,58	20,98	1,14E-02	
									1,01E-02
3,81	18,50	16,84	18,10	27,14	21,31	-1,49	19,82	9,77E-03	
									8,67E-03
4,76	18,50	15,85	17,62	26,43	20,05	-1,40	18,65	8,44E-03	
									7,52E-03
5,71	18,50	14,86	17,14	25,71	18,80	-1,31	17,49	7,36E-03	
									6,58E-03
6,67	18,50	13,87	16,67	25,00	17,55	-1,23	16,32	6,47E-03	

H	20,00
Gradient	6,52E-02
ΔN	7,97
N	224,88
$\delta_{\Delta N}$ (m)	1,60E-02
$\Sigma\delta_N$ (m)	1,90E-01
δ_τ (m)	1,90E-01
Δx	1,73
Compatibility criterion	0,00
Slip in the failure plane	0,11
x (m)	90,98

Step n°	4								
Position from slip surface (z)	Volumic weight (kN/m2)	τ_o (kN/m^2)	τ_{el} (kN/m^2)	c (kN/m^2)	τ	$\Delta\tau$	$\tau+\Delta\tau$	γ_τ	$\delta(\tau)$ (m)
0,00	18,50	20,80	20,00	30,00	24,48	-1,84	22,64	2,22E-02	
									1,69E-02
0,95	18,50	19,81	19,52	29,29	23,32	-1,75	21,56	1,33E-02	
									1,13E-02
1,90	18,50	18,82	19,05	28,57	22,15	-1,66	20,49	1,03E-02	
									8,84E-03
2,86	18,50	17,83	18,57	27,86	20,98	-1,58	19,41	8,25E-03	
									7,11E-03
3,81	18,50	16,84	18,10	27,14	19,82	-1,49	18,33	6,68E-03	
									5,78E-03
4,76	18,50	15,85	17,62	26,43	18,65	-1,40	17,25	5,46E-03	
									4,73E-03
5,71	18,50	14,86	17,14	25,71	17,49	-1,31	16,17	4,48E-03	
									3,90E-03
6,67	18,50	13,87	16,67	25,00	16,32	-1,23	15,10	3,71E-03	

H	20,00
Gradient	6,52E-02
ΔN	4,65
N	229,53
$\delta_{\Delta N}$ (m)	1,60E-02
$\Sigma\delta_N$ (m)	2,06E-01
δ_τ (m)	2,06E-01
Δx	1,69
Compatibility criterion	0,00
Slip in the failure plane	0,15
x (m)	92,66

$\tau + \Delta\tau = \tau_0$

Step n° 5									
Position from slip surface (z)	Volumic weight (kN/m2)	τ_o (kN/m²)	τ_{el} (kN/m²)	c (kN/m²)	τ	Δτ	τ+Δτ	γ_τ	δ(τ) (m)
0,00	18,50	20,80	20,00	30,00	22,64	-1,84	20,80	1,87E-02	
									1,37E-02
0,95	18,50	19,81	19,52	29,29	21,56	-1,75	19,81	9,97E-03	
									8,10E-03
1,90	18,50	18,82	19,05	28,57	20,49	-1,66	18,82	7,04E-03	
									5,76E-03
2,86	18,50	17,83	18,57	27,86	19,41	-1,58	17,83	5,06E-03	
									4,12E-03
3,81	18,50	16,84	18,10	27,14	18,33	-1,49	16,84	3,60E-03	
									2,89E-03
4,76	18,50	15,85	17,62	26,43	17,25	-1,40	15,85	2,47E-03	
									1,94E-03
5,71	18,50	14,86	17,14	25,71	16,17	-1,31	14,86	1,61E-03	
									1,22E-03
6,67	18,50	13,87	16,67	25,00	15,10	-1,23	13,87	9,53E-04	

H	20,00
Gradient	6,52E-02
ΔN	1,53
N	231,06
$\delta_{\Delta N}$ (m)	1,60E-02
$\Sigma\delta_N$ (m)	2,22E-01
δ_τ (m)	2,22E-01
Δx	1,66
Compatibility criterion	0,00
Slip in the failure plane	0,18
x (m)	94,33

$\tau + \Delta\tau = c_r$

Step n° 6									
Position from slip surface (z)	Volumic weight (kN/m2)	τ_o (kN/m²)	τ_{el} (kN/m²)	c (kN/m²)	τ	Δτ	τ+Δτ	γ_τ	δ(τ) (m)
0,00	18,50	20,80	20,00	30,00	20,80	-5,80	15,00	7,84E-03	
									3,43E-03
0,95	18,50	19,81	19,52	29,29	19,81	-5,53	14,29	-6,43E-04	
									-1,88E-03
1,90	18,50	18,82	19,05	28,57	18,82	-5,25	13,57	-3,30E-03	
									-3,94E-03
2,86	18,50	17,83	18,57	27,86	17,83	-4,97	12,86	-4,98E-03	
									-5,30E-03
3,81	18,50	16,84	18,10	27,14	16,84	-4,70	12,14	-6,14E-03	
									-6,23E-03
4,76	18,50	15,85	17,62	26,43	15,85	-4,42	11,43	-6,94E-03	
									-6,86E-03
5,71	18,50	14,86	17,14	25,71	14,86	-4,15	10,71	-7,46E-03	
									-7,24E-03
6,67	18,50	13,87	16,67	25,00	13,87	-3,87	10,00	-7,75E-03	

H	20,00
Gradient	6,52E-02
ΔN	-15,71
N	215,34
$\delta_{\Delta N}$ (m)	5,04E-02
$\Sigma\delta_N$ (m)	2,72E-01
δ_τ (m)	2,72E-01
Δx	5,41
Compatibility criterion	0,00
Slip in the failure plane	0,30
x (m)	99,74

Calculation of instability parameters:

Instability	
Δx	39,81
δ_τ (m)	0,45
L (m)	139,55
N (kN/m)	0,00

Summary of the results:

Results						
ΣΔx for stage 1 (m)	ΣΔx for stage 2 (m)	L_{crit} (m)	δ_{crit} (m)	N_{crit} (kN/m)	L_{instab} (m)	δ_{instab} (m)
85,49	8,84	94,33	0,22	231,06	139,55	0,45

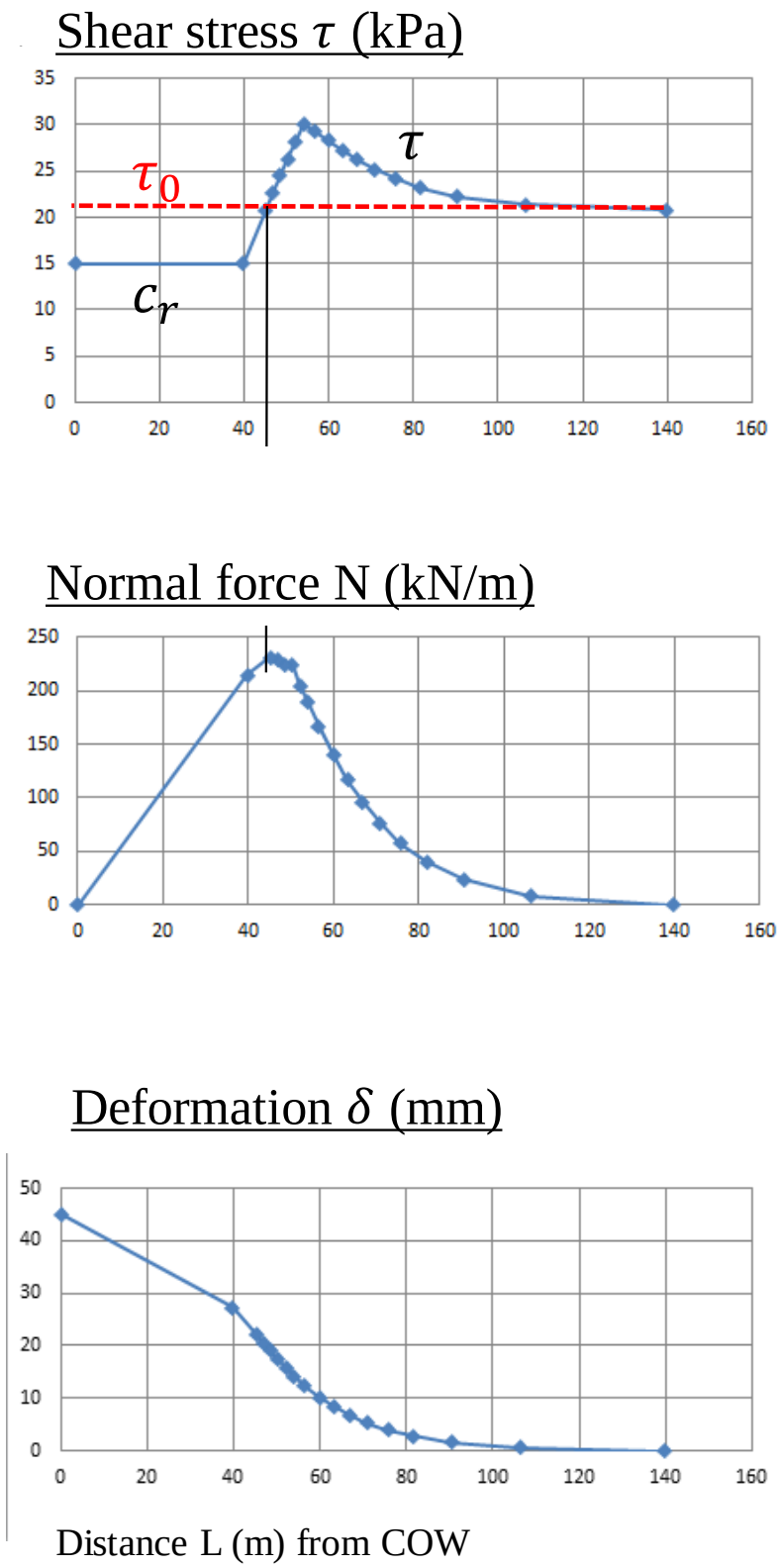

Figure C-1. Shear stresses τ, normal force N and deformation δ as function of the distance L from disturbing load N,

Table C-1 Summarry of calculations

Appendix C. Introductory Example

Step	x	L = 139,5 - x	$\tau+\Delta\tau$	τ_0	N	δ	Moment
	m	m	kPa		kN/m	mm	
0	0	139,5	20,8	20,8	0	0	a
I-1	33,13	106,37	21,3	20,8	8,28	0,571	
I-2	49,16	90,34	22,22	20,8	23,67	1,64	
I-3	57,82	81,68	23,19	20,8	40,13	2,79	
I-4	63,89	75,61	24,17	20,8	57,58	4,03	
I-5	68,67	70,83	25,18	20,8	76,1	5,36	
I-6	72,77	66,73	26,2	20,8	95,87	6,81	
I-7	76,32	63,18	27,23	20,8	117,18	8,41	
I-8	79,68	59,82	28,28	20,8	140,54	10,2	
I-9	83,01	56,49	29,33	20,8	167,15	12,3	
I-10	85,49	54,01	30	20,8	189,15	14,2	b
II-1	87,43	52,07	28,16	20,8	205,23	15,8	
II-2	89,24	50,26	26,32	20,8	224,88	17,4	
II-3	90,98	48,52	24,48	20,8	224,88	19	
II-4	92,66	46,84	22,64	20,8	229,53	20,6	
II-5	94,33	45,17	20,8	20,8	231,6	22,2	c
II-6	99,74	39,76	15	20,8	215,34	27,2	d
II-7	139,5	0	15	20,8	0	45	e

D. Calculations regarding Muskrat Falls Upper Clay Layer

This is the detailed calculation for the example of landslide investigation carried in chapter 5.2.3 with the excel spreadsheet developed during this work.

PARAMETERS														
Poisson ratio	Peak shear strength	Residual shear strength	Shear strength at surface	Sensitivity ratio	Shear stress at elastic limit	Deviator strain at elastic limit	Deviator strain at failure limit	Secant modulus in shear	Elastic modulus	Slip for residual shear strength	Depth of ground of the upper layer	Gradient of the slip surface	Thickness of the failure layer	Average density of the layer above
ν	c (kN/m^2)	c_R (kN/m^2)	c_s (kN/m^2)	c_R/c	τ_{el} (kN/m^2)	γ_{el} (%)	γ_f (%)	G (kN/m^2)	E_{mean} (kN/m^2)	δ_{cr} (m)	H (m)	β	Hc (m)	ρ (kN/m^2)
0,334	60	12	45	0,2	40	0,035	0,07	1142,8571	3000	0,3	28	0,04	15	18,8

Stage I:

Step n°	1								
Position from slip surface (z)	ρ_c (kN/m^2)	τ_o (kN/m^2)	τ_{el} (kN/m^2)	c(kN/m^2)	τ	$\Delta\tau$	$\tau+\Delta\tau$	γ_τ	$\delta(\tau)$ (m)
0,00	18,00	22,45	40,00	60,00	22,45	17,55	40,00	1,54E-02	
									1,09E-02
0,71	18,00	21,93	39,76	59,64	21,91	17,13	39,04	1,51E-02	
									1,07E-02
1,43	18,00	21,42	39,52	59,28	21,37	16,71	38,08	1,48E-02	
									1,05E-02
2,14	18,00	20,91	39,28	58,92	20,83	16,29	37,12	1,45E-02	
									1,03E-02
2,86	18,00	20,39	39,04	58,56	20,30	15,87	36,16	1,42E-02	
									1,01E-02
3,57	18,00	19,88	38,80	58,20	19,76	15,45	35,20	1,40E-02	
									9,88E-03
4,29	18,00	19,37	38,56	57,84	19,22	15,03	34,24	1,37E-02	
									9,70E-03
5,00	18,00	18,85	38,32	57,48	18,68	14,60	33,28	1,35E-02	

H1 (m)	29,02
H2 (m)	30,55
H (m)	29,78
Gradient	0,04
ΔN (kN/m)	335,74
N (kN/m)	335,74
$\delta_{\Delta N}$ (m)	7,19E-02
$\Sigma\delta_N$ (m)	7,19E-02
δ_τ (m)	7,19E-02
Δx (m)	38,26
Compatibility criterion	0,00
x (m)	38,26
Calculation	Solver OK
Condition for brittle failure	Brittle failure

(*) H_1 is the height of the right boarder of the upper part of the slice considered above the clay layer

(**) H_2 is the height of the left boarder of the upper part of the slice considered above the clay layer

(***) H is the average height of the slice considered above the clay layer $H = \frac{H1+H2}{2}$

Step n°	2								
Position from slip surface (z)	ρ_c (kN/m²)	τ_o (kN/m²)	τ_{el} (kN/m²)	c(kN/m²)	τ	Δτ	τ+Δτ	γ_τ	δ(τ) (m)
0,00	18,00	22,13	40,00	60,00	40,00	2,22	42,22	1,76E-02	
									1,25E-02
0,71	18,00	21,62	39,75	59,63	39,04	2,17	41,21	1,73E-02	
									1,22E-02
1,43	18,00	21,10	39,51	59,26	38,08	2,11	40,19	1,69E-02	
									1,20E-02
2,14	18,00	20,59	39,26	58,89	37,12	2,06	39,18	1,66E-02	
									1,17E-02
2,86	18,00	20,07	39,01	58,52	36,16	2,00	38,17	1,62E-02	
									1,15E-02
3,57	18,00	19,56	38,77	58,15	35,20	1,95	37,15	1,59E-02	
									1,12E-02
4,29	18,00	19,05	38,52	57,78	34,24	1,89	36,14	1,55E-02	
									1,10E-02
5,00	18,00	18,53	38,27	57,41	33,28	1,84	35,12	1,52E-02	

H1 (m)	28,92
H2 (m)	29,02
H (m)	28,97
Gradient	0,04
ΔN (kN/m)	46,55
N (kN/m)	382,29
δΔN (m)	1,01E-02
ΣδN (m)	8,20E-02
δτ (m)	8,20E-02
Δx (m)	2,45
Compatibility criterion	0,00
x (m)	40,71
Calculation	Solver OK
Condition for brittle failure	Brittle failure

Step n°	3								
Position from slip surface (z)	ρ_c (kN/m²)	τ_o (kN/m²)	τ_{el} (kN/m²)	c(kN/m²)	τ	Δτ	τ+Δτ	γ_τ	δ(τ) (m)
0,00	18,00	22,09	40,00	60,00	42,22	2,28	44,51	1,99E-02	
									1,40E-02
0,71	18,00	21,58	39,75	59,63	41,21	2,23	43,44	1,94E-02	
									1,37E-02
1,43	18,00	21,07	39,51	59,26	40,19	2,17	42,37	1,90E-02	
									1,34E-02
2,14	18,00	20,55	39,26	58,89	39,18	2,12	41,30	1,85E-02	
									1,31E-02
2,86	18,00	20,04	39,01	58,52	38,17	2,06	40,22	1,81E-02	
									1,28E-02
3,57	18,00	19,53	38,76	58,14	37,15	2,00	39,15	1,77E-02	
									1,25E-02
4,29	18,00	19,01	38,52	57,77	36,14	1,95	38,08	1,73E-02	
									1,22E-02
5,00	18,00	18,50	38,27	57,40	35,12	1,89	37,01	1,69E-02	

H1 (m)	28,84
H2 (m)	28,92
H (m)	28,88
Gradient	0,04
ΔN (kN/m)	44,54
N (kN/m)	426,83
δΔN (m)	9,78E-03
ΣδN (m)	9,18E-02
δτ (m)	9,18E-02
Δx (m)	2,09
Compatibility criterion	0,00
x (m)	42,80
Calculation	Solver OK
Condition for brittle failure	Brittle failure

Step n°	4								
Position from slip surface (z)	ρ_c (kN/m²)	τ_o (kN/m²)	τ_{el} (kN/m²)	c(kN/m²)	τ	Δτ	τ+Δτ	γ_τ	δ(τ) (m)
0,00	18,00	22,06	40,00	60,00	44,51	2,32	46,83	2,23E-02	
									1,57E-02
0,71	18,00	21,55	39,75	59,63	43,44	2,26	45,70	2,17E-02	
									1,53E-02
1,43	18,00	21,03	39,50	59,26	42,37	2,21	44,57	2,12E-02	
									1,49E-02
2,14	18,00	20,52	39,26	58,88	41,30	2,15	43,44	2,07E-02	
									1,46E-02
2,86	18,00	20,01	39,01	58,51	40,22	2,09	42,32	2,02E-02	
									1,42E-02
3,57	18,00	19,49	38,76	58,14	39,15	2,03	41,19	1,97E-02	
									1,39E-02
4,29	18,00	18,98	38,51	57,77	38,08	1,98	40,06	1,92E-02	
									1,35E-02
5,00	18,00	18,47	38,26	57,40	37,01	1,92	38,93	1,87E-02	

H1 (m)	28,76
H2 (m)	28,84
H (m)	28,80
Gradient	0,04
ΔN (kN/m)	47,19
N (kN/m)	474,02
δΔN (m)	1,04E-02
ΣδN (m)	1,02E-01
δτ (m)	1,02E-01
Δx (m)	2,00
Compatibility criterion	0,00
x (m)	44,80
Calculation	Solver OK
Condition for brittle failure	Brittle failure

Step n°	5								
Position from slip surface (z)	ρ_c (kN/m²)	τ_o (kN/m²)	τ_{el} (kN/m²)	c(kN/m²)	τ	Δτ	τ+Δτ	γ_τ	δ(τ) (m)
0,00	18,00	22,03	40,00	60,00	46,83	2,35	49,18	2,50E-02	
									1,76E-02
0,71	18,00	21,52	39,75	59,63	45,70	2,29	47,99	2,43E-02	
									1,71E-02
1,43	18,00	21,00	39,50	59,25	44,57	2,23	46,80	2,36E-02	
									1,66E-02
2,14	18,00	20,49	39,25	58,88	43,44	2,17	45,62	2,30E-02	
									1,62E-02
2,86	18,00	19,98	39,01	58,51	42,32	2,12	44,43	2,23E-02	
									1,57E-02
3,57	18,00	19,46	38,76	58,13	41,19	2,06	43,24	2,17E-02	
									1,53E-02
4,29	18,00	18,95	38,51	57,76	40,06	2,00	42,06	2,12E-02	
									1,49E-02
5,00	18,00	18,43	38,26	57,39	38,93	1,94	40,87	2,06E-02	

H1 (m)	28,68
H2 (m)	28,76
H (m)	28,72
Gradient	0,04
ΔN (kN/m)	50,55
N (kN/m)	524,57
δΔN (m)	1,13E-02
ΣδN (m)	1,13E-01
δτ (m)	1,13E-01
Δx (m)	1,95
Compatibility criterion	0,00
x (m)	46,75
Calculation	Solver OK
Condition for brittle failure	Brittle failure

Step n°	6								
Position from slip surface (z)	ρ_c (kN/m²)	τ_o (kN/m²)	τ_{el} (kN/m²)	c(kN/m²)	τ	Δτ	τ+Δτ	γ_τ	δ(τ) (m)
0,00	18,00	22,00	40,00	60,00	49,18	2,37	51,55	2,80E-02	
									1,97E-02
0,71	18,00	21,49	39,75	59,63	47,99	2,31	50,30	2,71E-02	
									1,91E-02
1,43	18,00	20,97	39,50	59,25	46,80	2,25	49,06	2,63E-02	
									1,85E-02
2,14	18,00	20,46	39,25	58,88	45,62	2,19	47,81	2,55E-02	
									1,79E-02
2,86	18,00	19,95	39,00	58,50	44,43	2,13	46,57	2,47E-02	
									1,74E-02
3,57	18,00	19,43	38,75	58,13	43,24	2,07	45,32	2,40E-02	
									1,69E-02
4,29	18,00	18,92	38,50	57,76	42,06	2,02	44,07	2,33E-02	
									1,64E-02
5,00	18,00	18,40	38,25	57,38	40,87	1,96	42,83	2,26E-02	

H1 (m)	28,60
H2 (m)	28,68
H (m)	28,64
Gradient	0,04
ΔN (kN/m)	54,52
N (kN/m)	579,09
δΔN (m)	1,23E-02
ΣδN (m)	1,26E-01
δτ (m)	1,26E-01
Δx (m)	1,92
Compatibility criterion	0,00
x (m)	48,67
Calculation	Solver OK
Condition for brittle failure	Brittle failure

Step n°	7								
Position from slip surface (z)	ρ_c (kN/m²)	τ_o (kN/m²)	τ_{el} (kN/m²)	c(kN/m²)	τ	Δτ	τ+Δτ	γ_τ	δ(τ) (m)
0,00	18,00	21,97	40,00	60,00	51,55	2,39	53,94	3,15E-02	
									2,21E-02
0,71	18,00	21,46	39,75	59,62	50,30	2,33	52,63	3,03E-02	
									2,13E-02
1,43	18,00	20,94	39,50	59,25	49,06	2,27	51,32	2,93E-02	
									2,06E-02
2,14	18,00	20,43	39,25	58,87	47,81	2,21	50,02	2,83E-02	
									1,99E-02
2,86	18,00	19,92	39,00	58,50	46,57	2,15	48,71	2,73E-02	
									1,92E-02
3,57	18,00	19,40	38,75	58,12	45,32	2,09	47,41	2,64E-02	
									1,86E-02
4,29	18,00	18,89	38,50	57,75	44,07	2,03	46,10	2,56E-02	
									1,80E-02
5,00	18,00	18,37	38,25	57,37	42,83	1,97	44,80	2,48E-02	

H1 (m)	28,52
H2 (m)	28,60
H (m)	28,56
Gradient	0,04
ΔN (kN/m)	59,54
N (kN/m)	638,64
δΔN (m)	1,37E-02
ΣδN (m)	1,40E-01
δτ (m)	1,40E-01
Δx (m)	1,94
Compatibility criterion	0,00
x (m)	50,61
Calculation	Solver OK
Condition for brittle failure	Brittle failure

Step n°	8								
Position from slip surface (z)	ρ_c (kN/m²)	τ_o (kN/m²)	τ_{el} (kN/m²)	c(kN/m²)	τ	Δτ	τ+Δτ	γ_τ	δ(τ) (m)
0,00	18,00	21,94	40,00	60,00	53,94	2,40	56,34	3,58E-02	
									2,50E-02
0,71	18,00	21,43	39,75	59,62	52,63	2,34	54,97	3,42E-02	
									2,39E-02
1,43	18,00	20,91	39,50	59,25	51,32	2,28	53,61	3,28E-02	
									2,29E-02
2,14	18,00	20,40	39,25	58,87	50,02	2,22	52,24	3,15E-02	
									2,20E-02
2,86	18,00	19,88	39,00	58,50	48,71	2,16	50,87	3,03E-02	
									2,12E-02
3,57	18,00	19,37	38,75	58,12	47,41	2,10	49,51	2,92E-02	
									2,05E-02
4,29	18,00	18,86	38,50	57,74	46,10	2,04	48,14	2,81E-02	
									1,98E-02
5,00	18,00	18,34	38,24	57,37	44,80	1,98	46,78	2,72E-02	

H1 (m)	28,44
H2 (m)	28,52
H (m)	28,48
Gradient	0,04
ΔN (kN/m)	66,58
N (kN/m)	705,22
δΔN (m)	1,58E-02
ΣδN (m)	1,55E-01
δτ (m)	1,55E-01
Δx (m)	2,01
Compatibility criterion	0,00
x (m)	52,61
Calculation	Solver OK
Condition for brittle failure	Brittle failure

Step n°	9								
Position from slip surface (z)	ρ_c (kN/m²)	τ_o (kN/m²)	τ_{el} (kN/m²)	c(kN/m²)	τ	Δτ	τ+Δτ	γ_τ	δ(τ) (m)
0,00	18,00	21,91	40,00	60,00	56,34	2,41	58,75	4,21E-02	
									2,91E-02
0,71	18,00	21,39	39,75	59,62	54,97	2,35	57,33	3,93E-02	
									2,73E-02
1,43	18,00	20,88	39,50	59,25	53,61	2,29	55,90	3,71E-02	
									2,58E-02
2,14	18,00	20,37	39,25	58,87	52,24	2,23	54,47	3,53E-02	
									2,46E-02
2,86	18,00	19,85	38,99	58,49	50,87	2,17	53,05	3,37E-02	
									2,36E-02
3,57	18,00	19,34	38,74	58,11	49,51	2,11	51,62	3,23E-02	
									2,26E-02
4,29	18,00	18,82	38,49	57,74	48,14	2,05	50,19	3,10E-02	
									2,17E-02
5,00	18,00	18,31	38,24	57,36	46,78	1,99	48,77	2,98E-02	

H1 (m)	28,36
H2 (m)	28,44
H (m)	28,40
Gradient	0,04
ΔN (kN/m)	78,61
N (kN/m)	783,83
δΔN (m)	1,93E-02
ΣδN (m)	1,75E-01
δτ (m)	1,75E-01
Δx (m)	2,21
Compatibility criterion	0,00
x (m)	54,82
Calculation	Solver OK
Condition for brittle failure	Brittle failure

Step n°	10								
Position from slip surface (z)	ρ_c (kN/m²)	τ_o (kN/m²)	τ_{el} (kN/m²)	c(kN/m²)	τ	Δτ	τ+Δτ	γ_τ	δ(τ) (m)
0,00	18,00	21,88	40,00	60,00	58,75	1,25	60,00	5,09E-02	
									3,35E-02
0,71	18,00	21,36	39,75	59,62	57,33	1,22	58,54	4,30E-02	
									2,96E-02
1,43	18,00	20,85	39,50	59,24	55,90	1,18	57,08	3,99E-02	
									2,77E-02
2,14	18,00	20,34	39,24	58,87	54,47	1,15	55,63	3,76E-02	
									2,62E-02
2,86	18,00	19,82	38,99	58,49	53,05	1,12	54,17	3,57E-02	
									2,49E-02
3,57	18,00	19,31	38,74	58,11	51,62	1,09	52,71	3,41E-02	
									2,38E-02
4,29	18,00	18,80	38,49	57,73	50,19	1,06	51,25	3,26E-02	
									2,28E-02
5,00	18,00	18,28	38,23	57,35	48,77	1,03	49,80	3,13E-02	

H1 (m)	28,30
H2 (m)	28,36
H (m)	28,33
Gradient	0,04
ΔN (kN/m)	55,00
N (kN/m)	838,83
δΔN (m)	1,40E-02
ΣδN (m)	1,89E-01
δτ (m)	1,89E-01
Δx (m)	1,47
Compatibility criterion	0,00
x (m)	56,29
Calculation	Solver OK
Condition for brittle failure	Brittle failure

Stage II:

Step n°	1								
Position from slip surface (z)	ρ_c (kN/m²)	τ_o (kN/m²)	τ_{el} (kN/m²)	c (kN/m²)	τ	Δτ	τ+Δτ	γ_τ	δ(τ) (m)
0,00	18,00	22,13	40,00	60,00	60,00	-7,57	52,43	4,40E-02	
									2,87E-02
0,71	18,00	21,62	39,75	59,62	58,54	-7,38	51,16	3,63E-02	
									2,49E-02
1,43	18,00	21,10	39,49	59,24	57,08	-7,19	49,89	3,34E-02	
									2,30E-02
2,14	18,00	20,59	39,24	58,86	55,63	-7,00	48,63	3,12E-02	
									2,16E-02
2,86	18,00	20,07	38,99	58,48	54,17	-6,81	47,36	2,94E-02	
									2,05E-02
3,57	18,00	19,56	38,74	58,10	52,71	-6,62	46,09	2,79E-02	
									1,94E-02
4,29	18,00	19,05	38,48	57,73	51,25	-6,43	44,83	2,65E-02	
									1,85E-02
5,00	18,00	18,53	38,23	57,35	49,80	-6,23	43,56	2,53E-02	

H1 (m)	28,24
H2 (m)	28,30
H (m)	28,27
Gradient	0,04
ΔN (kN/m)	51,35
N (kN/m)	890,19
δΔN (m)	1,54E-02
ΣδN (m)	2,04E-01
δτ (m)	2,04E-01
Δx (m)	1,51E+00
Compatibility criterion	0,00
Slip in the failure plane	0,05
x (m)	57,79
Calculation	Solver OK
Condition for brittle failure	Brittle failure

Step n°	2								
Position from slip surface (z)	ρ_c (kN/m²)	τ_o (kN/m²)	τ_{el} (kN/m²)	c (kN/m²)	τ	Δτ	τ+Δτ	γ_τ	δ(τ) (m)
0,00	18,00	22,09	40,00	60,00	52,43	-7,58	44,84	3,74E-02	
									2,40E-02
0,71	18,00	21,58	39,75	59,62	51,16	-7,39	43,77	2,98E-02	
									2,03E-02
1,43	18,00	21,07	39,49	59,24	49,89	-7,20	42,70	2,70E-02	
									1,86E-02
2,14	18,00	20,55	39,24	58,86	48,63	-7,01	41,62	2,50E-02	
									1,72E-02
2,86	18,00	20,04	38,99	58,48	47,36	-6,81	40,55	2,33E-02	
									1,62E-02
3,57	18,00	19,53	38,73	58,10	46,09	-6,62	39,47	2,19E-02	
									1,52E-02
4,29	18,00	19,01	38,48	57,72	44,83	-6,43	38,40	2,07E-02	
									1,44E-02
5,00	18,00	18,50	38,23	57,34	43,56	-6,24	37,32	1,97E-02	

H1 (m)	28,18
H2 (m)	28,24
H (m)	28,21
Gradient	0,04
ΔN (kN/m)	41,10
N (kN/m)	931,28
δΔN (m)	1,67E-02
ΣδN (m)	2,21E-01
δτ (m)	2,21E-01
Δx (m)	1,55E+00
Compatibility criterion	0,00
Slip in the failure plane	0,09
x (m)	59,34
Calculation	Solver OK
Condition for brittle failure	Brittle failure

Step n°	3								
Position from slip surface (z)	ρ_c (kN/m²)	τ_o (kN/m²)	τ_{el} (kN/m²)	c (kN/m²)	τ	Δτ	τ+Δτ	γ_τ	δ(τ) (m)
0,00	18,00	22,06	40,00	60,00	44,84	-7,59	37,26	3,08E-02	
									1,93E-02
0,71	18,00	21,55	39,75	59,62	43,77	-7,39	36,38	2,34E-02	
									1,57E-02
1,43	18,00	21,03	39,49	59,24	42,70	-7,20	35,49	2,07E-02	
									1,41E-02
2,14	18,00	20,52	39,24	58,86	41,62	-7,01	34,61	1,87E-02	
									1,28E-02
2,86	18,00	20,01	38,98	58,48	40,55	-6,82	33,73	1,72E-02	
									1,19E-02
3,57	18,00	19,49	38,73	58,10	39,47	-6,62	32,85	1,60E-02	
									1,10E-02
4,29	18,00	18,98	38,48	57,72	38,40	-6,43	31,97	1,49E-02	
									1,03E-02
5,00	18,00	18,47	38,22	57,34	37,32	-6,24	31,08	1,40E-02	

H1 (m)	28,12
H2 (m)	28,18
H (m)	28,15
Gradient	0,04
ΔN (kN/m)	28,27
N (kN/m)	959,55
δΔN (m)	1,67E-02
ΣδN (m)	2,37E-01
δτ (m)	2,37E-01
Δx (m)	1,49E+00
Compatibility criterion	0,00
Slip in the failure plane	0,14
x (m)	60,83
Calculation	Solver OK
Condition for brittle failure	Brittle failure

Step n°	4										
Position from slip surface (z)	ρ_c (kN/m²)	τ_0 (kN/m²)	τ_{el} (kN/m²)	c (kN/m²)	τ	$\Delta\tau$	$\tau+\Delta\tau$	γ_τ	$\delta(\tau)$ (m)		
0,00	18,00	22,03	40,00	60,00	37,26	-7,59	29,66	2,42E-02		H1 (m)	28,06
									1,47E-02	H2 (m)	28,12
0,71	18,00	21,52	39,75	59,62	36,38	-7,40	28,97	1,69E-02		H (m)	28,09
									1,11E-02	Gradient	0,04
1,43	18,00	21,00	39,49	59,24	35,49	-7,21	28,29	1,43E-02		ΔN (kN/m)	16,59
									9,58E-03	N (kN/m)	976,15
2,14	18,00	20,49	39,24	58,86	34,61	-7,01	27,60	1,25E-02		δΔN (m)	1,67E-02
									8,45E-03	ΣδN (m)	2,54E-01
2,86	18,00	19,98	38,98	58,47	33,73	-6,82	26,91	1,11E-02		δτ (m)	2,54E-01
									7,56E-03	Δx (m)	1,45E+00
3,57	18,00	19,46	38,73	58,09	32,85	-6,63	26,22	1,00E-02		Compatibility criterion	0,00
									6,82E-03	Slip in the failure plane	0,19
4,29	18,00	18,95	38,47	57,71	31,97	-6,43	25,53	9,08E-03		x (m)	62,28
									6,21E-03	Calculation	Solver OK
5,00	18,00	18,43	38,22	57,33	31,08	-6,24	24,84	8,29E-03		Condition for brittle failure	Brittle failure

$$\tau + \Delta\tau = \tau_0$$

Step n°	5										
Position from slip surface (z)	ρ_c (kN/m²)	τ_0 (kN/m²)	τ_{el} (kN/m²)	c (kN/m²)	τ	$\Delta\tau$	$\tau+\Delta\tau$	γ_τ	$\delta(\tau)$ (m)		
0,00	18,00	22,00	40,00	60,00	29,66	-7,66	22,00	1,75E-02		H1 (m)	28,00
									9,94E-03	H2 (m)	28,06
0,71	18,00	21,49	39,75	59,62	28,97	-7,47	21,51	1,03E-02		H (m)	28,03
									6,50E-03	Gradient	0,04
1,43	18,00	20,97	39,49	59,24	28,29	-7,27	21,01	7,89E-03		ΔN (kN/m)	5,54
									5,05E-03	N (kN/m)	981,69
2,14	18,00	20,46	39,24	58,85	27,60	-7,08	20,52	6,24E-03		δΔN (m)	1,68E-02
									4,01E-03	ΣδN (m)	2,71E-01
2,86	18,00	19,95	38,98	58,47	26,91	-6,88	20,03	4,99E-03		δτ (m)	2,71E-01
									3,21E-03	Δx (m)	1,45E+00
3,57	18,00	19,43	38,73	58,09	26,22	-6,69	19,53	4,01E-03		Compatibility criterion	0,00
									2,58E-03	Slip in the failure plane	0,24
4,29	18,00	18,92	38,47	57,71	25,53	-6,49	19,04	3,21E-03		x (m)	63,73
									2,06E-03	Calculation	Solver OK
5,00	18,00	18,40	38,22	57,32	24,84	-6,30	18,55	2,56E-03		Condition for brittle failure	Brittle failure

$$\tau + \Delta\tau = c_r$$

Step n°	6								
Position from slip surface (z)	ρ_c (kN/m^2)	τ_0 (kN/m^2)	τ_{el} (kN/m^2)	c (kN/m^2)	τ	$\Delta\tau$	$\tau+\Delta\tau$	γ_τ	$\delta(\tau)$ (m)
0,00	18,00	21,97	40,00	60,00	37,26	-25,26	12,00	8,78E-03	
									3,76E-03
0,71	18,00	21,46	39,75	59,62	36,38	-24,62	11,76	1,76E-03	
									4,47E-04
1,43	18,00	20,94	39,49	59,24	35,49	-23,98	11,52	-5,06E-04	
									-8,91E-04
2,14	18,00	20,43	39,24	58,86	34,61	-23,34	11,28	-1,99E-03	
									-1,80E-03
2,86	18,00	19,92	38,99	58,48	33,73	-22,70	11,03	-3,06E-03	
									-2,48E-03
3,57	18,00	19,40	38,73	58,10	32,85	-22,05	10,79	-3,87E-03	
									-2,99E-03
4,29	18,00	18,89	38,48	57,72	31,97	-21,41	10,55	-4,49E-03	
									-3,38E-03
5,00	18,00	18,37	38,22	57,34	31,08	-20,77	10,31	-4,96E-03	

H1 (m)	28,00
H2 (m)	28,33
H (m)	28,17
Gradient	0,04
ΔN (kN/m)	22,10
N (kN/m)	912,28
δΔN (m)	8,87E-02
ΣδN (m)	2,93E-01
δτ (m)	2,93E-01
Δx (m)	8,31E+00
Compatibility criterion	0,00
Slip in the failure plane	0,30
x (m)	72,04
Calculation	Solver OK
Condition for brittle failure	Brittle failure

Calculation of instability parameters:

Instability	
Δx	91,49422616
δ_τ (m)	0,786587926
L	163,5358295
N	0

Summary of the results:

Results									
ΣΔx for stage 1	ΣΔx for stage 2	L_{crit} (m)	δ_{crit} (m)	N_{crit} (kN/m)	L_{instab} (m)	δ_{instab} (m)	Safety Factor	Calculation	Brittle failure
56,29	7,44	63,73	0,27	981,69	163,54	0,79	0,09	Solver OK	Brittle failure

Table D-1. Summary of calcualtions

Step	x m	L = 163,53 - x m	$\tau+\Delta\tau$ kPa	τ_0	N kN/m	d mm
0	0	163,53	22,45	22,45	0	0
I-1	38,26	125,27	40	22,45	335,74	0,07
I-2	40,71	122,82	42,22	22,13	382,29	0,08
I-3	42,8	120,73	44,51	22,09	426,83	0,09
I-4	44,8	118,73	46,83	22,06	474,02	0,1
I-5	46,75	116,78	49,18	22,03	524,57	0,11
I-6	48,67	114,86	51,55	22	579,09	0,12
I-7	50,61	112,92	53,94	21,97	638,64	0,14
I-8	52,61	110,92	56,34	21,94	705,22	0,155
I-9	54,82	108,71	58,75	21,91	783,83	0,175
I-10	56,29	107,24	60	21,88	838,83	0,189
II-1	57,79	105,74	52,43	22,13	890,19	0,204
II-2	59,34	104,19	44,84	22,09	931,28	0,221

II-3	60,83	102,7	37,26	22,06	959,55	0,237
II-4	62,28	101,25	29,66	22,03	976,15	0,254
II-5	63,73	99,8	22	22	981,69	0,271
II-6	72,04	91,49	12	21,97	912,28	0,293
II-7	163,53	0	12	22	0	0,79

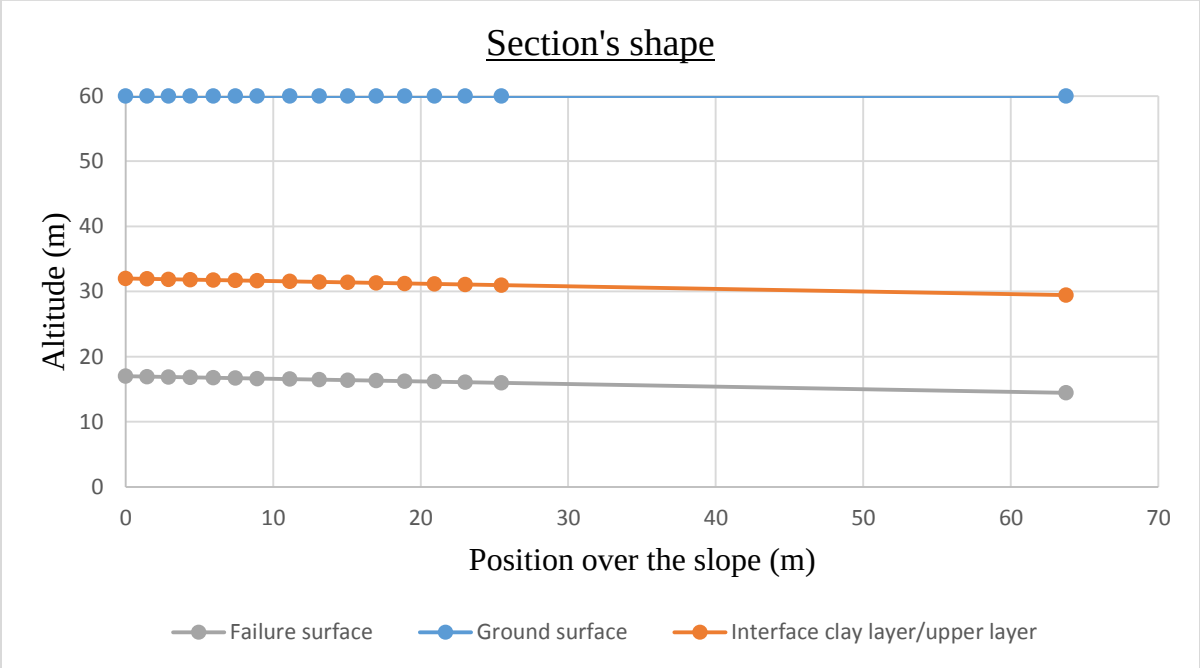

Figure D-1, Shape of geometric simplification of the North Spur studied

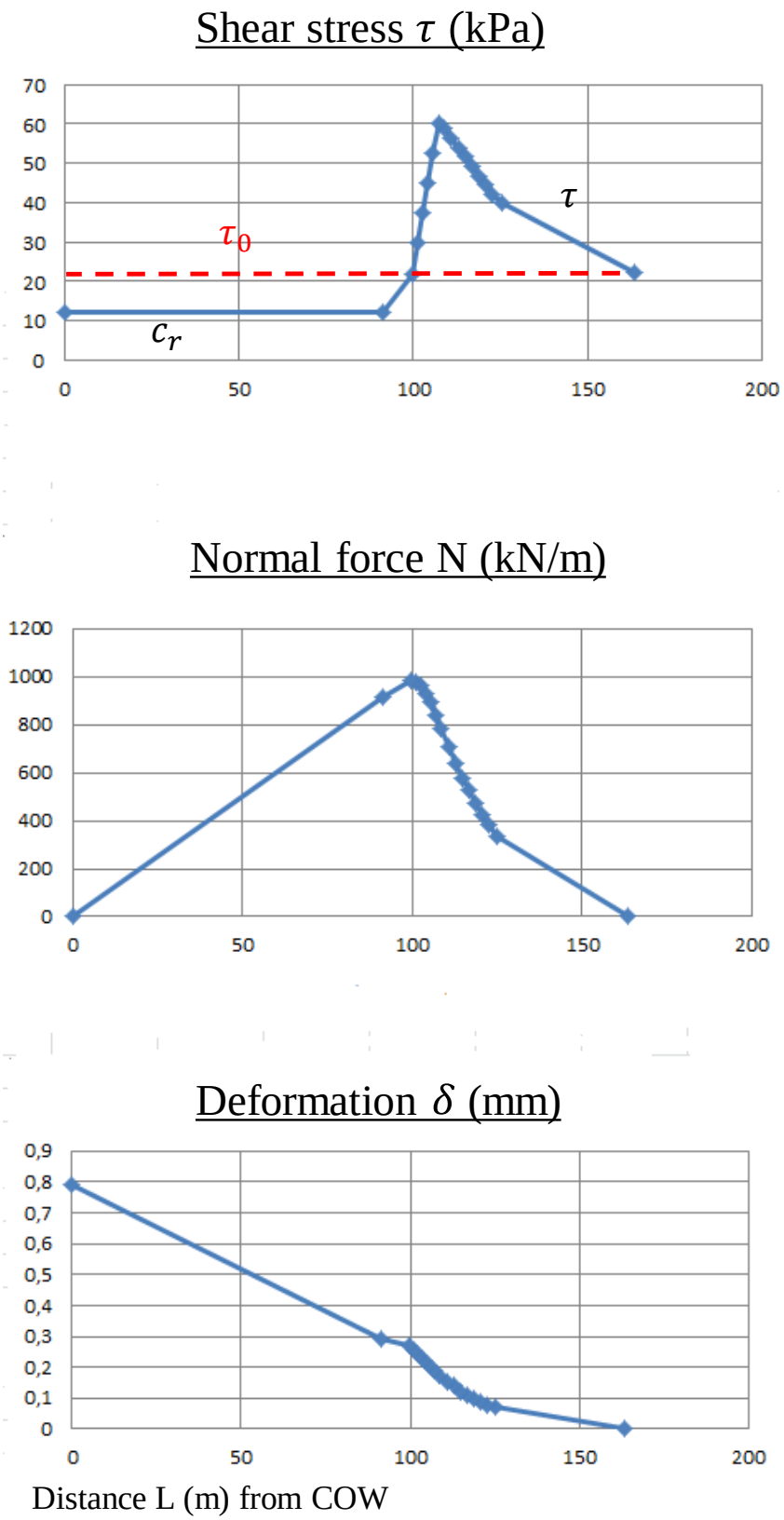

Figure D-2. Shear stresses τ, normal force N and deformation δ as function of the distance *L* from the Cut-Off Wall

An alternative more detailed study of the load N_q is given below

For this investigation the total additional load N_q likely to trigger progressive failure is set to be the pressure acting on the cut-off wall. However, this choice will be discussed in chapter 6.

We consider that the upper layers is a "heterogeneous" mix of clays, silts and sands having an average humid mass weight of $\rho g = \gamma$ = 18,8 kN/m^3 and a weight in water of γ' = 8,8 kN/m^3
Its active Rankine pressure coefficient is taken as $K_a = 0{,}3$

Concerning the clay layer studied, it is assumed to have water saturated mass density γ_c = 18,0 kN/m^3 and its weight in water γ_c' = 8,8 kN/m^3
Its effective cohesion is $c' = 6\ kPa$.

The triggering load is defined as:

$$N_q = K_a g\left[\frac{1}{2}\rho {H_d}^2 + \rho(H - H_d)^2 + \frac{1}{2}\rho'(H - H_d)^2\right] + \rho g(H - H_d) * H_c + \rho' g(H - H_d) * H_c + \frac{1}{2}\rho'_c g {H_c}^2 - 2c' H_c + \frac{1}{2}\rho_w g {H_w}^2$$

$$N_q = 0{,}3 * \left[\frac{1}{2} * 18{,}8 * 21^2 + 18{,}8 * (28 - 21)^2 + \frac{1}{2} * 8{,}8(28 - 21)^2\right] + 18{,}8 * (28 - 21) * 15 + 8{,}8 * (28 - 21) * 15 + \frac{1}{2} * 8 * 15^2 - 2 * 6 * 15 + \frac{1}{2} * 10 * 22^2 = 1243{,}6 + 276{,}4 + 64{,}7 + 1974 + 924 + 900 - 180 + 2420 = 7622{,}7\ \text{kN/m}$$

The maximal load, reached when the reservoir is full is:

$$N_q = 7627\ kN/m$$

E. Calculations regarding Muskrat Falls Lower Clay Layer

This is the detailed calculation for one example of landslide investigation carried in chapter 5.3.3 with the excel spreadsheet developed during this work.

PARAMETERS													
Poisson ratio	Peak shear strength	Residual shear strength	Shear strength at surface	Sensitivity ratio	Shear stress at elastic limit	Deviator strain at elastic limit	Deviator strain at failure limit	Secant modulus in shear	Elastic modulus	Slip for residual shear strength	Depth of ground of the upper layer	Thickness of the failure layer	Average density of the layer above
ν	c (kN/m^2)	c_R (kN/m^2)	c_s (kN/m^2)	c_R/c	τ_{el} (kN/m^2)	γ_{el} (%)	γ_f (%)	G (kN/m^2)	E_{mean} (kN/m^2)	δ_{cr} (m)	H (m)	Hc (m)	ρ (kN/m^2)
0,334	60	12	45	0,2	40	0,035	0,07	1142,8571	3000	0,3	50	10	18,8

Stage 1:

Step n° 1									
Position from slip surface (z)	ρ_c (kN/m^2)	τ_0 (kN/m^2)	τ_{el} (kN/m^2)	c (kN/m^2)	τ	$\Delta\tau$	$\tau+\Delta\tau$	γ_τ	$\delta(\tau)$ (m)
0,00	18,00	28,17	40,00	60,00	28,17	11,83	40,00	1,04E-02	
									4,93E-03
0,48	18,00	27,83	39,91	59,87	27,92	11,73	39,64	1,04E-02	
									4,94E-03
0,95	18,00	27,48	39,82	59,73	27,67	11,62	39,29	1,04E-02	
									4,95E-03
1,43	18,00	27,14	39,73	59,60	27,42	11,52	38,93	1,04E-02	
									4,95E-03
1,90	18,00	26,80	39,64	59,47	27,17	11,41	38,58	1,04E-02	
									4,96E-03
2,38	18,00	26,46	39,56	59,33	26,92	11,31	38,22	1,04E-02	
									4,97E-03
2,86	18,00	26,11	39,47	59,20	26,67	11,20	37,87	1,05E-02	
									4,98E-03
3,33	18,00	25,77	39,38	59,07	26,42	11,10	37,51	1,05E-02	

H1 (m)	52,72
H2 (m)	54,46
H (m)	53,59
Gradient	0,04
ΔN (kN/m)	256,87
N (kN/m)	256,87
$\delta_{\Delta N}$ (m)	3,47E-02
$\Sigma\delta_N$ (m)	3,47E-02
δ_τ (m)	3,47E-02
Δx (m)	43,42
Compatibility criterion	0,00
x (m)	43,42
Calculation	Solver OK
Condition for brittle failure	Brittle failure

(*) H_1 is the height of the right boarder of the upper part of the slice considered above the clay layer

(**) H_2 is the height of the left boarder of the upper part of the slice considered above the clay layer

(***) H is the average height of the slice considered above the clay layer $H = \frac{H1+H2}{2}$

Step n° 2									
Position from slip surface (z)	ρ_c (kN/m^2)	τ_0 (kN/m^2)	τ_{el} (kN/m^2)	c (kN/m^2)	τ	$\Delta\tau$	$\tau+\Delta\tau$	γ_τ	$\delta(\tau)$ (m)
0,00	18,00	27,80	40,00	60,00	40,00	2,22	42,22	1,27E-02	
									6,03E-03
0,48	18,00	27,45	39,91	59,86	39,64	2,20	41,85	1,27E-02	
									6,03E-03
0,95	18,00	27,11	39,82	59,73	39,29	2,18	41,47	1,27E-02	
									6,02E-03
1,43	18,00	26,77	39,73	59,59	38,93	2,16	41,10	1,26E-02	
									6,02E-03
1,90	18,00	26,43	39,64	59,46	38,58	2,14	40,72	1,26E-02	
									6,02E-03
2,38	18,00	26,08	39,55	59,32	38,22	2,12	40,34	1,26E-02	
									6,01E-03
2,86	18,00	25,74	39,46	59,19	37,87	2,10	39,97	1,26E-02	
									6,01E-03
3,33	18,00	25,40	39,37	59,05	37,51	2,08	39,59	1,26E-02	

H1 (m)	52,55
H2 (m)	52,72
H (m)	52,64
Gradient	0,04
ΔN (kN/m)	55,11
N (kN/m)	311,98
δΔN (m)	7,45E-03
ΣδN (m)	4,21E-02
δτ (m)	4,21E-02
Δx (m)	4,14
Compatibility criterion	0,00
x (m)	47,56
Calculation	Solver OK
Condition for brittle failure	Brittle failure

Step n°	3								
Position from slip surface (z)	ρ_c (kN/m^2)	τ_o (kN/m^2)	τ_{el} (kN/m^2)	c (kN/m^2)	τ	$\Delta\tau$	$\tau+\Delta\tau$	γ_τ	$\delta(\tau)$ (m)
0,00	18,00	27,74	40,00	60,00	42,22	2,28	44,51	1,49E-02	
									7,10E-03
0,48	18,00	27,40	39,91	59,86	41,85	2,26	44,11	1,49E-02	
									7,07E-03
0,95	18,00	27,05	39,82	59,73	41,47	2,24	43,71	1,48E-02	
									7,05E-03
1,43	18,00	26,71	39,73	59,59	41,10	2,22	43,32	1,48E-02	
									7,03E-03
1,90	18,00	26,37	39,64	59,46	40,72	2,20	42,92	1,47E-02	
									7,01E-03
2,38	18,00	26,02	39,55	59,32	40,34	2,18	42,53	1,47E-02	
									7,00E-03
2,86	18,00	25,68	39,46	59,18	39,97	2,16	42,13	1,47E-02	
									6,98E-03
3,33	18,00	25,34	39,36	59,05	39,59	2,14	41,73	1,46E-02	

H1 (m)	52,42
H2 (m)	52,55
H (m)	52,49
Gradient	0,04
ΔN (kN/m)	51,73
N (kN/m)	363,71
δΔN (m)	7,10E-03
ΣδN (m)	4,92E-02
δτ (m)	4,92E-02
Δx (m)	3,31
Compatibility criterion	0,00
x (m)	50,87
Calculation	Solver OK
Condition for brittle failure	Brittle failure

Step n°	4								
Position from slip surface (z)	ρ_c (kN/m^2)	τ_o (kN/m^2)	τ_{el} (kN/m^2)	c (kN/m^2)	τ	$\Delta\tau$	$\tau+\Delta\tau$	γ_τ	$\delta(\tau)$ (m)
0,00	18,00	27,69	40,00	60,00	44,51	2,32	46,83	1,74E-02	
									8,25E-03
0,48	18,00	27,34	39,91	59,86	44,11	2,30	46,41	1,73E-02	
									8,21E-03
0,95	18,00	27,00	39,82	59,73	43,71	2,28	45,99	1,72E-02	
									8,17E-03
1,43	18,00	26,66	39,73	59,59	43,32	2,26	45,58	1,71E-02	
									8,13E-03
1,90	18,00	26,32	39,64	59,45	42,92	2,24	45,16	1,70E-02	
									8,09E-03
2,38	18,00	25,97	39,55	59,32	42,53	2,22	44,74	1,70E-02	
									8,06E-03
2,86	18,00	25,63	39,45	59,18	42,13	2,20	44,32	1,69E-02	
									8,03E-03
3,33	18,00	25,29	39,36	59,05	41,73	2,17	43,91	1,68E-02	

H1 (m)	52,30
H2 (m)	52,42
H (m)	52,36
Gradient	0,04
ΔN (kN/m)	55,50
N (kN/m)	419,20
δΔN (m)	7,69E-03
ΣδN (m)	5,69E-02
δτ (m)	5,69E-02
Δx (m)	3,09
Compatibility criterion	0,00
x (m)	53,96
Calculation	Solver OK
Condition for brittle failure	Brittle failure

Step n°	5								
Position from slip surface (z)	ρ_c (kN/m^2)	τ_o (kN/m^2)	τ_{el} (kN/m^2)	c (kN/m^2)	τ	$\Delta\tau$	$\tau+\Delta\tau$	γ_τ	$\delta(\tau)$ (m)
0,00	18,00	27,64	40,00	60,00	46,83	2,35	49,18	2,01E-02	
									9,52E-03
0,48	18,00	27,30	39,91	59,86	46,41	2,33	48,74	1,99E-02	
									9,46E-03
0,95	18,00	26,96	39,82	59,73	45,99	2,31	48,30	1,98E-02	
									9,39E-03
1,43	18,00	26,61	39,73	59,59	45,58	2,28	47,86	1,97E-02	
									9,33E-03
1,90	18,00	26,27	39,64	59,45	45,16	2,26	47,42	1,95E-02	
									9,27E-03
2,38	18,00	25,93	39,54	59,32	44,74	2,24	46,98	1,94E-02	
									9,21E-03
2,86	18,00	25,58	39,45	59,18	44,32	2,22	46,55	1,93E-02	
									9,16E-03
3,33	18,00	25,24	39,36	59,04	43,91	2,20	46,11	1,92E-02	

H1 (m)	52,18
H2 (m)	52,30
H (m)	52,24
Gradient	0,04
ΔN (kN/m)	59,78
N (kN/m)	478,98
δΔN (m)	8,41E-03
ΣδN (m)	6,54E-02
δτ (m)	6,54E-02
Δx (m)	2,94
Compatibility criterion	0,00
x (m)	56,89
Calculation	Solver OK
Condition for brittle failure	Brittle failure

Step n°	6								
Position from slip surface (z)	ρ_c (kN/m²)	τ_o (kN/m²)	τ_{el} (kN/m²)	c (kN/m²)	τ	Δτ	τ+Δτ	γ_τ	δ(τ) (m)
0,00	18,00	27,60	40,00	60,00	49,18	2,37	51,55	2,31E-02	
									1,10E-02
0,48	18,00	27,25	39,91	59,86	48,74	2,35	51,09	2,29E-02	
									1,09E-02
0,95	18,00	26,91	39,82	59,73	48,30	2,33	50,63	2,27E-02	
									1,08E-02
1,43	18,00	26,57	39,73	59,59	47,86	2,31	50,17	2,25E-02	
									1,07E-02
1,90	18,00	26,22	39,63	59,45	47,42	2,28	49,71	2,23E-02	
									1,06E-02
2,38	18,00	25,88	39,54	59,31	46,98	2,26	49,25	2,21E-02	
									1,05E-02
2,86	18,00	25,54	39,45	59,18	46,55	2,24	48,79	2,19E-02	
									1,04E-02
3,33	18,00	25,20	39,36	59,04	46,11	2,22	48,32	2,18E-02	

H1 (m)	52,07
H2 (m)	52,18
H (m)	52,12
Gradient	0,04
ΔN (kN/m)	64,98
N (kN/m)	543,97
δΔN (m)	9,34E-03
ΣδN (m)	7,47E-02
δτ (m)	7,47E-02
Δx (m)	2,85
Compatibility criterion	0,00
x (m)	59,75
Calculation	Solver OK
Condition for brittle failure	Brittle failure

Step n°	7								
Position from slip surface (z)	ρ_c (kN/m²)	τ_o (kN/m²)	τ_{el} (kN/m²)	c (kN/m²)	τ	Δτ	τ+Δτ	γ_τ	δ(τ) (m)
0,00	18,00	27,55	40,00	60,00	51,55	2,39	53,94	2,66E-02	
									1,26E-02
0,48	18,00	27,21	39,91	59,86	51,09	2,37	53,45	2,63E-02	
									1,25E-02
0,95	18,00	26,87	39,82	59,73	50,63	2,34	52,97	2,60E-02	
									1,23E-02
1,43	18,00	26,52	39,73	59,59	50,17	2,32	52,49	2,57E-02	
									1,22E-02
1,90	18,00	26,18	39,63	59,45	49,71	2,30	52,01	2,54E-02	
									1,20E-02
2,38	18,00	25,84	39,54	59,31	49,25	2,28	51,52	2,52E-02	
									1,19E-02
2,86	18,00	25,49	39,45	59,18	48,79	2,26	51,04	2,49E-02	
									1,18E-02
3,33	18,00	25,15	39,36	59,04	48,32	2,23	50,56	2,47E-02	

H1 (m)	51,95
H2 (m)	52,07
H (m)	52,01
Gradient	0,04
ΔN (kN/m)	71,96
N (kN/m)	615,93
δΔN (m)	1,06E-02
ΣδN (m)	8,53E-02
δτ (m)	8,53E-02
Δx (m)	2,86
Compatibility criterion	0,00
x (m)	62,60
Calculation	Solver OK
Condition for brittle failure	Brittle failure

Step n°	8								
Position from slip surface (z)	ρ_c (kN/m²)	τ_o (kN/m²)	τ_{el} (kN/m²)	c (kN/m²)	τ	Δτ	τ+Δτ	γ_τ	δ(τ) (m)
0,00	18,00	27,50	40,00	60,00	53,94	2,40	56,34	3,10E-02	
									1,46E-02
0,48	18,00	27,16	39,91	59,86	53,45	2,38	55,83	3,05E-02	
									1,44E-02
0,95	18,00	26,82	39,82	59,72	52,97	2,36	55,33	3,00E-02	
									1,42E-02
1,43	18,00	26,48	39,72	59,59	52,49	2,34	54,82	2,95E-02	
									1,40E-02
1,90	18,00	26,13	39,63	59,45	52,01	2,31	54,32	2,91E-02	
									1,38E-02
2,38	18,00	25,79	39,54	59,31	51,52	2,29	53,82	2,87E-02	
									1,36E-02
2,86	18,00	25,45	39,45	59,17	51,04	2,27	53,31	2,83E-02	
									1,34E-02
3,33	18,00	25,11	39,36	59,04	50,56	2,25	52,81	2,80E-02	

H1 (m)	51,83
H2 (m)	51,95
H (m)	51,89
Gradient	0,04
ΔN (kN/m)	82,48
N (kN/m)	698,41
δΔN (m)	1,26E-02
ΣδN (m)	9,79E-02
δτ (m)	9,79E-02
Δx (m)	2,98
Compatibility criterion	0,00
x (m)	65,59
Calculation	Solver OK
Condition for brittle failure	Brittle failure

Step n°	9								
Position from slip surface (z)	ρ_c (kN/m^2)	τ_o (kN/m^2)	τ_{el} (kN/m^2)	c (kN/m^2)	τ	Δτ	τ+Δτ	γ_τ	δ(τ) (m)
0,00	18,00	27,45	40,00	60,00	56,34	2,41	58,75	3,72E-02	
									1,75E-02
0,48	18,00	27,11	39,91	59,86	55,83	2,39	58,23	3,62E-02	
									1,70E-02
0,95	18,00	26,77	39,82	59,72	55,33	2,37	57,70	3,53E-02	
									1,66E-02
1,43	18,00	26,43	39,72	59,59	54,82	2,35	57,17	3,45E-02	
									1,63E-02
1,90	18,00	26,08	39,63	59,45	54,32	2,33	56,65	3,38E-02	
									1,59E-02
2,38	18,00	25,74	39,54	59,31	53,82	2,30	56,12	3,32E-02	
									1,56E-02
2,86	18,00	25,40	39,45	59,17	53,31	2,28	55,59	3,26E-02	
									1,54E-02
3,33	18,00	25,06	39,36	59,03	52,81	2,26	55,07	3,20E-02	

H1 (m)	51,70
H2 (m)	51,83
H (m)	51,76
Gradient	0,04
ΔN (kN/m)	102,55
N (kN/m)	800,95
δΔN (m)	1,65E-02
ΣδN (m)	1,14E-01
δτ (m)	1,14E-01
Δx (m)	3,41
Compatibility criterion	0,00
x (m)	69,00
Calculation	Solver OK
Condition for brittle failure	Brittle failure

Step n°	10								
Position from slip surface (z)	ρ_c (kN/m^2)	τ_o (kN/m^2)	τ_{el} (kN/m^2)	c (kN/m^2)	τ	Δτ	τ+Δτ	γ_τ	δ(τ) (m)
0,00	18,00	27,41	40,00	60,00	58,75	1,25	60,00	4,60E-02	
									2,08E-02
0,48	18,00	27,07	39,91	59,86	58,23	1,24	59,46	4,13E-02	
									1,92E-02
0,95	18,00	26,72	39,82	59,72	57,70	1,22	58,92	3,95E-02	
									1,85E-02
1,43	18,00	26,38	39,72	59,59	57,17	1,21	58,39	3,82E-02	
									1,79E-02
1,90	18,00	26,04	39,63	59,45	56,65	1,20	57,85	3,71E-02	
									1,74E-02
2,38	18,00	25,70	39,54	59,31	56,12	1,19	57,31	3,61E-02	
									1,70E-02
2,86	18,00	25,35	39,45	59,17	55,59	1,18	56,77	3,53E-02	
									1,66E-02
3,33	18,00	25,01	39,35	59,03	55,07	1,17	56,23	3,46E-02	

H1 (m)	51,60
H2 (m)	51,70
H (m)	51,65
Gradient	0,04
ΔN (kN/m)	77,47
N (kN/m)	878,42
δΔN (m)	1,31E-02
ΣδN (m)	1,27E-01
δτ (m)	1,27E-01
Δx (m)	2,42
Compatibility criterion	0,00
x (m)	71,42
Calculation	Solver OK
Condition for brittle failure	Brittle failure

Stage 2:

Step n°	1								
Position from slip surface (z)	ρ_c (kN/m^2)	τ_o (kN/m^2)	τ_{el} (kN/m^2)	c (kN/m^2)	τ	Δτ	τ+Δτ	γ_τ	δ(τ) (m)
0,00	18,00	27,80	40,00	60,00	60,00	-6,44	53,56	4,00E-02	
									1,80E-02
0,48	18,00	27,45	39,91	59,86	59,46	-6,38	53,08	3,54E-02	
									1,64E-02
0,95	18,00	27,11	39,82	59,72	58,92	-6,32	52,60	3,36E-02	
									1,57E-02
1,43	18,00	26,77	39,72	59,58	58,39	-6,26	52,12	3,23E-02	
									1,51E-02
1,90	18,00	26,43	39,63	59,45	57,85	-6,20	51,65	3,12E-02	
									1,47E-02
2,38	18,00	26,08	39,54	59,31	57,31	-6,14	51,17	3,03E-02	
									1,43E-02
2,86	18,00	25,74	39,45	59,17	56,77	-6,08	50,69	2,96E-02	
									1,39E-02
3,33	18,00	25,40	39,35	59,03	56,23	-6,02	50,21	2,89E-02	

H1 (m)	51,39
H2 (m)	51,60
H (m)	51,49
Gradient	0,06
ΔN (kN/m)	100,31
N (kN/m)	978,74
δΔN (m)	2,08E-02
ΣδN (m)	1,48E-01
δτ (m)	1,48E-01
Δx (m)	3,46
Compatibility criterion	0,00
Slip in the failure plane	0,04
x (m)	74,88
Calculation	Solver OK
Condition for brittle failure	Brittle failure

Step n°	2								
Position from slip surface (z)	ρ_c (kN/m²)	τ_0 (kN/m²)	τ_{el} (kN/m²)	c (kN/m²)	τ	$\Delta\tau$	$\tau+\Delta\tau$	γ_τ	$\delta(\tau)$ (m)
0,00	18,00	27,74	40,00	60,00	53,56	-6,45	47,11	3,44E-02	
									1,53E-02
0,48	18,00	27,40	39,91	59,86	53,08	-6,39	46,69	2,98E-02	
									1,38E-02
0,95	18,00	27,05	39,81	59,72	52,60	-6,33	46,27	2,81E-02	
									1,31E-02
1,43	18,00	26,71	39,72	59,58	52,12	-6,27	45,85	2,68E-02	
									1,25E-02
1,90	18,00	26,37	39,63	59,44	51,65	-6,21	45,43	2,58E-02	
									1,21E-02
2,38	18,00	26,02	39,54	59,30	51,17	-6,15	45,01	2,50E-02	
									1,17E-02
2,86	18,00	25,68	39,44	59,16	50,69	-6,09	44,60	2,42E-02	
									1,14E-02
3,33	18,00	25,34	39,35	59,02	50,21	-6,03	44,18	2,36E-02	

H1 (m)	51,12
H2 (m)	51,39
H (m)	51,26
Gradient	0,08
ΔN (kN/m)	75,75
N (kN/m)	1054,49
δΔN (m)	2,22E-02
ΣδN (m)	1,70E-01
δτ (m)	1,70E-01
Δx (m)	3,35
Compatibility criterion	0,00
Slip in the failure plane	0,08
x (m)	78,23
Calculation	Solver OK
Condition for brittle failure	Brittle failure

Step n°	3								
Position from slip surface (z)	ρ_c (kN/m²)	τ_0 (kN/m²)	τ_{el} (kN/m²)	c (kN/m²)	τ	$\Delta\tau$	$\tau+\Delta\tau$	γ_τ	$\delta(\tau)$ (m)
0,00	18,00	27,69	40,00	60,00	47,11	-6,46	40,64	2,88E-02	
									1,26E-02
0,48	18,00	27,34	39,91	59,86	46,69	-6,40	40,29	2,43E-02	
									1,11E-02
0,95	18,00	27,00	39,81	59,72	46,27	-6,34	39,93	2,26E-02	
									1,05E-02
1,43	18,00	26,66	39,72	59,58	45,85	-6,28	39,57	2,13E-02	
									9,93E-03
1,90	18,00	26,32	39,63	59,44	45,43	-6,22	39,21	2,04E-02	
									9,51E-03
2,38	18,00	25,97	39,53	59,30	45,01	-6,16	38,85	1,96E-02	
									9,15E-03
2,86	18,00	25,63	39,44	59,16	44,60	-6,10	38,50	1,89E-02	
									8,83E-03
3,33	18,00	25,29	39,35	59,02	44,18	-6,04	38,14	1,82E-02	

H1 (m)	50,81
H2 (m)	51,12
H (m)	50,97
Gradient	0,10
ΔN (kN/m)	50,83
N (kN/m)	1105,32
δΔN (m)	2,22E-02
ΣδN (m)	1,93E-01
δτ (m)	1,93E-01
Δx (m)	3,14
Compatibility criterion	0,00
Slip in the failure plane	0,12
x (m)	81,37
Calculation	Solver OK
Condition for brittle failure	Brittle failure

Step n°	4								
Position from slip surface (z)	ρ_c (kN/m²)	τ_0 (kN/m²)	τ_{el} (kN/m²)	c (kN/m²)	τ	$\Delta\tau$	$\tau+\Delta\tau$	γ_τ	$\delta(\tau)$ (m)
0,00	18,00	27,64	40,00	60,00	40,64	-6,47	34,17	2,32E-02	
									9,98E-03
0,48	18,00	27,30	39,91	59,86	40,29	-6,41	33,87	1,87E-02	
									8,50E-03
0,95	18,00	26,96	39,81	59,72	39,93	-6,35	33,58	1,70E-02	
									7,83E-03
1,43	18,00	26,61	39,72	59,58	39,57	-6,29	33,28	1,59E-02	
									7,33E-03
1,90	18,00	26,27	39,62	59,44	39,21	-6,23	32,98	1,49E-02	
									6,92E-03
2,38	18,00	25,93	39,53	59,29	38,85	-6,17	32,69	1,41E-02	
									6,58E-03
2,86	18,00	25,58	39,44	59,15	38,50	-6,11	32,39	1,35E-02	
									6,29E-03
3,33	18,00	25,24	39,34	59,01	38,14	-6,05	32,09	1,29E-02	

H1 (m)	50,45
H2 (m)	50,81
H (m)	50,63
Gradient	0,12
ΔN (kN/m)	29,42
N (kN/m)	1134,74
δΔN (m)	2,22E-02
ΣδN (m)	2,15E-01
δτ (m)	2,15E-01
Δx (m)	3,01
Compatibility criterion	0,00
Slip in the failure plane	0,16
x (m)	84,38
Calculation	Solver OK
Condition for brittle failure	Brittle failure

$$\tau + \Delta\tau = \tau_0$$

Step n°	5								
Position from slip surface (z)	ρ_c (kN/m²)	τ_o (kN/m²)	τ_{el} (kN/m²)	c (kN/m²)	τ	Δτ	τ+Δτ	γ_τ	δ(τ) (m)
0,00	18,00	27,60	40,00	60,00	34,17	-6,58	27,60	1,75E-02	
									7,26E-03
0,48	18,00	27,25	39,91	59,86	33,87	-6,51	27,36	1,30E-02	
									5,81E-03
0,95	18,00	26,91	39,81	59,72	33,58	-6,45	27,13	1,14E-02	
									5,16E-03
1,43	18,00	26,57	39,72	59,57	33,28	-6,39	26,89	1,03E-02	
									4,68E-03
1,90	18,00	26,22	39,62	59,43	32,98	-6,33	26,66	9,38E-03	
									4,29E-03
2,38	18,00	25,88	39,53	59,29	32,69	-6,27	26,42	8,65E-03	
									3,97E-03
2,86	18,00	25,54	39,43	59,15	32,39	-6,20	26,19	8,03E-03	
									3,70E-03
3,33	18,00	25,20	39,34	59,00	32,09	-6,14	25,95	7,50E-03	

H1 (m)	50,00
H2 (m)	50,45
H (m)	50,22
Gradient	0,15
ΔN (kN/m)	9,81
N (kN/m)	1144,55
δΔN (m)	2,26E-02
ΣδN (m)	2,37E-01
δτ (m)	2,37E-01
Δx (m)	2,98
Compatibility criterion	0,00
Slip in the failure plane	0,20
x (m)	87,37
Calculation	Solver OK
Condition for brittle failure	Brittle failure

$$\tau + \Delta\tau = c_r$$

Step n°	6								
Position from slip surface (z)	ρ_c (kN/m²)	τ_o (kN/m²)	τ_{el} (kN/m²)	c (kN/m²)	τ	Δτ	τ+Δτ	γ_τ	δ(τ) (m)
0,00	18,00	27,55	40,00	60,00	40,64	-28,64	12,00	3,89E-03	
									8,02E-04
0,48	18,00	27,21	39,91	59,86	40,29	-28,38	11,91	-5,25E-04	
									-6,12E-04
0,95	18,00	26,87	39,82	59,72	39,93	-28,12	11,81	-2,05E-03	
									-1,22E-03
1,43	18,00	26,52	39,72	59,59	39,57	-27,85	11,72	-3,09E-03	
									-1,66E-03
1,90	18,00	26,18	39,63	59,45	39,21	-27,59	11,62	-3,89E-03	
									-2,00E-03
2,38	18,00	25,84	39,54	59,31	38,85	-27,33	11,53	-4,53E-03	
									-2,28E-03
2,86	18,00	25,49	39,45	59,17	38,50	-27,06	11,43	-5,06E-03	
									-2,51E-03
3,33	18,00	25,15	39,36	59,03	38,14	-26,80	11,34	-5,50E-03	

H1 (m)	50,00
H2 (m)	53,43
H (m)	51,72
Gradient	0,15
ΔN (kN/m)	-28,09
N (kN/m)	950,65
δΔN (m)	1,42E-01
ΣδN (m)	2,91E-01
δτ (m)	2,91E-01
Δx (m)	22,87
Compatibility criterion	0,00
Slip in the failure plane	0,30
x (m)	110,24
Calculation	Solver OK
Condition for brittle failure	Brittle failure

Calculation of the instability parameters

Instability	
Δx	61,1334455
δ_τ (m)	0,477802731
L	171,3721942
N	0

Summary of the results:

Results									
ΣΔx for stage 1	ΣΔx for stage 2	L_{crit} (m)	δ_{crit} (m)	N_{crit} (kN/m)	L_{instab} (m)	δ_{instab} (m)	Safety Factor	Calculation	Brittle failure
71,42	15,95	87,37	0,24	1144,55	171,37	0,48	0,07	Solver OK	Brittle failure

Shape of the section studied:

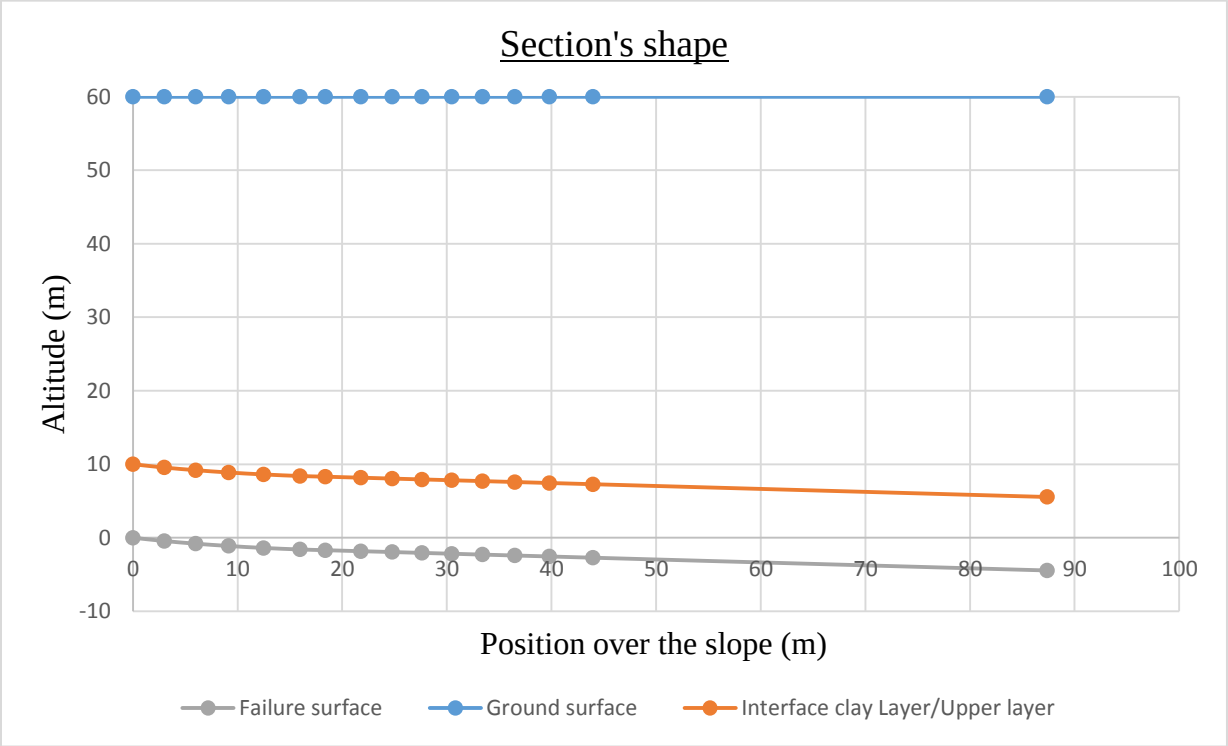

Figure E-3 Shape of geometric simplification of the North Spur studied

Table E-1. Summary of calculations

Step	x	L = 171,37 - x	τ+Δτ	τ_0	N	d	
	m	m	kPa		kN/m	mm	
0	0	171,37	28,17		0	0	a
I-1	43,42	127,95	40	28,17	8,28	0,571	
I-2	47,46	123,91	42,22	27,18	23,67	1,64	
I-3	50,87	120,5	44,51	27,74	40,13	2,79	
I-4	53,96	117,41	46,83	27,69	57,58	4,03	
I-5	56,89	114,48	49,18	27,64	76,1	5,36	
I-6	59,75	111,62	51,56	27,6	95,87	6,81	
I-7	62,6	108,77	53,94	27,55	117,18	8,41	
I-8	65,59	105,78	56,34	27,4	140,54	10,2	
I-9	69	102,37	58,75	27,45	167,15	12,3	
I-10	71,42	99,95	60	27,41	189,15	14,2	b
II-1	74,88	96,49	53,56	27,8	205,23	15,8	
II-2	78,23	93,14	47,11	27,74	224,88	17,4	
II-3	81,37	90	40,64	27,69	224,88	19	
II-4	84,38	86,99	34,17	27,64	229,53	20,6	
II-5	87,37	84	27,6	27,6	231,6	22,2	c
II-6	110,24	61,13	12	27,55	215,34	27,2	d
II-7	171,37	0	12	27,5	0	45	e

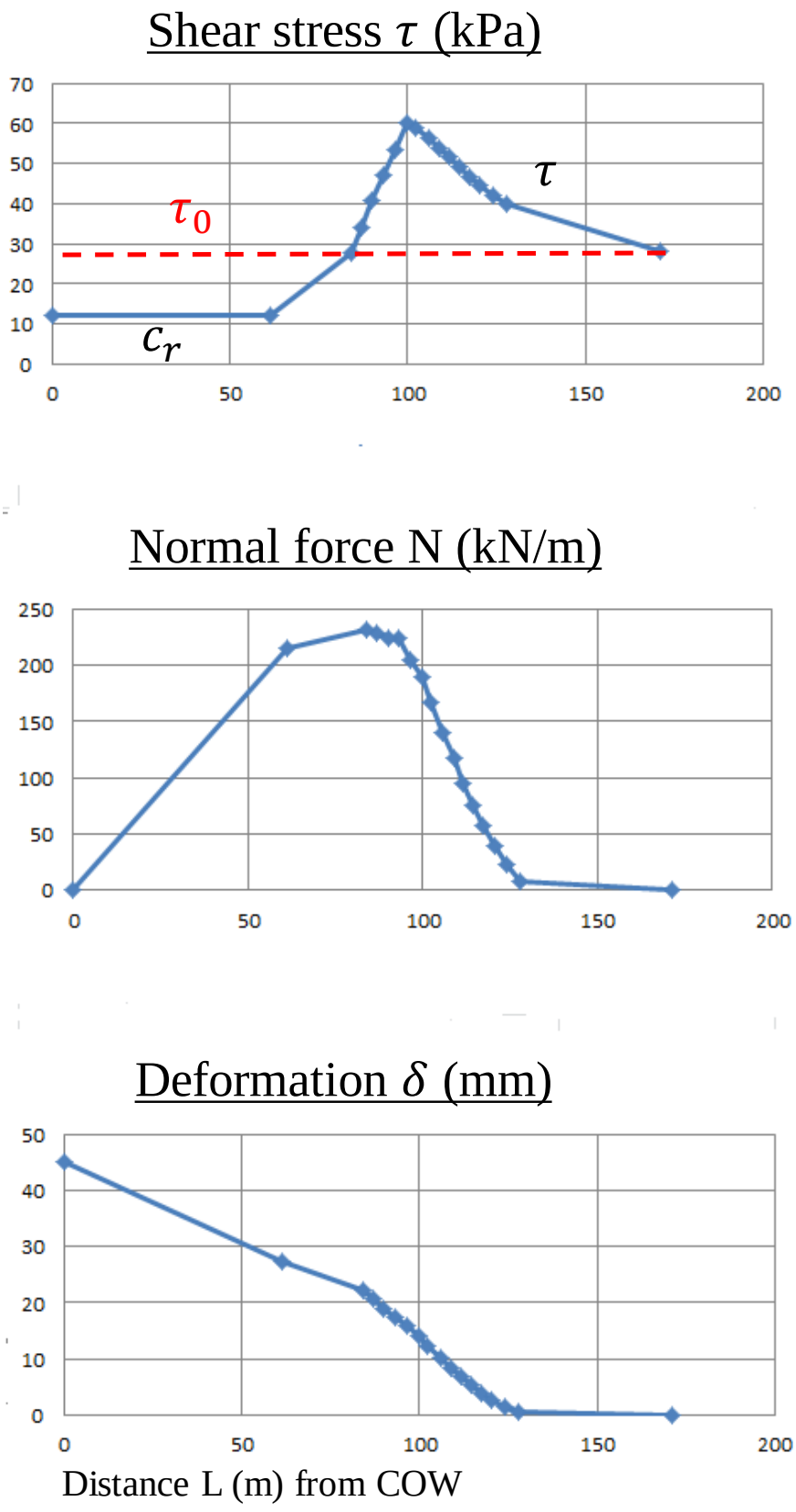

Figure E-2. Shear stresses τ, normal force N and deformation δ as function of the distance L from disturbing load N,

An alternative way more conservative way of estimating Nq is given below.

$$N_q = K_a g \left[\frac{1}{2}\rho {H_d}^2 + \rho(H - H_d)^2 + \frac{1}{2}\rho'(H - H_d)^2\right] + \rho g(H - H_d) * H_c + \rho' g(H - H_d) * H_c + \frac{1}{2}{\rho'}_c g {H_c}^2 - 2c' H_c + \frac{1}{2}\rho_w g {H_w}^2$$

$$N_q = 0{,}3 * 1 * \left[\frac{1}{2} * 18{,}8 * 21^2 + 18{,}8 * (50 - 21)^2 + \frac{1}{2} * 8{,}8 * (50 - 21)^2\right] + 18{,}8 * (50 - 21) * 10 + 8{,}8 * (50 - 21) * 10 + \frac{1}{2} * 8 * 10^2 - 2 * 6 * 10 + \frac{1}{2} * 10 * 39^2$$

The maximal load, reached when the reservoir is full is:

$$N_q \approx 22986\ kN/m$$

About the author

Robin Dury was born on September 15, 1994 in Saint-Etienne, France. He attended primary and secondary school in Sorbiers and La Talaudiere. He studied sciences at high school in Saint-Etienne and graduated in 2012 with honors. Afterwards, he went to the engineering school INSA de Lyon to study civil engineering. After 4 years spent at INSA Lyon where he studied mostly geotechnics and structural analysis, he went in 2016 to Luleå Tekniska Universitet in order to do his last year of Master Degree before graduation. Then he wrote this thesis at the Department of Civil, Environmental and Natural Resources Engineering.